DOKUZ EYLÜL UNIVERSITY
GRADUATE SCHOOL OF NATURAL AND APPLIED SCIENCES

VIBRATION CONTROL OF A STRUCTURE WITH ACTIVE MASS SYSTEMS

by
Rafet Can ÜMÜTLÜ

August, 2022
İZMİR

VIBRATION CONTROL OF A STRUCTURE WITH ACTIVE MASS SYSTEMS

A Thesis Submitted to the
Graduate School of Natural and Applied Sciences of Dokuz Eylül University
In Partial Fulfillment of the Requirements for the Degree of Doctor of Philosophy in Mechatronic Engineering

by

Rafet Can ÜMÜTLÜ

August, 2022
İZMİR

Ph.D. THESIS EXAMINATION RESULT FORM

We have read the thesis entitled "**VIBRATION CONTROL OF A STRUCTURE WITH ACTIVE MASS SYSTEMS**" completed by **RAFET CAN ÜMÜTLÜ** under supervision of **PROF.DR. HASAN ÖZTÜRK** and we certify that in our opinion it is fully adequate, in scope and in quality, as a thesis for the degree of Doctor of Philosophy**.**

.....

Prof. Dr. Hasan ÖZTÜRK

_____

Supervisor

.....	.....
Prof. Dr. Zeki KIRAL	Assoc. Prof. Dr. Savaş ŞAHİN
_____	_____
Thesis Committee Member	Thesis Committee Member
.....	.....
Prof. Dr. Lale Canan DÜLGER	Prof. Dr. Levent ÇETİN
_____	_____
Examining Committee Member	Examining Committee Member

_____

Prof. Dr. Okan FISTIKOĞLU

Director

Graduate School of Natural and Applied Sciences

ACKNOWLEDGMENTS

First of all, I would like to express my deepest gratitude to my supervisor, Prof. Dr. Hasan Öztürk, for all his efforts, who guided me with his valuable opinions at every moment I needed during my Ph.D. thesis.

I am sincerely grateful to Assoc. Prof. Barış Bıdıklı, who first introduced me to Lyapunov-based controller design. I would like to thank him for his help, guidance, and criticism throughout the course of this work.

I would like to also thank my thesis committee members: Prof. Dr. Zeki Kıral and Assoc. Prof. Savaş Şahin for their help with valuable suggestions and discussions.

The eighth chapter of this thesis was created during my time as visiting researcher at the University of Exeter. I would like to thank Prof. Dr. Aleksandar Pavic and Prof. Dr. Paul Reynolds, members of the University of Exeter, for their invaluable opinions, suggestions, and time devoted to me.

This thesis was supported by the Scientific and Technological Research Council of Turkey (TUBITAK) 2211-A program. I am grateful for this scholarship.

I would like to acknowledge the financial support from the Scientific and Technological Research Council of Turkey (TUBITAK) 2214-A.

I would like to express my deepest gratitude to my mother Fidan Ümütlü and my father Muammer Ümütlü for their loving support and efforts.

Finally, I would like to thank my dear wife, Hatice Cansu Ayaz Ümütlü, for her understanding, patience, endless love, and continuous support throughout my Ph.D. thesis.

Rafet Can ÜMÜTLÜ

VIBRATION CONTROL OF A STRUCTURE WITH ACTIVE MASS SYSTEMS

ABSTRACT

Strong earthquake-induced vibrations that endanger human life and the structural integrity of structures as well as wind-induced vibrations of skyscrapers are examples of vibrations in buildings whose amplitudes aimed to be decreased. In order to reduce these types of structural vibrations, active mass damper systems are often used in literature and full-scale applications.

In this thesis, the focus is on controller design for ATMD systems in order to reduce the vibration of multi-story buildings, especially earthquake-induced vibrations. Stability of the structure and control mass is guaranteed by Lyapunov-based stability analysis. Robust adaptive backstepping controller, which is a full state feedback control method, is enriched with a new linear regression based design. In this way, the designed controller achieves its control purpose by using fewer sensors feedback. In Lyapunov-based controller designs within the scope of this thesis, the structural parameters are not used and the unknown structural parameters are compensated using adaptive compensation terms. Afterward, a Lyapunov-based controller is designed for a nonlinear structure model that is exposed to nonlinear disturbances and the stability of the structure is ensured while achieving the control purpose. Finally, a controller design based on the natural frequency of the structure has been strengthened with a control structure that limits the range of motion of the controller.

As a result, this thesis theoretically proved that vibrations occurring in engineering structures can be controlled by compensating for unknown structural parameters with active mass systems. Stability of the structure for all positive control gains while achieving the control objective is guaranteed by Lyapunov-based stability analysis.

Keywords: Active vibration control, Lyapunov-based control, Backstepping control, Nonlinear control, Robust adaptive control

BİR YAPININ AKTİF KÜTLE SİSTEMLERİ İLE TİTREŞİM KONTROLÜ

ÖZ

İnsan hayatını ve yapıların yapısal bütünlüğünü tehlikeye atan güçlü deprem kaynaklı titreşimler ile gökdelenlerin rüzgar kaynaklı titreşimleri, genliği azaltılmaya çalışılan binalardaki titreşimlere örnektir. Literatürde ve tam ölçekli uygulamalarda yapısal titreşimleri sönümlemek amacı ile aktif kütle damper sistemleri uygulamaları ile sıklıkla karşılaşılmaktadır.

Bu tez kapsamında çok katlı yapıların başta deprem kaynaklı titreşimleri olmak üzere titreşim genliklerini düşürmek amacı ile ATMD sistemler için kontrolcü tasarımı üzerine odaklanılmıştır. Lyapunov tabanlı kararlılık analizi ile ilk olarak yapının daha sonra ise hem yapının hem kontrol kütlesinin kararlılığı garanti altına alınmıştır. Bir tam durum geri besleme kontrol yöntemi olan uyarlanabilir gürbüz geriadımlamalı kontrolcü, yeni doğrusal regresyon temelli bir tasarım ile zenginleştirilmiştir. Bu sayede tasarlanan kontrolcü, daha az sensör verisi kullanarak kontrol amacına ulaşmaktadır. Lyapunov tabanlı kontrolcü tasarımlarında yapı parametreleri kontrolcü tasarımında kullanılmamıştır ve bilinmeyen yapısal parametreler uyarlamalı telafi terimleri kullanılarak telafi edilmiştir. Daha sonra, doğrusal olmayan bozucu etkiye maruz kalan ve doğrusal olmayan bir yapı modeli için Lyapunov tabanlı kontrolcü tasarlanarak yapının kararlılığı kontrol amacına ulaşırken garanti edilmiştir. Son olarak yapının doğal frekansını baz alan bir kontrolcü tasarımı kontrolcü kütle hareket aralığı sınırlayıcı bir kontrol yapısı ile güçlendirilmiştir.

Sonuç olarak, bu tez mühendislik yapılarında meydana gelen titreşimlerin aktif kütle sistemleri ile bilinmeyen yapı parametreleri telafi edilerek kontrol edilebileceğini teorik olarak kanıtlamıştır. Kontrol amacına ulaşırken bütün pozitif kontrol kazançları için yapının kararlılığı Lyapunov tabanlı kararlılık analizi ile garanti altına alınmıştır.

Anahtar Kelimeler: Aktif titreşim kontrolü, Lyapunov tabanlı kontrol, Geriadımlamalı kontrol, Doğrusal olmayan kontrol, Uyarlamalı gürbüz control

CONTENTS

Page

LIST OF FIGURES

Page

LIST OF TABLES

Page

CHAPTER ONE
INTRODUCTION

1.1 Introduction

The vibration of flexible structures is a major challenge caused by external factors such as earthquakes and wind. With the developing world and increasing population, the demand for high-rise buildings is increasing in many earthquake regions. The destructive effects of earthquakes on buildings and human life are one of the biggest problems encountered in daily life as seen in Figure 1.1. Some of the most catastrophic earthquakes in recent years that have resulted in considerable casualties are listed in Table 1.1.

Table 1.1 Some major earthquakes and loss of life (Spence & So, 2021)

Location	Date	Magnitude	Loss of Life
Turkey, Kocaeli	17/08/1999	7.6	17,127
Japan, Kobe	17/01/1995	6.9	6,434
Iran,Bam	26/12/2003	6.6	26,271
China, Sichuan	12/05/2008	8.0	87,587
Indonesia, Yogyakarta	27/05/2006	6.4	28,903

The data is a reminder of humanity's vulnerability to natural hazards. The protection of civil structures from natural hazards, especially earthquakes, is undoubted of great importance worldwide. The buildings are being developed in order to be more resistant to such external effects. Engineering structures are in continuous development to satisfy the increasing human needs depending on the developing technology throughout the history of humanity. Building structures also have to evolve to fulfill human needs in this context. Today, engineering structures have to overcome two essential requirements. First, engineering structures must have sufficient strength against external influences. Second, engineering structures must be as light as possible to reduce costs and reduce our carbon footprint. Inevitably, designing more flexible structures using lightweight materials is the only solution engineers have come up with to this problem.

Figure 1.1 Examples of major damage to structures caused by some major earthquakes (Christenson, 2001)

In addition to strengthening building structures, supporting buildings with technologies and systems that can protect them against the destructive effects of earthquakes have become the frequently preferred protection methods. This fact has been leading scientists to conduct research on this topic for many years. Undoubtedly, damping these vibrations as quickly as possible is one of the most effective methods to prevent loss of life and property. The demand for earthquake protection systems to protect buildings and people in the face of earthquakes is rapidly increasing. From the viewpoint of the theory of control, this purpose is considered a subtitle of vibration control. Damping the undesired vibrations of the building during the earthquake by producing a vibrational response in the reverse direction is the main aim of these types of vibration control studies. Earthquake-induced vibrations can be reduced by passive and active vibration control methods. There has been an increasing number of studies on this subject in recent years.

Vibration isolation using rubber bearings is one of the most popular methods of passive vibration control. Base isolators are flexible isolation devices, placed between the building structure and the foundation for reducing seismic wave propagation into the structure (Yu & Thenozhi, 2016). The addition of this device will increase the flexibility of the structure, hence, the structural time period. For that reason, isolators reduce the propagation of high-frequency signals from the ground to the structure. They are one of the popular techniques applied widely in bridges (Aly, 2014a).

Another passive control method is a tuned mass damper (TMD). It is based on the simple idea of transferring the kinetic energy of the vibrating structure to a properly tuned and specially designed single degree of freedom oscillator (Aly, 2014b; Kamgar et al., 2018; Khatibinia et al., 2020; Petrini et al., 2020). The TMD has been used very successfully in many applications, including the mitigation of the wind response of tall buildings, wind turbines, and power transmission lines, and the vibration alleviation in cars, helicopters, and spacecraft (Fuller et al., 1997; Kaynia et al., 1981; Nagarajaiah & Varadarajan, 2005; Preumont et al., 2014; Varadarajan & Nagarajaiah, 2004). Some of the full-scale applications of TMD systems are shown in Figure 1.2 (a). The floors where the TMD system is located in the Taipei 101 building are shown in Figure 1.2 (b). The actual image of the 660 tons TMD system in the Taipei 101 building is shown in Figure 1.2 (c).

TMD system supported with an actuator is called an active tuned mass damper (ATMD) system. In ATMD systems, the mass movement is provided via a control force that is applied from the actuator input in addition to spring and damping elements. Owing to this structure, the vibrational response in the inverse direction of undesired vibrations can be produced and it can be used to reduce undesired vibrations (Soong & Spencer, 1992). The Kyobashi Seiwa Building and ATMD system, which is one of the full-scale applications of ATMD systems, is shown in Figure 1.3.

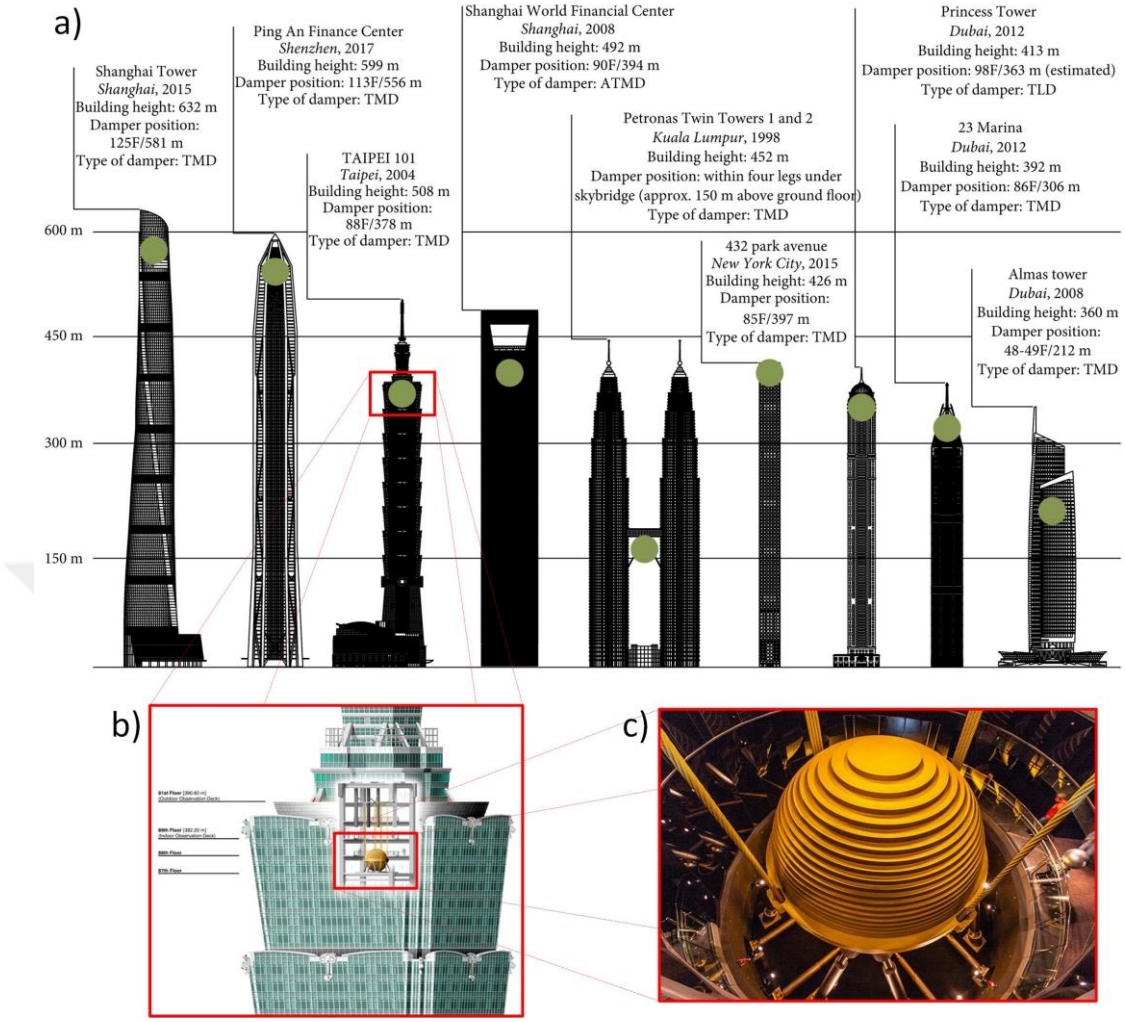

Figure 1.2 (a) Some of the full-scale applications of TMD systems by Rahmani and Könke (2019), (b) The floors where the TMD system is located in the Taipei 101 building by Someformofhuman (n.d.), (c) The actual image of the 660 tons TMD system in the Taipei 101 building by Paul Blair (n.d.)

TMD systems are designed considering the first natural frequency of the structures, but the ATMD system can work with several vibration modes. It is quite appropriate to use ATMD systems in structures where multi-mode damping is required, in structures that need faster vibration damping compared to passive vibration damping devices, or in structures where a smaller TMD mass is desired. However, depending on the parameters of the structure and the ATMD, the energy requirements of the systems used for vibration damping can be quite high (C. Li & Cao, 2019a; Yu & Thenozhi, 2016). This is an undesirable situation in control systems as it may increase the needed control effort. The most common and natural method to add viscous damping to the structure is to design a velocity feedback controller in ATMD systems.

However, this simple controller has one major drawback, for large values of control gain, the system tends to be unstable. Designing a controller that cannot guarantee the stability of the system for ATMD system may cause resonation and this situation may be more harmful than the earthquake. Considering this problem, it must be theoretically guaranteed that the designed controller can provide the zero convergence of all displacements on which the actuator is effective and assure the overall system's stability for all of the control process.

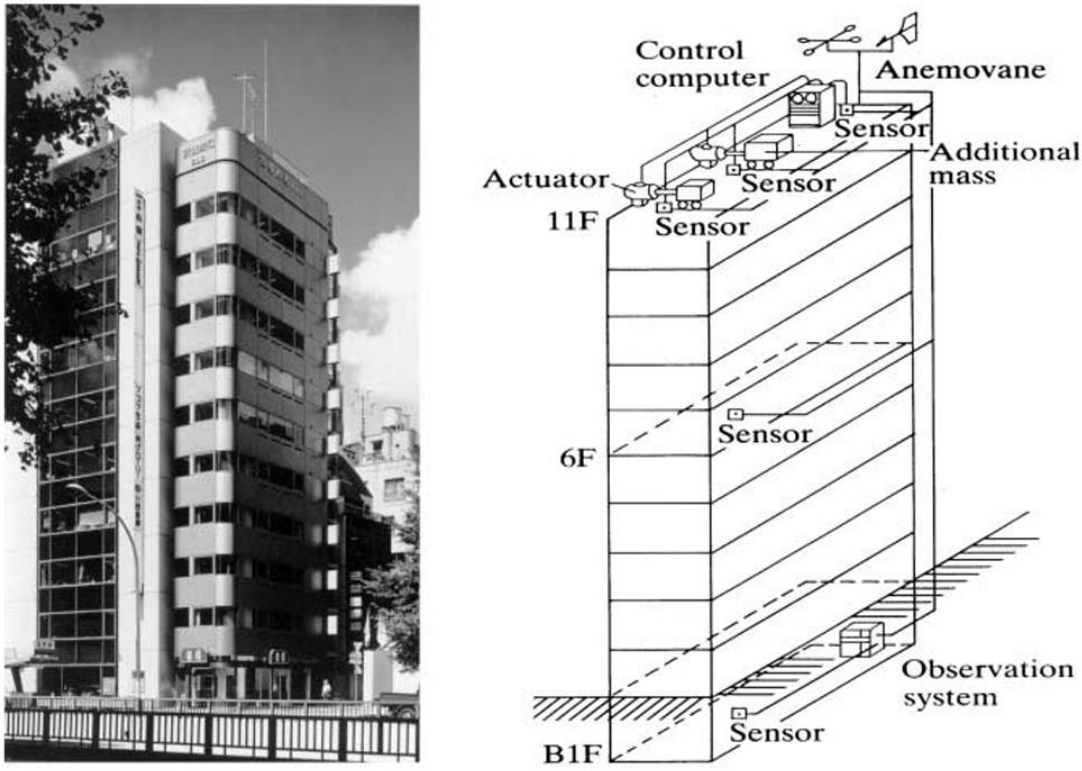

Figure 1.3 The vibration of the Kyobashi Seiwa Building is mitigated with the ATMD system (Soong & Spencer, 2002)

1.2 Literature Review

1.2.1 Tuned Mass Damper

In an important part of such vibration control studies, placing the TMD system on top of the building and damping the unwanted vibrations in the structure with the help of TMD has become the basic approach with the low cost and simplicity of TMD

systems. The mechanism of passive TMD, which is designed and placed in accordance with the structure of the building, does not contain any active component, sensor, or control unit. There is no opportunity to intervene against changing situations during the process. Schematic representations of conventional structure and structure with TMD are shown in Figure 1.4.

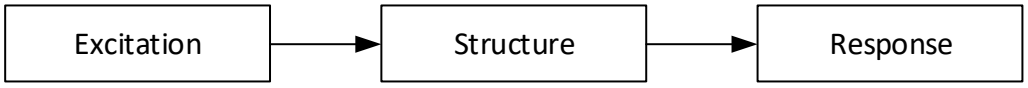

a) Conventional structure

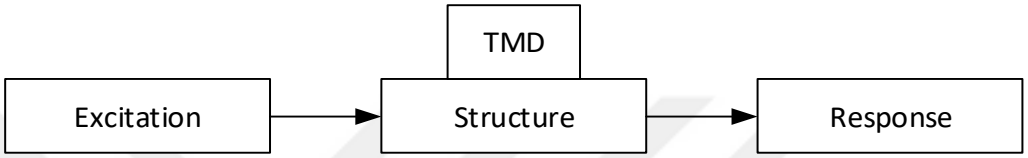

b) Structure with TMD

Figure 1.4 Schematic representations of conventional structure and structure with TMD

The schematic representation of some TMD types is shown in Figure 1.5. In pendulum-type TMDs (PTMD) (a, b, d, and e) and rolling bearing TMD, the restoring force is provided by gravity. In TMDs using springs (c, d, and f) and TMD using rubber (h) restoring force is provided by auxiliary elements such as spring and rubber. Undamped systems (a, e, and g types) can be used in TMD systems, damping force can be created with a shock absorber (b, c, d, and f types) or rubber material can be used to produce damping force as well as spring force (type h). (Cheng et al., 2008)

TMD systems, the first examples of which were encountered in North America in the 1970s, were used in economically developed countries with relatively small TMD samples in the 1980s. TMD systems started to be used popularly in the 1990s in Japan, which is often exposed to strong earthquakes and has to build tall buildings because of its limited residential area. Nowadays, TMD systems are widely used all over the world. Some examples of TMD systems used in buildings are shown chronologically in Table 1.2 (Gutierrez Soto & Adeli, 2013). The number of TMD systems listed in this table constitutes an insignificant part of the total number of TMD systems.

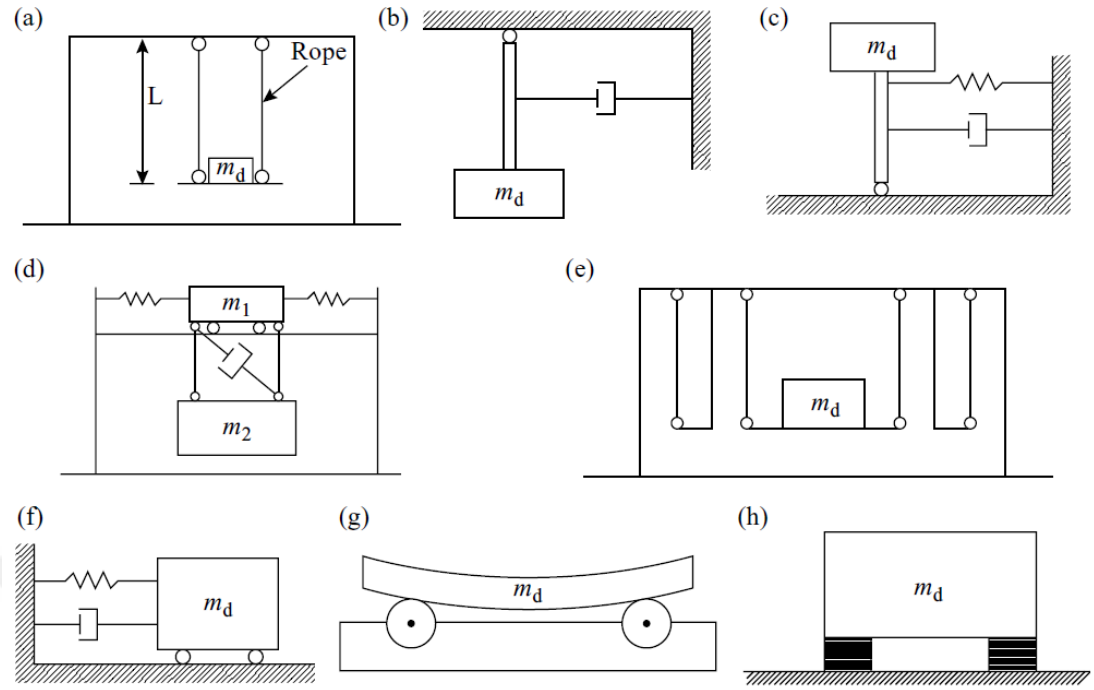

Figure 1.5 Types of TMDs: (a) pendulum type TMD (PTMD), (b) PTMD with damper, (c) inverted PTMD with spring and damper, (d) TMD and PTMD with damper, (e) multistage PTMD, (f) classical TMD, (g) TMD with rolling bearings, and (e) mass with rubber (Cheng et al., 2008)

Tablo 1.2 Full-scale implementations of TMD systems (Gutierrez Soto & Adeli, 2013)

Location	**Building**	**Year completed**	**Type of structure**	**Number of stories**	**Height**	**Controller type**
Toronto, Canada	CN Tower	1976	Tower	-	553 m	PTMD Weight = 18 t
Boston, MA, USA	John Hancock	1976	Building	60	241 m	TMD Weight = 600 t
New York, USA	Citycorp Center	1978	Building	59	278 m	TMD Weight = 370 t
Sydney, Australia	Sydney Tower	1980	Tower	-	305 m	TMD Weight = 220 t
Nurnberg, Germany	Deutsche Bundespost	1982	Tower	-	278 m	TMD Weight = 1.5 t
Yanbu, Saudi Arabia	Yanbu Cement Plant	1984	Chimney	-	81 m	TMD Weight = 10 t
Fukuoka, Japan	Fukuoka Tower	1989	Tower	-	234 m	TMD Weight = 55 t

Table 1.2 Continues

Berlin, Germany	Fernsehturm Tower	1990	Tower	-	368 m	TMD Weight = 1.5 t
Osaka, Japan	Crystal Tower	1990	Building	37	157 m	PTMD Weight = 540 t
Kobe, Japan	P&G Japan Headquarters	1993	Building	31	131 m	TMD Weight = 270 t
Hamamatsa, Japan	Act City	1994	Building	45	213 m	TMD Weight = 180 t
Fukuoka, Japan	Sea Hawk Hotel and Resort	1995	Building	36	143 m	TMD Weight = 132 t
Regensburg, Germany	Regensburg Siemens Building	1995	Building	-	-	TMD
Karlsruhe, Germany	Karlsruhe Building	1996	Building	-	-	TMD
Dubai, U.A.E.	Hotel Burj-Al-Arab	1997	Building	60	321 m	TMD Weight = 55 t
Kuala Lumpur, Malaysia	Petronas Twin Towers	1997	Building	88	451.9 m	TMD
Kau-Shon, Taiwan	TC Tower	1997	Building	85	348 m	TMD Weight = 100 t
Taipei, Taiwan	Taipei 101	2004	Building	101	449 m	TMD Weight = 730 t,
Jiaxing, China	Hangzhou Bay Bridge Tower	2009	Tower	-	130 m	TMD Weight = 110 t
Tokyo, Japan	Tokyo Skytree	2012	Tower	-	634.0 m	TMD Weight = 100 t

Since Frahm was granted a US patent for a device termed a dynamic vibration absorber in 1911, TMD systems have been the most widely used technology to mitigate the vibrations in structures (Frahm, 1911). Frahm recommended that the rolling motion of ships be controlled using a spring-mass system without damping element components. For a single frequency, the developed system demonstrated the

capacity to adjust the main system's amplitude to virtually zero (Elias & Matsagar, 2017). The basic ideas of TMD systems were theoretically developed by Ormondroyd & Den, (1928). They discovered that when a spring mass system is added to an undamped SDOF structure driven by a sinusoidal force at the resonance frequency, the resulting new two-mass system reduces vibration on the main structure. They emphasized that if the added spring mass system was chosen to be the same as that of the natural frequency main system, the structural response was greatly damped (Živanović et al., 2005). For an undamped structure exposed to harmonic external stimulation over a broad frequency range, Brock, (1947) defined the process for selecting the optimal TMD parameters. Snowdon, (1959) demonstrated the steady-state behavior of TMD. Vickery & Davenport, (1970) studied the behavior of wind response of tower type structures. Wirsching & Campbell, (1973) used TMD systems to reduce the structural response that occurs in structures under random stimulation. TMD systems were utilized by Weisner, (1979) to lessen the impact of wind on tall structures. Many studies (Luft, 1979; Randall et al., 1981; Warburton & Ayorinde, 1980) have suggested some of the simplest optimization techniques for passive TMD. The first studies on the reduction of earthquake-induced structural vibrations with TMD were made by Kaynia et al. (1981). In an unusual finding, Sladek & Klingner, (1983) conducted a theoretical analysis on the use of TMD to minimize the seismic response of buildings, and concluded that TMDs are ineffective for decreasing earthquake-induced vibrations in tall structures. Despite, some exception studies, it is an indisputable fact with numerous publications in the literature and many real-world applications that TMD systems are a very effective tool in reducing seismic and wind-induced vibrations that occur in such structures (Andersen et al., 2001; Constantinou et al., 1998; Kareem et al., 1999; Ricciardelli & Vickery, 1999; Shing et al., 1996).

Rasouli & Yahyai, (2002) found that TMD systems show maximum vibration reduction performance in scenarios where the structures are excited with a frequency close to the structure resonance frequency. Krenk (2005), with the optimal TMD parameters suggested in his study, showed that the first natural frequency of the structure and the TMD natural frequency in the frequency response are of equal amplitude and provide effective damping. Many studies have been done while working

on the optimal control of structures using TMD. TMD behavior is defined by the control mass, the spring adjusted to the structure frequency, and the damper used, and all optimal TMD designs focus on optimizing these parameters. The determination of the optimal values of these parameters for different purposes such as reducing maximum and root mean squire (RMS) of acceleration and displacements of structure and for different excitation types such as harmonic, pink, and white noise has been studied by many researchers (M. M. Ali & Moon, 2007; Bekdaş & Nigdeli, 2013; Ghosh & Basu, 2007; Hoang et al., 2008; Marian & Giaralis, 2014).

The findings mentioned above demonstrate that TMD systems are improving day by day and are now becoming more and more efficient. Although TMD systems are very effective in the fundamental frequency region of the structure, they cannot be a completely reliable system in damping the vibrations of the structure. As the name suggests, TMD systems are designed to mitigate vibrations in a certain mode only. Generally, TMD systems tuned to the first mode frequency, which is the dominant mode of the structures, have little or no effect on reducing the vibrations in other modes. These systems are only effective in this small frequency range. They can leave the structure vulnerable to vibrations that will occur with an external force effect that will trigger a different natural frequency.

1.2.2 Active Tuned Mass Damper

The vibration response is produced by moving the mass of the TMD system via a spring and a damping element in some of these studies while the spring and the damping elements are supported with an actuator in some other structures. Similar to other vibration control approaches realized in many different systems, according to the presence of the actuator, these systems are called passive or active vibration control systems. In an active control system, apart from the spring, damper and actuator, unlike TMD systems, there is a large power source for the actuator to operate, sensors to measure the structural responses, and a controller that drives the actuator via control signal in the light of an algorithm determined for generating the required power. A

schematic representation of the structure with the ATMD system is shown in Figure 1.6.

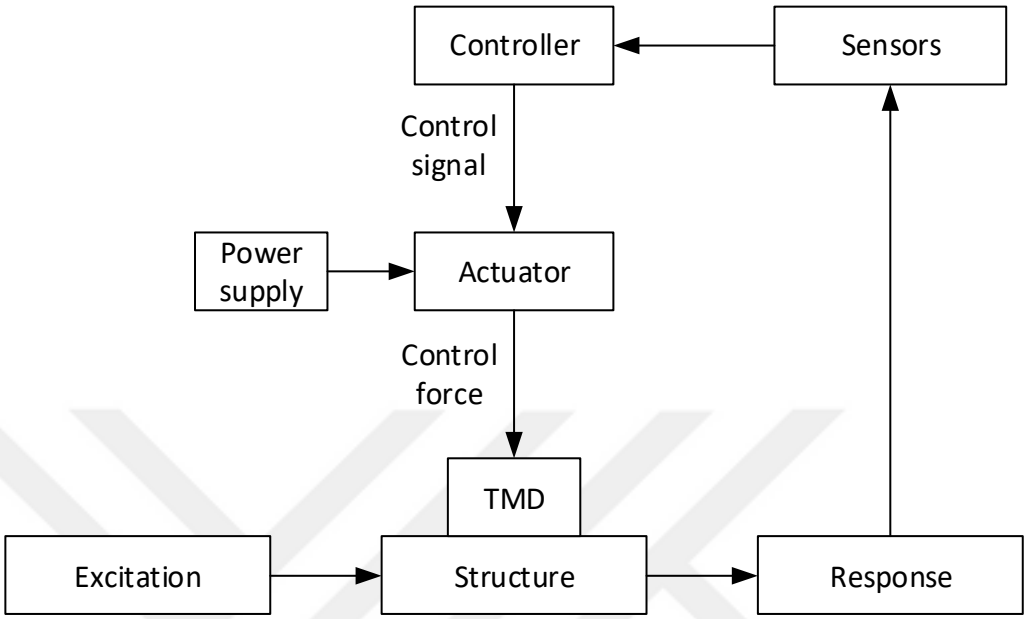

Figure 1.6 A schematic representation structure with the ATMD system

The first instance of active vibration control was a steamboat, which dates back to the beginning of the 20th century (Mallock, 1905). The vibrations of the twin-engine steamship's engines are reduced by operating at the same speed but in opposite phases (Dench et al., 2013; Tokhi et al., 2002). Until the middle of the 20th century, maritime has been leading the active vibration damping studies. Hort (1934) showed that an actively driven tank, in which water is pumped between tanks on both sides of the ship, reduces the rolling motion of the ships. Allan (1945) presented that the roll stabilization of ships is improved with the use of active fins.

The concept of controlling seismic vibrations in structures was first introduced by Japanese researchers Kobori and Minai in 1960. The conclusion of the studies: unless the earthquake motion can be predicted with precision, the vibration of the structure should be controlled through the building structure (Kobori & Minai, 1960). The idea of using active control strategies to dampen vibrations in structures started in the 1970s. Yao proposed a system whose behavior changes automatically in structures under the influence of unpredictable forces caused by external effects (Yao, 1972).

Thus, this system would be able to produce a response that would dampen structural vibration under all possible loading conditions (Cheng et al., 2008).

The full-scale implementation of ATMD systems was realized in 1989. The first full-scale ATMD system is installed in the 11-story Kyobashi Seiwa Building as shown in Figure 1.3 (Soong & Spencer, 2002). There are two ATMDs in the structure, one to suppress transverse vibrations and the other to suppress torsional vibrations. The first ATMD weighs four tons while the second ATMD weighs one ton. Some full-scale applications had to overcome large physical constraints. The most well-known example is the Nanjing Communications tower. The structural safe load carrying limits of the tower limited the tipper to 60 tons (Soong & Spencer, 2002). Due to the lack of sufficient movement space, the controller mass is supported by mechanical springs. In some structures, such as Ando Nishikicho, there are specially created systems called DUOX systems, where TMD and ATMD systems are used simultaneously. In this system, the ATMD system is placed on a conventional TMD system placed on the building. Some examples of full-scale ATMD systems used in buildings are shown chronologically in Table 1.3.

Tablo 1.3 Full-scale implementations of ATMD systems

Location	**Building**	**Year completed**	**Type of structure**	**Number of stories**	**Height**	**Controller type**
Tokyo, Japan	Kyobashi Seiwa Center	1989	Building	11	33 m	ATMD Weight = 5 t
Tokyo, Japan	Sendagaya INTES	1992	Building	11	58 m	ATMD Weight = 72 t
Osaka, Japan	Hankyu Chayamachi Building	1992	Building	-	34 m	ATMD
Osaka, Japan	Kansai International airport	1992	Tower	-	86 m	ATMD Weight = 10 t
Kobe, Japan	Rokko Island	1993	Building	36	117 m	ATMD Weight = 270 t

Table 1.3 Continues

Tokyo, Japan	C Office Tower	1993	Building	32	130 m	ATMD Weight = 200 t
Kanasawa, Japan	KS Project	1993	Tower	-	121 m	ATMD Weight = 100 t
Tokyo, Japan	MKD8 Hikarigaoka	1993	Building	30	100 m	ATMD
Tokyo, Japan	Riverside Sumida	1994	Building	33	133 m	ATMD Weight = 30 t
Tokyo, Japan	Shinjuku Park Tower	1994	Building	33	227 m	ATMD Weight = 330 t
Miyazaki, Japan	Hotel Ocean 45	1994	Building	43	-	ATMD
Hiroshima, Japan	RIHGA Royal Hotel	1994	Building	35	-	ATMD
Tokyo, Japan	Hikarigaoko City Building	1994	Building	46	-	ATMD
Osaka, Japan	Rinku Gate Tower	1995	Building	56	-	ATMD
Chiba, Japan	Otis Shibyama Test Tower	1998	Tower	39	-	ATMD
Nanjing, China	Nanjing Tower	1999	Tower	-	310 m	ATMD Weight = 60 t
Tokyo, Japan	Triton Square office complex	2001	Building	-	195 m	ATMD Weight =140 t
Shanghai, China	Shanghai World Financial Center	2008	Building	101	492 m	ATMD
Guangzhou, China	Canton Tower	2010	Tower	85	600 m	ATMD & TMD Weight = 50 t & 600 t

In (Dyke et al., 1996) acceleration-feedback approach was used as a controller of the ATMD system for reducing the response of the seismically excited three-story structure. In the mentioned study efficiency of the overall system was demonstrated via experimental results. The active mass control system was able to achieve an approximate 80 percent reduction in RMS acceleration responses, with a significant response reduction in all three modes of the system.

Adhikari et al., (1998) designed a sliding mode controller (SMC) for ATMD systems that reduce the vibration of a tall building and compare results with a linear quadratic gaussian (LQG) controller. In this study, wavelet analysis was used together with the model reduction method. Then, a study is carried out to eliminate the effects of neglected high modes on control performance. Mamat et al., (2020) designed an adaptive controller using SMC and fuzzy logic control. In Soleymani et al., (2018) a two-loop SMC in conjunction with a dynamic state predictor was used to produce the necessary control signal for an ATMD system. Integrated damage detection and semi-active control strategies based on semi-ATMD structure were presented by Karami et al., (2019). Fuzzy sliding mode control (Alli & Yakut, 2005; Thenozhi & Yu, 2013, 2014), Neural base sliding mode controller (Yakut & Alli, 2011), and optimal sliding mode controller (Khatibinia et al., 2020) have taken their place in ATMD control literature as other SMC methods.

The Proportional-integral-derivative (PID) controller is the most widely used controller for the ATMD system, it is often preferred in order to compare the controllers designed in the studies in the literature (Etedali et al., 2013, 2018; Etedali & Tavakoli, 2017; Kayabekir et al., 2020). The PID controller and SMC were other preferred methods to produce the control signal needed by the ATMD system (Guclu, 2006). Guclu & Yazici, (2008) designed a fuzzy logic controller for both the active base isolator and ATMD, and compared the performance of the controller to the PID controller to reduce the vibrations of a 15-story structure. Heidari et al., (2018), designed a hybrid controller for the ATMD control system which is used as a PID controller and a linear quadratic regulator (LQR) control algorithm.

Pourzeynali et al., (2007) designed the genetic algorithms and fuzzy logic based controller for ATMD systems on the 11-story structure. The proposed controller was compared with the linear quadratic regulator (LQR) control methods. Etedali & Tavakoli, (2017) designed optimized PD and PID controllers for an 11-story building structure. They compared the proposed controller with the LQR controller and simulated both controllers with four different earthquakes. As a result of their study, they claimed that LQR did not perform well in strong earthquakes, but optimized PD and PID control strategies were significantly successful. Akyürek & Suksawang, (2021) proposed a new active integrated control system using LQR to mitigate the torsional vibrations of buildings under bidirectional ground motions using ATMD systems.

Aly, (2014) proposed robust ATMD for reduced wind induced vibration on high rise structures. The performance of the proposed controller is increased by using LQG and fuzzy logic controllers. Shariatmadar & Razavi, (2014) combined fuzzy logic controller and particle swarm optimization to control the vibration of the 11-story structure. According to the study, the proposed controller reduced peak displacement of the top floor by about 30 percent compared with the fuzzy logic controller. Lavasani et al., (2020) designed two different types of fuzzy logic controllers with the Lion Pride Optimization algorithm to mitigate the vertical ground motion on the suspension bridge.

Palazzo & Petti, (1999) proposed H_2 and H_∞ control methods. Both methods were numerically compared to control the seismic response of a system equipped with ATMD and a base isolator. In (Huo et al., 2008), robust H_∞ control was applied for active structural vibration suppression using an ATMD. designed an H_∞ controller for ATMD systems, four of which are placed on the wind turbine blades. Each ATMD is individually driven by a velocity feedback control loop to dampen the vibration of the blades. In the study, decentralized controlled and centrally controlled ATMD systems were compared and it was concluded that they had similar performance values. Yazici et al., (2012) studied to design robust, state-feedback, delay-dependent H_∞ controller for ATMD systems to reduce structural vibration related to earthquakes. Li & Adeli,

(2016) designed new discrete-time robust H_2/H_∞control algorithm for vibration mitigation of structure with ATMD systems. This controller reduced the response of structure and overcome the parametric uncertainties of structure.

Chen et al., (2011) designed the LQG controller for the ATMD system for a real cable stayed bridge under construction. Collins et al., (2006) studied the control strategy on the bang-bang controller with the control force applied to the TMD to shape the frequency response function (FRF) of the structure. Block pulse functions were utilized as control signals of an ATMD system placed at the top of a ten-story building by Younespour & Ghaffarzadeh, (2015). Negative acceleration feedback control (Talib et al., 2019; D.-H. Yang et al., 2017) is another preferred control design on this subject in recent years. In addition to the aforementioned studies, ATMD systems were used together with various control algorithms. C. Li & Cao, (2019) used dynamic magnification factors of the structure with particle swarm optimization to design the ATMD system. C. Li & Cao, (2019b) used an Active tuned tandem mass damper to mitigate the seismic vibration.

There is limited usage of Lyapunov-based control designs with ATMD systems in this research area. Hacioglu & Yagiz, (2012) utilized an adaptive backstepping control to reach a similar purpose. In the mentioned structure, the vibration of a nine-story building exposed to an earthquake was tried to be damped via a Lyapunov-based adaptive control design based on the backstepping control approach. Xu et al., (2020) investigated the Lyapunov-based active vibration control for seismic excited adjacent buildings with ATMD systems. X. Chen et al., (2016) designed Lyapunov based semi-active controller for an adaptive base isolation system. The backstepping controller is more frequently employed in studies when MR dampers are used, even if there are few examples of it being used with ATMD systems to minimize structural vibration in the literature (S. F. Ali & Ramaswamy, 2009; Ouyang, Shi, et al., 2019; Shan et al., 2018; Zapateiro et al., 2009) and active base isolators (Ouyang, Shan, et al., 2019; Pozo et al., 2006) In some studies (Amini & Ghaderi, 2013; Ghaderi & Amini, 2017), earthquake-induced vibrations were dampened by applying force to the multiple floors of the building with actuators placed in another rigid structure with using the

backstepping controller. Xu et al., (2020) designed a Lyapunov based controller for two ATMDs. They were placed on top of the overall adjacent two buildings with viscoelastic dampers.

In addition to the studies where the stability of the structure is guaranteed with a Lyapunov-based control, with some special controller designs, stability can be guaranteed for large control gains as long as certain conditions are met. One of these control methods, α controller, was presented by Collette and Chesné. The α controller provides a great advantage in ATMD systems compared to Classic control methods. Collette & Chesné, (2016) proposed an α controller for mitigating resonant vibration amplitudes of the three DOF structure by using ATMD systems. The proposed controller structure is a revised version of the classic velocity feedback controller. Chesné & Collette, (2018) designed an α controller and experimentally controlled the vibration of SDOF structure with the ATMD system. Two poles and two zeros are added to the control law in order to prevent the structure from going into the unstable region at high control gain values. Paknejad et al., (2022) designed a resonant force feedback controller for active vibration damping of mechanical systems. This controller uses an α controller technique to dampen a target mode resonance and is based on a second-order low pass filter.

1.3 Research Aim and Objectives

In this thesis, the designed backstepping controller, linear regression based robust adaptive controller, and alfa controller for use with the ATMD system are discussed. The main purpose of the thesis is to design controllers for ATMD systems used to reduce vibrations caused by external effects such as earthquake and wind forces in multi-story buildings and to obtain a generalizable control design for these systems. Another important aim is to support generalized controllers designed for ATMD control systems with stability analyses to ensure system stability so that they can be used safely in any system with similar mathematical models.

The main contributions of the controllers designed within the scope of this thesis to the literature and the objectives of the thesis can be summarized as follows:

- To design a controller that can overcome parametric uncertainties with its adaptive structure and can be generalized for these types of systems contrary to its counterparts in this research area.

- To ensure the stability of the structure and the stability of the control mass, which has not been studied in the literature before, with a robust controller design while achieving the control purpose in ATMD systems.

- To design a controller that can overcome sensor precision problems owing to its structure that requires less measurement compared to its counterparts in this research area.

- To design a controller that can achieve the control purpose and maintain the stability of the structure in case of parametric uncertainty for multi-story nonlinear structures under the influence of earthquakes and nonlinear disturbances.

- To design a controller that limits the ATMD stroke within specified limits to prevent unexpected excessive movement of the controller mass while reducing structural vibration

1.4 Thesis Outline

Chapter 2 presents the robust adaptive controller design to dampen the vibration of a nine-story building where the ATMD system is used under earthquake effect. While achieving the control purpose, the stability of the structure is guaranteed by the Lyapunov-based stability analysis. In the controller design, a generalized robust design independent of structural parameters is obtained.

Chapter 3 presents the backstepping controller design to reduce the amplitude of vibration of an n-story structure using the ATMD system. Using Lyapunov-based arguments, theoretically, it has been proven that the designed controller can maintain the stability of the structure and controller mass while achieving this main control objective. The parametric uncertainty is coped with via adaptive compensation rules proposed in accordance with available system states. The designed controller has been tested with simulation studies for Kocaeli and El Centro earthquakes in a nine-story building.

Chapter 4 proposes a novel linear regression model based controller design for the ATMD systems. To achieve this goal, a control design that does not need any information about system parameters and is capable to provide the main control objective just by using states of the last floor as feedback information is implemented. As a result of the theoretical analysis based on Lyapunov-based arguments, it is mathematically proven that the system stability is guaranteed throughout the entire control process while achieving the main control objective. In this study, the designed controller is simulated on two different building models, one of which is nine-story and the other one is fifteen-story.

Chapter 5 details the dimensionless performance criteria chosen to test and compare controllers designed for ATMD systems in linear structures within the scope of this thesis. These criteria, which have been used in many publications in recent years, are used to compare and evaluate the response using the RMS and peak values of the acceleration and displacement measurements.

Chapter 6 presents the Lyapunov based controller for the ATMD system used in structures under the effect of unknown nonlinear disturbance effects. Nonlinear disturbance represents possible uncertain external effects such as measurement noise, unmodeled dynamics, etc. during control design to increase the efficiency of control designs.

Chapter 7 proposes the controller for mitigating the vibration of the nonlinear multi-story building which is reconstructed by adding nonlinear disturbance to represent unknown external effects. In order to obtain the robust structure of the controller, unknown structural parameters are compensated by using adaptive compensation terms. With the controller design supported by Lyapunov-based stability analysis, the stability of the structure is theoretically guaranteed while achieving the main control goal. Performance analyzes of the designed controllers are carried out with simulation studies.

Chapter 8 proposes a velocity feedback α controller design for ATMD systems using to reduce vibration of structures. With this control strategy, which is based on the natural frequency of the structure, it is possible to work with high control gains that conventional velocity feedback controls cannot reach. The proposed controller is powered by a nonlinear damping approach for ATMD stroke limitation.

Chapter 9 presents the general conclusions obtained for the controllers designed for ATMD systems in this thesis.

CHAPTER TWO
A ROBUST ADAPTIVE CONTROL DESIGN FOR ATMD SYSTEMS OF MULTI-STORY BUILDINGS

2.1 Introduction

In this chapter, a robust adaptive controller is designed to be used in an ATMD system that can be employed to mitigate undesired vibrations that occurred on the multi-story buildings during the earthquake. To realize the controller design, all of the system parameters are assumed to be unknown and the adaptive structure of the designed controller is obtained by designing adaptive compensation rules for system parameters. A backstepping control design approach is utilized for the control design by considering the appropriateness of the system's structure of multi-story buildings having an ATMD system at the top of the structure. The proposed control design is supported by a Lyapunov-based stability analysis where it is proven that the designed controller is able to protect the overall system's stability while reaching the main control purpose. In addition to these, in the simulation studies realized for a nine-story building under the effect of four major earthquakes, it is shown that the designed controller can be used to reach the main control purpose efficiently.

The investigations mentioned in the introduction chapter and the other studies about this subject are indicated that ATMD is generally combined with robust control strategies. The main reason for this choice is that the robust control strategy is one of the most feasible ways to cope with parametric uncertainties. In general, it has been considered that, even if the ATMD system is designed while the building is being constructed, it is not a realistic approach to design the control input of this system on the assumption that all of or some of the building parameters are perfectly known. Moreover, it should be possible to make this system available for buildings that have already been completed. In this case, it becomes more important to use the ATMD system with robust controller designs. However, guaranteeing the system's stability is one of the most critical parts of robust controller designs. However, since the control gains of these types of controllers are determined without knowing anything about the

system parameters, the overall system can easily be destabilized. Designing a controller for the ATMD system that cannot guarantee the overall system's stability during the control process may result in loss of life and property, and even demolition of the building. When this issue is considered it is a necessity to support the designed robust controller with a theoretical stability analysis that is able to guarantee the overall system's stability. In the literature, there are a few available studies where the robust control design is supported with this type of stability analysis and in some of these studies, control designs were based on the assumption that system parameters are partially known.

Designing a robust adaptive controller that meets the aforementioned requirements while damping the undesired vibrations of multi-story buildings under the effect of an earthquake when it is used in conjunction with the ATMD system is the main aim of this chapter. The designed controller is based on the assumption that all of the parameters of the building are uncertain. Owing to this approach, a general control design that can be used effectively for the ATMD system designed for multi-story buildings having different structures is obtained. The parametric uncertainties are coped with by designing adaptive compensation rules for unknown system parameters. The backstepping control approach is utilized by considering the appropriate structure of the controlled system for these types of control designs. The designed controller is supported by a Lyapunov-based stability analysis to prove that it is able to protect the stability of the overall system during the control process. The performance demonstration of the designed controller has been realized by using a Matlab-Simulink based simulation study.

2.2 Control Design and Analysis

In this section proposed control design and related stability analysis are based on a general model representation that is similar to the system model of multi-story buildings having an ATMD system at the top. Presenting a general control scheme that can be adapted to these types of buildings having different model structures is the main purpose of this choice. In the following section, the proposed control structure is

specified for a nine-story building that is preferred for the performance demonstration of the designed controller. According to the backstepping control approach, first, a virtual controller is designed and it is shown that the main control purpose can be reached when the designed virtual controller is substituted one of the system states. Then, the actual control input is designed to make the error between the virtual controller and the substituted system state zero. All of the mentioned procedure is given mathematically in a detailed manner in the following parts of this section.

The dynamic model of a system is given in the following form

$$x = \xi_n \tag{2.1}$$

$$\begin{aligned} p_1\ddot{\xi}_n = {} & p_2 f_1(\dot{\xi}_n, \dot{\xi}_{n-1}) + p_3 f_2(\dot{\xi}_{n+1}, \dot{\xi}_n) \\ & + p_4 f_3(\xi_n, \xi_{n-1}) + p_5 f_4(\xi_{n+1}, \xi_n) + u \end{aligned} \tag{2.2}$$

where $x, \xi_{n+1}, \xi_n, \xi_{n-1} \in \mathbb{R}$ and their first and second time derivatives denote the system states, n denotes degree-of-freedom of the system, $p_i \in \mathbb{R}$ for $i = 1, \dots, 5$ denote the constant system parameters, $f_j(\cdot) \in \mathbb{R}$ for $j = 1, \dots, 4$ denote the functions of system states whose gains are equal to ± 1 and $u \in \mathbb{R}$ denotes the control input. The given model provides the following properties.

Property 2.1. All of the system states are available.

Property 2.2. p_1 is a positive constant.

Property 2.3. Functions denoted by $f_j(\cdot)$ for $j = 1, \dots, 4$ are available owing to availability of system states.

Obtaining the result that guarantees zero convergence of x is the main purpose of the control design. The following auxiliary error is defined to help the mentioned aim

$$e \triangleq u_v - \dot{\xi}_n \tag{2.3}$$

where $u_v \in \mathbb{R}$ denotes the virtual control input. The system parameters denoted by p_i for $i = 1, \dots, 5$ are assumed to be completely unknown. Robust structure of the designed controller is provided via their adaptive compensations denoted by $\hat{p}_i \in \mathbb{R}$ and the additional auxiliary errors are defined as follows to show the difference between system parameters and their adaptive compensations

$$\tilde{p}_i \triangleq \hat{p}_i - p_i \text{ for } i = 1 \; to \; 5. \tag{2.4}$$

For the virtual controller design, the open-loop system can be obtained by taking the time derivative of Equation (2.1)

$$\dot{x} = \dot{\xi}_n. \tag{2.5}$$

After that point, the virtual controller is designed as follows to be substituted with $\dot{\xi}_n$

$$u_v = -g_1 x \tag{2.6}$$

where $g_1 \in \mathbb{R}^+$ denotes the positive constant control gain. The closed-loop system is obtained as follows when u_v is substituted with $\dot{\xi}_n$ in Equation (2.5)

$$\dot{x} = -g_1 x. \tag{2.7}$$

By using a Lyapunov-based preliminary analysis, it is possible to show that the designed virtual controller can be used to reach the control purpose. To show this result mathematically a nonnegative function denoted by $V_1(x) \in \mathbb{R}^+$ is defined as

$$V_1 \triangleq \frac{1}{2} x^2. \tag{2.8}$$

Time derivative of Equation (2.8) is obtained as

$$\dot{V}_1 = -g_1 x^2 \tag{2.9}$$

where Equation (2.7) is utilized. From Equation (2.8) and its time derivative in equation (9) it is clear that it is possible to obtain a semi-global asymptotic stability result for x in the sense that

$$x \to 0 \text{ as } t \to \infty \tag{2.10}$$

and the process needed to obtain Equation (2.10) can be shortened as desired with the appropriate selection of the control gain g_1. Since the validity of the aforementioned analysis is directly related with the $e \to 0$ condition, control input u must be designed to satisfy both of this condition and the main control purpose. The remaining part of the design and analysis is devoted to reach this result.

The open-loop system is obtained as follows when the time derivative of Equation (2.3) is pre-multiplied with p_1

$$p_1 \dot{e} = p_1 \dot{u}_v - p_2 f_1 - p_3 f_2 - p_4 f_3 - p_5 f_4 - u \tag{2.11}$$

where Equation (2.2) is utilized. The above equation can be rearranged as

$$\begin{aligned} p_1 \dot{e} = (\tilde{p}_1 - \hat{p}_1) g_1 \dot{\xi}_n + (\tilde{p}_2 - \hat{p}_2) f_1 + (\tilde{p}_3 - \hat{p}_3) f_2 \\ + (\tilde{p}_4 - \hat{p}_4) f_3 + (\tilde{p}_5 - \hat{p}_5) f_4 - u \end{aligned} \tag{2.12}$$

where Equations (2.4) and (2.5), time derivative of Equation (2.6) and Equation (2.7) are utilized. The control input is designed as

$$u = -\hat{p}_1 g_1 \dot{\xi}_n - \hat{p}_2 f_1 - \hat{p}_3 f_2 - \hat{p}_4 f_3 - \hat{p}_5 f_4 + g_2 e \tag{2.13}$$

where $g_2 \in \mathbb{R}^+$ is positive constant control gain. The closed-loop system is obtained as follows when Equation (2.13) is substituted in Equation (2.12)

$$p_1\dot{e} = \tilde{p}_1 g_1 \dot{\xi}_n + \tilde{p}_2 f_1 + \tilde{p}_3 f_2 + \tilde{p}_4 f_3 + \tilde{p}_5 f_4 - g_2 e. \tag{2.14}$$

Another Lyapunov-based stability analysis is used to show semi-global asymptotic stability both of x and e. The nonnegative Lyapunov function candidate $V(e, \tilde{p}_1, \tilde{p}_2, \tilde{p}_3, \tilde{p}_4, \tilde{p}_5) \in \mathbb{R}^+$ is defined as

$$V \triangleq V_1 + \frac{1}{2} p_1 e^2 + \frac{1}{2} \sum_{i=1}^{5} \tilde{p}_i^2. \tag{2.15}$$

Time derivative of Equation (2.15) is obtained in the following form when Equations (2.4), (2.9), and (2.14) are utilized

$$\begin{aligned} \dot{V} = -g_1 x^2 - g_2 e^2 + \tilde{p}_1\left(\dot{\tilde{p}}_1 + g_1 \dot{\xi}_n e\right) + \tilde{p}_2\left(\dot{\tilde{p}}_2 + f_1 e\right) \\ + \tilde{p}_3\left(\dot{\tilde{p}}_3 + f_2 e\right) + \tilde{p}_4\left(\dot{\tilde{p}}_4 + f_3 e\right) + \tilde{p}_5\left(\dot{\tilde{p}}_5 + f_4 e\right). \end{aligned} \tag{2.16}$$

From the above equation, it can be seen that the time derivative of the Lyapunov function candidate can be upper bounded as

$$\dot{V} \leq -\beta \|\mathbf{z}\|^2 \tag{2.17}$$

where $\mathbf{z} \in \mathbb{R}^2$ is a vector defined as

$$\mathbf{z} \triangleq [x \quad e]^T \tag{2.18}$$

and $\beta \in \mathbb{R}^+$ denotes a positive constant selected as

$$\beta = \min\{g_1, g_2\} \tag{2.19}$$

if adaptive compensations are updated according to following update rules

$$\dot{\hat{p}}_1 = -g_1 \dot{\xi}_n e \tag{2.20}$$

$$\dot{\hat{p}}_\ell = -f_{\ell-1} e \text{ for } \ell = 2, \dots, 5. \tag{2.21}$$

Remark 2.1. At this point, it should be noted that the above update rules are not designed to identify the exact numerical values of uncertain parameters. They are used to obtain finite numerical values that can be used to reach the main control purpose. Their numerical values can be ignored as long as they guarantee the semi-global asymptotic stability of x and e and change in a finite interval.

From Equation (2.15) and the bound of its time derivative Equation (2.17), it is seen that $\mathbf{z}(t) \in \mathcal{L}_\infty$. Boundedness of this term guarantees the boundedness of x and e. From its design in Equation (2.6), it is seen that boundedness of x guarantees the boundedness of u_v. Boundedness of the virtual control input can be utilized along with the boundedness of e and its definition in Equation (2.3) to show that $\dot{\xi}_n \in \mathcal{L}_\infty$. Boundedness of $\dot{\xi}_n$ is utilized along with Equation (2.1) and the time derivative of Equation (2.7) to show that $\ddot{\xi}_n \in \mathcal{L}_\infty$ and can be utilized with the time derivative of Equation (2.6) to show that $\dot{u}_v \in \mathcal{L}_\infty$. Boundedness of $\dot{u}_v$ and boundedness of $\ddot{\xi}_n$ can be used along with the time derivative of Equation (2.3) to show that $\dot{e} \in \mathcal{L}_\infty$. Boundedness of $\dot{\xi}_n$ and $\dot{e}$ guarantees the boundedness of $\dot{\mathbf{z}}(t)$**.** All of the remaining signals under the closed-loop operation can be shown via standard signal chasing arguments. To show that $\mathbf{z}(t) \in \mathcal{L}_2$, integration of Equation (2.17) that can be obtained as follows is utilized

$$\int_0^\infty \|\mathbf{z}(\sigma)\|^2 d\sigma \leq \frac{V(0)}{\beta}. \tag{2.22}$$

Boundedness of the time derivative of $\mathbf{z}(t)$ can be utilized along with $\mathbf{z}(t) \in \mathcal{L}_2 \cap \mathcal{L}_\infty$ and Barbalat's Lemma (Krstic et al., 1995) to prove semi-global asymptotic stability of $\mathbf{z}(t)$ that guarantees the main purpose of the control design mathematically expressed as

$$x, e \to 0 \text{ as } t \to \infty \tag{2.23}$$

2.3 Control Design for the ATMD System of a Nine-Story Building

The control design presented in the previous section is adapted for the ATMD system that is used for a nine-story building exposed to the earthquake in this section. By considering the completeness and clearness of the study at first the dynamic model of the building with an ATMD system on the top is introduced. Then, it is shown that how the control design presented in the previous section and the adaptive rules in Equations (2.20) and (2.21) can be adapted for this building.

The dynamic model of the nine-story building (Hacioglu & Yagiz, 2012) whose structure shown in Figure 2.1 is given as

$$m_n\ddot{y}_n + b_n(\dot{y}_n - \dot{y}_{n-1}) - b_{n+1}(\dot{y}_{n+1} - \dot{y}_n) + k_n(y_n - y_{n-1}) - k_{n+1}(y_{n+1} - y_n) = 0 \text{ for } n = 1, \dots, 8 \tag{2.24}$$

$$m_9\ddot{y}_9 + b_9(\dot{y}_9 - \dot{y}_8) - b_d(\dot{y}_{10} - \dot{y}_9) + k_9(y_9 - y_8) - k_d(y_{10} - y_9) = u_f \tag{2.25}$$

$$m_d\ddot{y}_{10} + b_d(\dot{y}_{10} - \dot{y}_9) + k_d(y_{10} - y_9) = -u_f \tag{2.26}$$

where m_j, k_j and $b_j \in \mathbb{R}$ for $j = 1, \dots, 9$ denotes mass, stiffness coefficients, and damping coefficient of j^{th} floor, respectively while $y_j \in \mathbb{R}$ represents the displacement of the j^{th} floor. At this point, it is noted that $\dot{y}_j$ and $\ddot{y}_j \in \mathbb{R}$ denotes velocity and acceleration of j^{th} floor, respectively. Mass, stiffness coefficient, and damping coefficient of the ATMD system placed on the top of the highest floor as it is shown in Figure 2.1 are denoted by m_d, k_d and $b_d \in \mathbb{R}$, respectively while the force applied to the ATMD system and the displacement of tuned mass caused by this force are denoted by u_f and $y_{10} \in \mathbb{R}$, respectively. Displacement and velocity of ground motion are represented by y_0 and $\dot{y}_0 \in \mathbb{R}$, respectively. The general control approach that is applied to these types of systems for reaching control purposes is given in the following remark.

Remark 2.2. In these types of structures, the highest floor is one of the floors where the highest impact of the earthquake is observed. By considering this fact and the rigidity of the building, it can be considered that damping the vibration of the highest floor is enough to dampen the vibration of all remaining floors. To reduce the vibration of the highest floor, the ATMD system is placed at the top of the building and it is provided that the applied input force is directly effective on this floor.

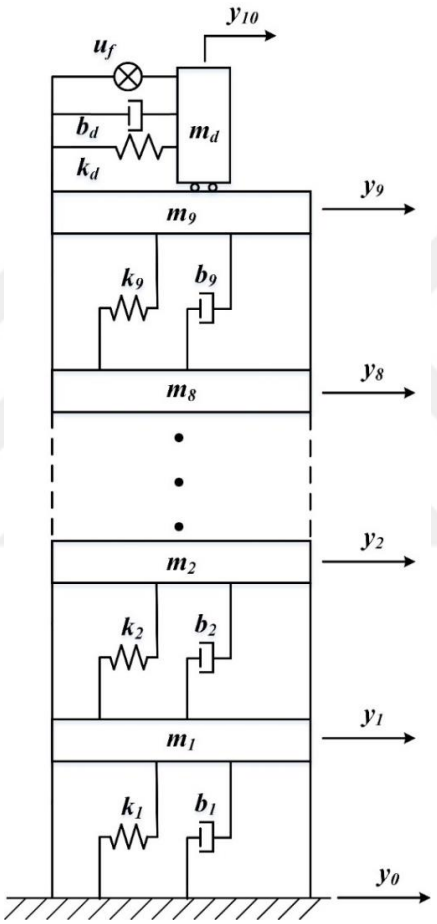

Figure 2.1 Nine-story building structure under earthquake excitation and controlled via ATMD system placed on the top

According to the dynamic model of the top floor of the building in Equation (2.25), the control design in Equation (2.13) can be adapted to this system as

$$u_f = \hat{m}_9 g_1 \dot{y}_9 + \hat{b}_9(\dot{y}_9 - \dot{y}_8) - \hat{b}_d(\dot{y}_{10} - \dot{y}_9) + \hat{k}_9(y_9 - y_8) - \hat{k}_d(y_{10} - y_9) + g_2 e \tag{2.27}$$

with the update rules of adaptive compensations of uncertain parameters given as

$$\dot{\hat{m}}_9 = -g_1 \dot{y}_9 e \tag{2.28}$$

$$\dot{\hat{b}}_9 = -(\dot{y}_9 - \dot{y}_8)e \tag{2.29}$$

$$\dot{\hat{k}}_9 = -(y_9 - y_8)e \tag{2.30}$$

$$\dot{\hat{b}}_d = -(\dot{y}_{10} - \dot{y}_9)e \tag{2.31}$$

$$\dot{\hat{k}}_d = -(y_{10} - y_9)e \tag{2.32}$$

2.4 Simulation Studies

For the simulation studies, the nine-story building whose numerical parameters are presented in Table 2.1 (Hacioglu & Yagiz, 2012) was used. This building is exposed to four strong earthquake records to show the efficiency of the method against earthquakes having different intensity and duration. Two pulse-like and two non-pulse-like records shown in Figure 2.2 were chosen to reach the mentioned aim (Kardoutsou et al., 2017). These earthquakes are Kocaeli Earthquake (1999, Yarimca station, closest distance to fault 4.83km), Kobe Earthquake (1995, Shin-Osaka station, closest distance to fault 19.15km), El Centro Earthquake (1940, CA - Array station 9, closest distance to fault 6.09 km), and Imperial Valley-06 Earthquake (1979, Aeropuerto Mexicali station, closest distance to fault 3.2km). For representing the external effects, measurement noise, and possible sensor precision problems, additive white Gaussian noise (AWGN) was added to all measurement values.

Table 2.1 Parameters of the nine-story building and the ATMD system

Parameter	Value $\times 10^3$ (kg)	Parameter	Value $\times 10^6$ (N/m)	Parameter	Value $\times 10^3$ (Ns/m)
m_1	450	k_1	18.05	b_1	26.17
m_2	345	k_2	340	b_2	490
m_3	345	k_3	326	b_3	467
m_4	345	k_4	285	b_4	410
m_5	345	k_5	269	b_5	386
m_6	345	k_6	243	b_6	348

Table 2.1 Continues

m_7	345	k_7	207	b_7	298
m_8	345	k_8	169	b_8	243
m_9	345	k_9	137	b_9	196
m_d	69	k_d	0.3365	b_d	152.39

Remark 2.3. At this point, it should be noted that the numerical parameters in Table 2.1 were just used in simulation studies. They were not utilized in the robust adaptive control design.

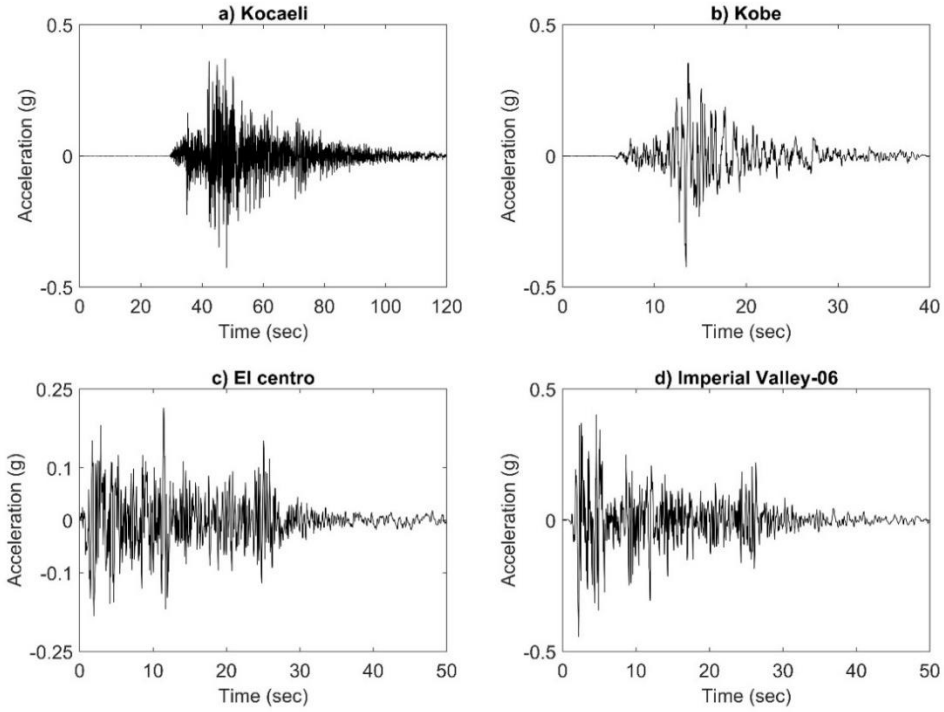

Figure 2.2 Acceleration of earthquakes a) Kocaeli, b) Kobe, c) El Centro, d) Imperial Valley-06

2.4.1 Simulation Studies for ATMD System with Backstepping Controller

The control design in Equation (2.27) was applied from the actuator input and the control gains were selected as follows via trial and error method

$$g_1 = 410, g_2 = 3520 \tag{2.33}$$

Figure 2.3 represents the vibration of the top floor for three cases which are uncontrolled system (i.e., there is no effective system on the building), the tuned mass damper (TMD) system (i.e., there is no actuator input for the tuned mass damper system) and the active tuned mass damper (ATMD) system in which the designed robust backstepping controller was used. Although the TMD system provided better results compared to the uncontrolled system, vibration amplitudes were quite high compared to ATMD. With the used adaptive backstepping controller, the ATMD system appeared to significantly reduce the vibration of the last floor of the structure. With this controller, it absorbed the earthquake-induced vibrations of the building in a short time.

The applied control forces to the auxiliary mass to reach the control purpose which is another important parameter in ATMD control approaches are shown in Figure 2.4. As seen in this figure, the control purpose is reached with a reasonable control force for all earthquakes.

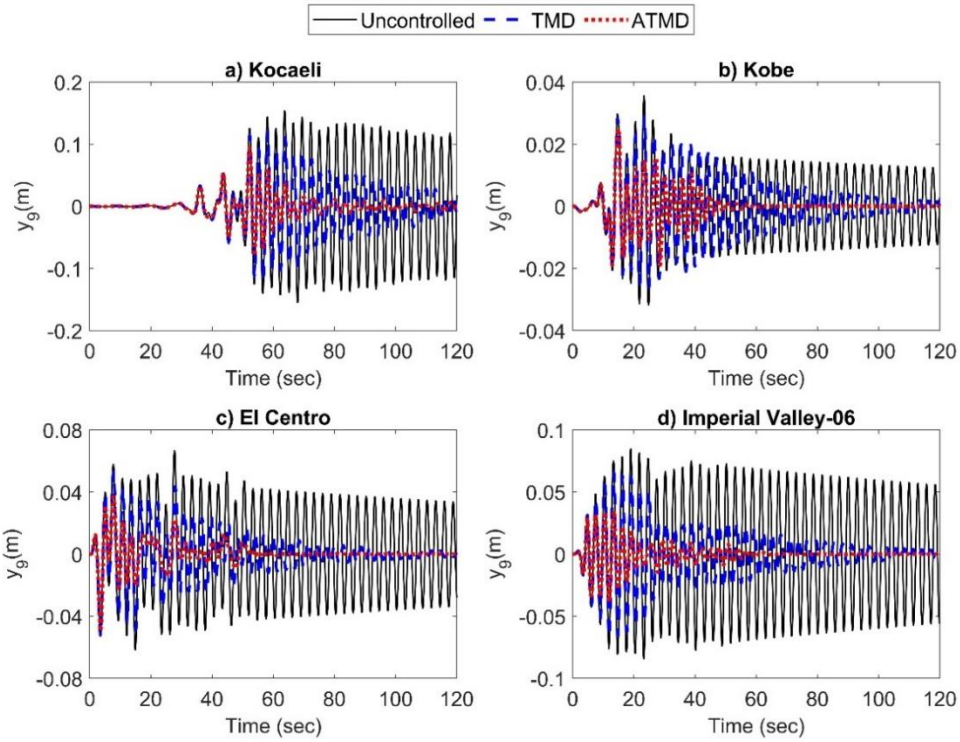

Figure 2.3 Displacements of the top floor of the building during the four different earthquakes

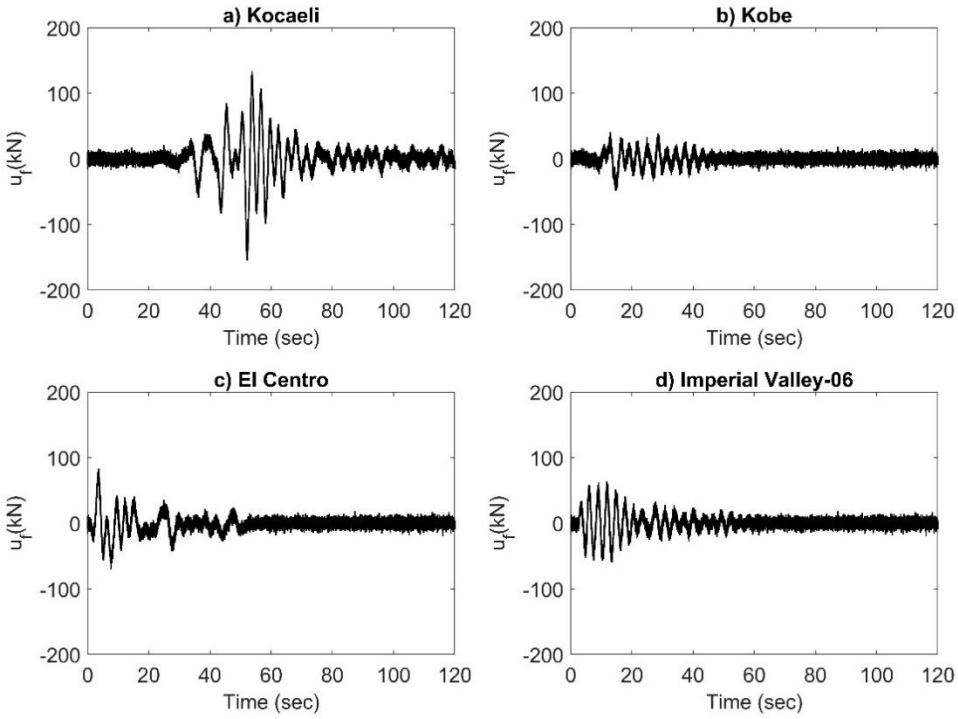

Figure 2.4 Control forces

The efficiency of ATMD system on damping the undesired vibrations of the building floors can be seen from the maximum and root-mean-squared values of their displacements presented in Figures 2.5 and 2.6, respectively. From these figures, it can be seen that TMD is effective in damping external vibrations as earthquakes in such structures. However, as seen in Figures 2.5 and 2.6, the best performance in the meaning of damping the vibration is ensured via ATMD system.

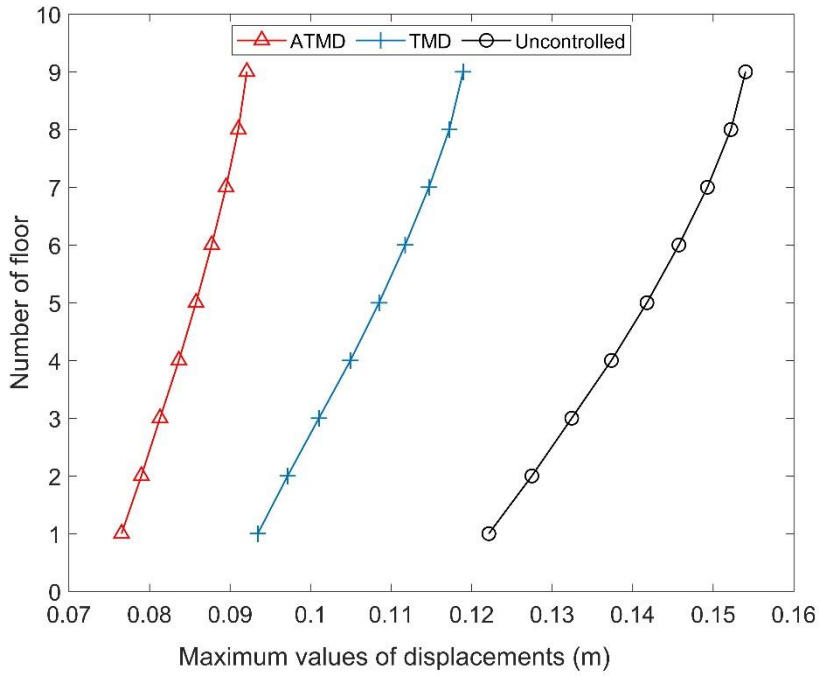

Figure 2.5 Maximum displacements of the floors

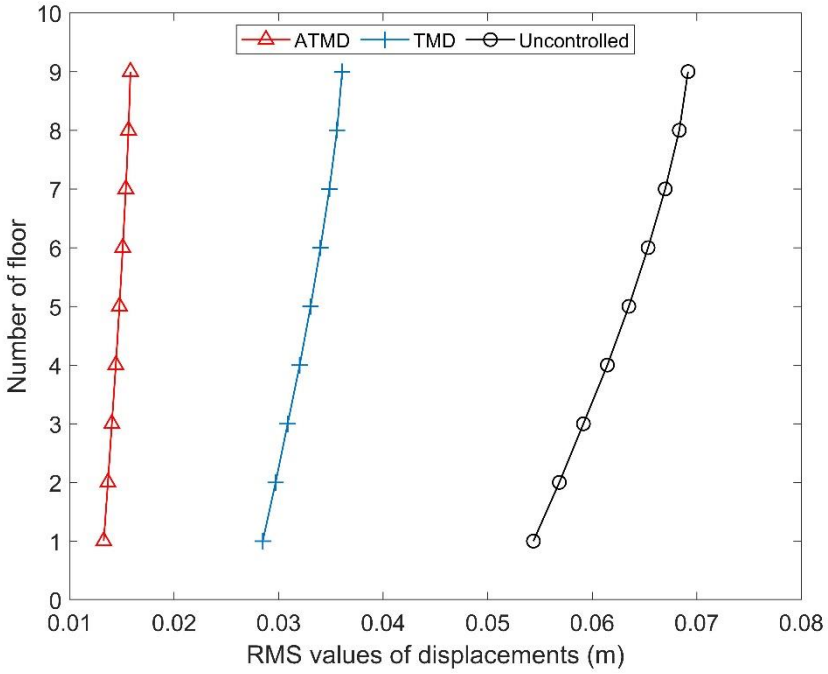

Figure 2.6 RMS values of the displacements of the floors

Figure 2.7 demonstrates the adaptive compensations of the uncertain parameters for four different earthquakes. Figure 2.7(a), 2.7(b), 2.7(c), 2.7(d) and 2.7(e) show

$\hat{k}_9, \hat{b}_9, \hat{m}_9, \hat{k}_d$ and $\hat{b}_d$, respectively. As previously mentioned in Remark 1; the compensation parameters are used to achieve the control purpose. Their numerical values are insignificant providing that changing in a finite interval. From this figure, it is seen that they change in a finite interval while the control purpose is reached.

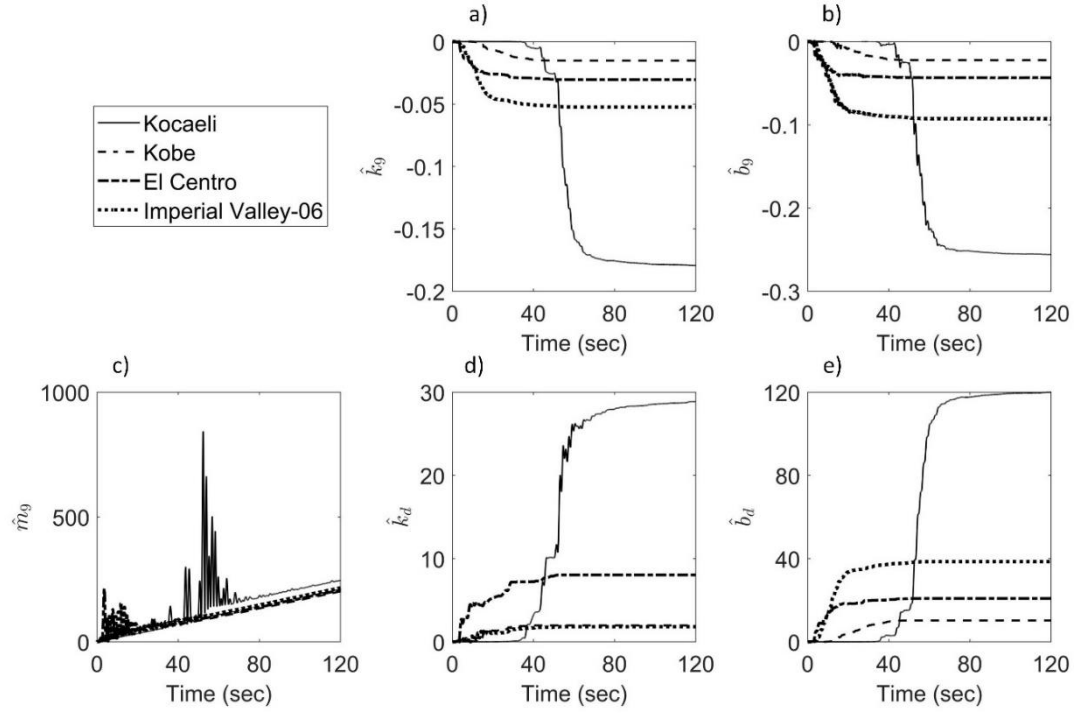

Figure 2.7 Adaptive compensations of uncertain parameters

2.4.2 Comparative Simulation Studies

The performance of the designed controller is compared with its robust counterpart. PID controller is preferred for comparison purposes. Its commonly used in these types of systems is the main reason for this choice. The proportional (P), integral (I) and derivative (D) control gains of the PID controller are selected as follows by trial and error method until the displacement response of the controller designed in this chapter is obtained. In order to achieve this, the areas under the last story displacement result were taken into account.

$$P = 1000000, I = 1000, D = 950 \tag{2.34}$$

The displacement of the top floor, one of the most important performance outputs of the backstepping and PID controllers, is shown in Figure 2.8.

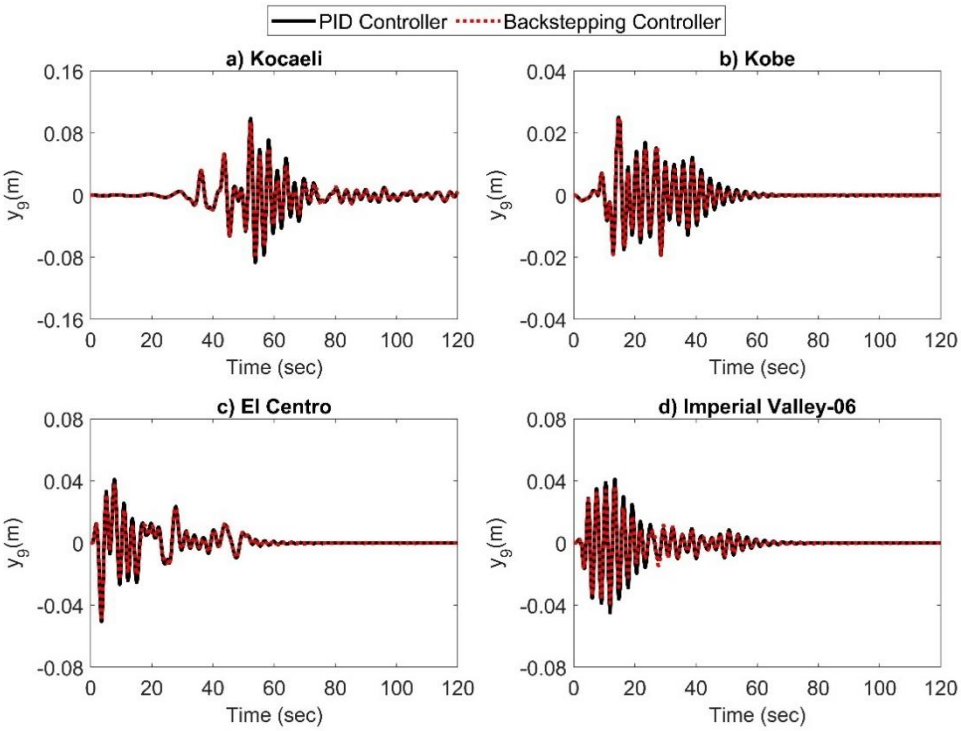

Figure 2.8 Displacements of top floor for backstepping controller and PID controller

Displacement of the tuned mass and the control force needed to reach the control purpose are shown in Figures 2.9 and 2.10, respectively. From Figures 2.8, 2.9 and 2.10 it can be observed that the PID controller needed much more control force than the designed controller to show the similar performance in terms of vibration damping. This result is important since it is a significant part of actuator selection. It shows that in the presence of measurement noise and possible sensor precision problems, the control purpose can be reached by using a smaller capacity actuator.

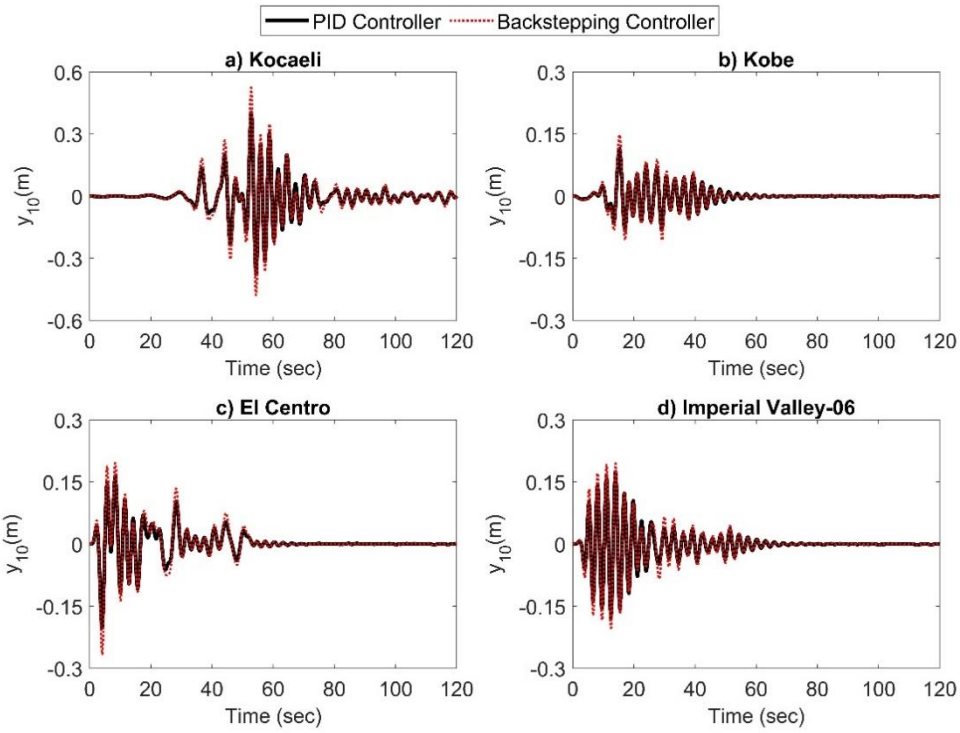

Figure 2.9 Displacement of the tuned mass for backstepping controller and PID controller

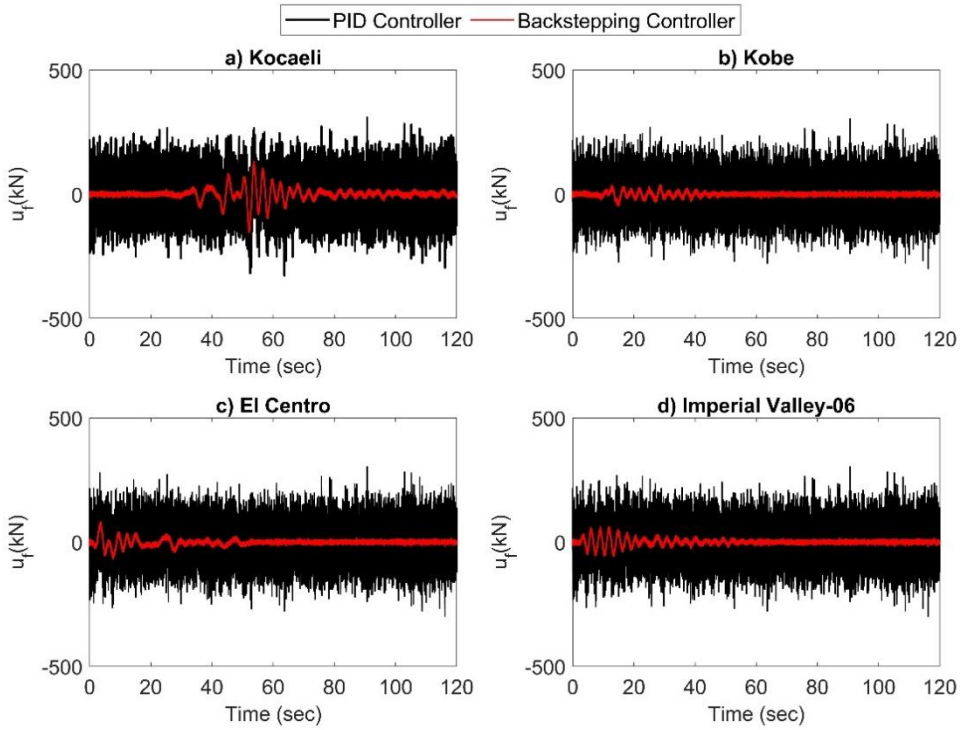

Figure 2.10 Control forces for backstepping controller and PID controller

2.5 Conclusions

In this chapter, a novel robust adaptive controller is designed to use in ATMD systems of multi-story buildings. The control design is based on the backstepping control approach and its theoretical proof was done via Lyapunov-based arguments. Owing to the Lyapunov-based stability analysis presented in the study, it is theoretically guaranteed that the designed controller can protect the system's stability while reaching the main control purpose as long as the constant control gains are selected as positive numerical values. When the importance of this subject in using ATMD systems is considered, this fact can be considered as one of the most advantageous aspects of the designed controller. Owing to the robust structure of the designed controller and adaptive compensation rules proposed in the study, a general controller structure that can be used in ATMD systems of multi-story buildings having different structures is obtained. This situation can be considered as another important development of this study. Finally, the performance demonstration of the designed controller is realized via numerical simulation results. In these results, the effectiveness of the designed controller in terms of damping the undesired vibrations occurred on the building is demonstrated. Comparative simulation studies are also conducted and presented. From these results, it can be seen that the designed controller reaches the control aim by needing much less control effort than its commonly preferred robust counterpart.

CHAPTER THREE
A BACKSTEPPING CONTROLLER DESIGN WITH STABILITY ANALYSIS FOR THE STRUCTURE AND ATMD SYSTEM

3.1 Introduction

Control strategies just dependent on the availability of system states are commonly preferred for the control design of ATMD systems. The capability of these types of controllers in terms of coping with parametric uncertainty may be considered as the main reason of this choice. Even where the controller is designed in building construction, it should be kept in mind that it is not a realistic approach to know all or some of the building parameters with certain accuracy and to use these parameters while designing the control system. Moreover, the control system to be designed should be available not only for a single building but also for buildings that have already been completed. Considering the mentioned situations, it is seen that a system parameters free control design is suitable for this type of system. In studies where system parameters are not known in the literature, unknown system parameters are often estimated by system identification methods (Concha et al., 2016; Ghaderi & Amini, 2020). However, the structure created in this chapter is completely different from this, and is based on compensating for unknown system parameters. In Chapter Two only controlled the vibration of the structure and have not to deal with the vibration of the controller mass as in the other studies in the literature. However, considering that it is important to control the vibration of the controller mass, this study was conducted, unlike similar studies in the literature and previous chapter by the authors. Designing a controller that cannot guarantee the stability of the system for ATMD system may cause resonation and this situation may be more harmful than the earthquake. Considering this problem, it must be theoretically guaranteed that the designed controller can provide the zero convergence of all displacements on which the actuator is effective and assure the overall system's stability for all of the control process. In addition to these, even if the control gains are adjusted properly control effort necessity of control designs where all system parameters are assumed to be uncertain may be quite high since they work according to the worst-case scenario

without using any information about the system. When the structure of a multi-story building with ATMD system is analyzed it is observed that the actuator input is both effective on the displacement of controller mass and the displacement of the last floor. The reverse force utilized to damp the undesired vibrations is produced by moving ATMD system and at the end of the process vibration of the building is eliminated by eliminating the vibration of the top floor via this force. However, during this process vibration of ATMD system must remain within a reasonable interval and it must converge to zero as the vibration of the building is damped. Otherwise, the controller mass, whose stability is not guaranteed, may be the source of the vibration in the structure after a certain point. Because of this situation, the effect of the single actuator input onto the displacement of ATMD system and the displacement of the top floor should be considered together. This necessity makes the control problem a little bit harder since it converges the overall system to a system where more than one occurred vibrations are tried to be damped via single actuator input. There is no available system in the literature where all of the aforementioned situations were considered during the control design and proven theoretically.

The main purpose of this chapter is to design a controller that can provide the aforementioned control purposes without using the knowledge of system parameters but their compensation terms proposed in accordance with the available system states overcome all the problems mentioned above when used as the actuator of the ATMD system placed on the last floor of multi-story buildings. The motivation for this approach is that controllers equipped with this type of compensation rules require much less control effort than conventional system parameter independent controller designs, as has been proven many times in the control literature for the control of different systems. Considering its suitability to such ATMD systems, the backstepping control approach is used to design the controller. The theoretical part of the design is supported via Lyapunov-based arguments to prove that the designed controller is able to provide the zero convergence of all necessary displacements and maintain the stability of the overall system while the control process. The numerical simulation of the designed controller is carried out using Matlab / Simulink with simulation studies performed on a nine-story building model exposed to a strong earthquake.

3.2 System Model and Properties

In this section system model and properties utilized to propose the presented controller are presented in a detailed manner. In the first subsection, system properties and the system states that are available for the control design are given. At this point it should be stated that these properties are not restrictive assumptions, they are properties valid for all multi story buildings. Then, the dynamic model of the multi story building is presented as a separate subsection.

3.2.1 System Properties

The following properties are valid for the n-story building shown in Figure 3.1;

Property 3.1. This manuscript considers a linear multi story one-dimensional shear building model equipped with viscous dampers.

Property 3.2. Geometrical nonlinearities are not considered in the system model.

Property 3.3. Displacement of the mass placed at the top of the building, displacement of the top floor, and displacement of the floor under the top floor are denoted by y_d, y_n and $y_{n-1} \in \mathbb{R}$, respectively and their time derivative denoted by $\dot{y}_d$, $\dot{y}_n$ and $\dot{y}_{n-1} \in \mathbb{R}$, respectively are measurable.

3.2.2 System Model

The dynamic model of the n-story building shown in Figure 3.1; is given as (Hacioglu & Yagiz, 2012; Ümütlü et al., 2021)

$$m_i\ddot{y}_i + b_i(\dot{y}_i - \dot{y}_{i-1}) - b_{i+1}(\dot{y}_{i+1} - \dot{y}_i) + k_i(y_i - y_{i-1}) - k_{i+1}(y_{i+1} - y_i) = 0 \text{ for } i = 1, \dots, n-1 \quad (3.1)$$

$$m_n\ddot{y}_n + b_n(\dot{y}_n - \dot{y}_{n-1}) - b_d(\dot{y}_d - \dot{y}_n) + k_n(y_n - y_{n-1}) - k_d(y_d - y_n) = u_f \quad (3.2)$$

$$m_d\ddot{y}_d + b_d(\dot{y}_d - \dot{y}_n) + k_d(y_d - y_n) = -u_f \tag{3.3}$$

where $m_j \in \mathbb{R}$ represents mass coefficient, $k_j \in \mathbb{R}$ represents stiffness coefficient and $b_j \in \mathbb{R}$ represents the damping coefficient for the floor number given as $j = 1, \dots, n$. j^{th} floor's displacement is represented by $y_j \in \mathbb{R}$ and first and second-time derivatives of the displacement represent the related floor's velocity and acceleration. As in Figure 3.1, ATMD system has a tuned movable mass whose movement is provided via force input represented by $u_f \in \mathbb{R}$. As a result of the common effect of spring and damping elements and the applied force the mentioned mass moves in the horizontal axis and this movement is represented via displacement denoted by $y_d \in \mathbb{R}$. Mathematical expression of this movement is given with the help of mass coefficient $m_d \in \mathbb{R}$, stiffness coefficient $k_d \in \mathbb{R}$ and damping coefficient $b_d \in \mathbb{R}$ in the above model. The earthquake induced ground motion is denoted by $y_0 \in \mathbb{R}$ while its first time derivative represents the ground motion's velocity.

As it can be seen from Equation (3.2) and Equation (3.3), the input force applied from the actuator input is effective onto the displacements of ATMD system and the top floor. Multi-story buildings tend to oscillate according to the first mode shape(Rana & Soong, 1998). Damping the vibration of the last floor during an earthquake is seen as the main necessity to mitigate the vibration of the building in these types of applications. Considering these issues, the following combined system model where the effect of the control force onto the displacements of ATMD system and the top floor can be represented together can be obtained by utilizing Equation (3.2) and Equation (3.3)

$$\mathbf{P_1}\ddot{\mathbf{y}}_\mathbf{c} + \mathbf{P_2}\mathbf{f_1} + \mathbf{P_3}\mathbf{f_2} = \mathbf{g}u_f \tag{3.4}$$

$$\mathbf{x} = \mathbf{y_c} \tag{3.5}$$

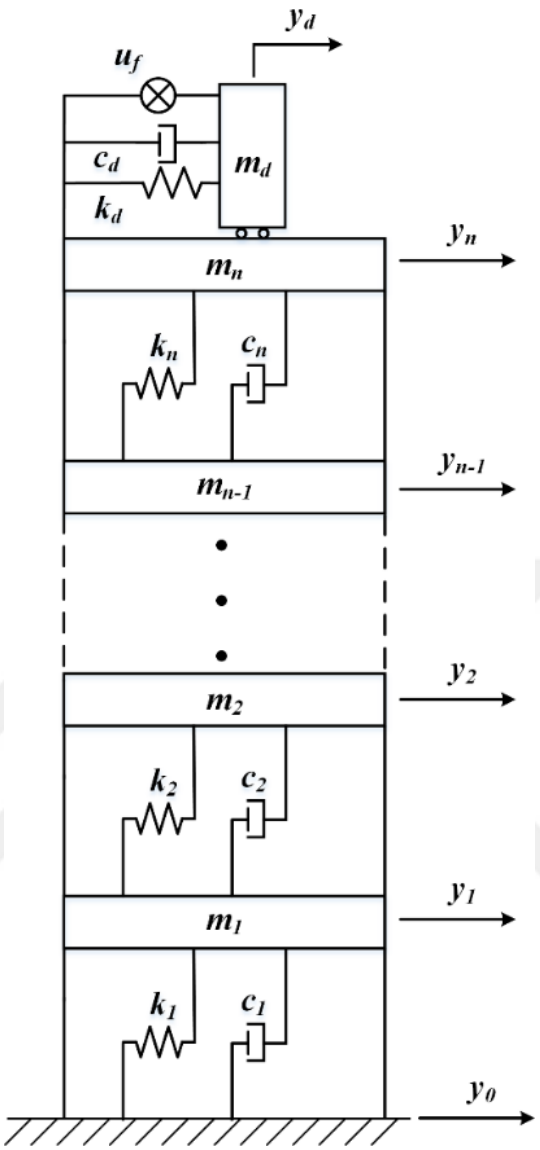

Figure 3.1 Model of Multi-story building structure with ATMD system

where $\mathbf{y_c} \triangleq [y_n \quad y_d]^{\mathrm{T}} \in \mathbb{R}^2$ denotes the vector of system states while function vectors of measurable system states having unity gains are denoted by and defined as $\mathbf{f_1} \triangleq [\dot{y}_n - \dot{y}_{n-1} \quad \dot{y}_d - \dot{y}_n]^{\mathrm{T}}$, $\mathbf{f_2} \triangleq [y_n - y_{n-1} \quad y_d - y_n]^{\mathrm{T}} \in \mathbb{R}^2$. $\mathbf{P_1}$, $\mathbf{P_2}$ and $\mathbf{P_3} \in \mathbb{R}^{\mathbf{2\times 2}}$ are the matrices of constant system parameters and defined as $\mathbf{P_1} \triangleq \begin{bmatrix} m_n & 0 \\ 0 & m_d \end{bmatrix}$, $\mathbf{P_2} \triangleq \begin{bmatrix} b_n & -b_d \\ 0 & b_d \end{bmatrix}$, $\mathbf{P_3} \triangleq \begin{bmatrix} k_n & k_d \\ 0 & k_d \end{bmatrix}$ and $\mathbf{g} \triangleq [1 \quad -1]^T \in \mathbb{R}^2$ denotes the constant input gain vector. The control input is denoted by $u \in \mathbb{R}$ and the following properties are ensured for the given system.

Property 3.4. Since the system states $\dot{y}_d, \dot{y}_n, \dot{y}_{n-1}, y_d, y_n$ and y_{n-1} are measurable states, the f_1 and f_2 vectors consisting of these states are available.

Property 3.5. Because of the uncertainty of system parameters P_1, P_2 and P_3 are uncertain matrices. Owing to the structure of the controller system input gain vector g is known and can be used in the control design.

Remark 3.1. The control design proposed and presented in this chapter is based on the backstepping control design approach and generally, this approach is developed to deal with the systems in a strict-feedback form. Although, it seems in a slightly different form the system model is given in Equation (3.4) and Equation (3.5) is a modified form of the strict-feedback form that can be given as

$$\dot{\mathbf{x}} = \dot{\mathbf{y}}_\mathbf{c} \tag{3.6}$$

$$\ddot{\mathbf{y}}_\mathbf{c} = \mathbf{f_{sb}}(\mathbf{x}, \dot{\mathbf{y}}_\mathbf{c}, t) + \mathbf{G}u_f \tag{3.7}$$

where $\mathbf{f_{sb}}(\mathbf{x}, \dot{\mathbf{y}}_\mathbf{c}, t) \triangleq -\mathbf{P_1^{-1}}(\mathbf{P_2 f_1} + \mathbf{P_3 f_2})$ and $\mathbf{G} = \mathbf{P_1^{-1}g}$. However, this model is given in the form of Equation (3.4) and Equation (3.5) by considering its suitability for the presentation of the control design and analysis procedure proposed in the following section.

3.3 Backstepping Control System Design

In this section, the design procedure of the control input that is able to dampen the vibration of the displacements of the ATMD system and the top floor while protecting the stability of the overall system is introduced. The backstepping control approach is utilized to reach this purpose. Firstly, the virtual control input is designed and it is proven that achieving the primary control aim is possible when this design is replaced with one of the system states. The actual control input design is presented after this design and it is shown that this design makes the auxiliary error zero that is defined as the difference between the virtual control input and the state in which virtual control input is used instead of it.

The auxiliary error $\mathbf{e} \in \mathbb{R}^2$ is defined as

$$\mathbf{e} \triangleq \mathbf{u_v} - \dot{\boldsymbol{y}}_{\boldsymbol{c}} \tag{3.8}$$

where the virtual control input is represented by $\mathbf{u_v} \in \mathbb{R}^{\mathbf{2}}$. The parametric uncertainty is coped with via adaptive compensations of matrices of uncertain system parameters. The adaptive compensation errors of ℓ^{th} column of the matrices of uncertain system parameters $\mathbf{P_1}$, $\mathbf{P_2}$ and $\mathbf{P_3}$ are defined as

$$\tilde{\mathbf{p}}_{\mathbf{k}\boldsymbol{\ell}} \triangleq \hat{\mathbf{p}}_{\boldsymbol{k}\boldsymbol{\ell}} - \mathbf{p}_{\mathbf{k}\boldsymbol{\ell}} \text{ for } k = 1,2,3 \text{ and } \ell = 1,2 \tag{3.9}$$

and these uncertain matrices are adaptively compensated as

$$\hat{\mathbf{P}}_{\mathbf{k}} = [\hat{\mathbf{p}}_{\boldsymbol{k1}} \quad \hat{\mathbf{p}}_{\boldsymbol{k2}}] \text{ for } k = 1,2,3 \tag{3.10}$$

while matrices of adaptive compensation errors are defined as

$$\tilde{\mathbf{P}}_{\mathbf{k}} \triangleq [\tilde{\mathbf{p}}_{\mathbf{k1}} \quad \tilde{\mathbf{p}}_{\mathbf{k2}}] \text{ for } k = 1,2,3. \tag{3.11}$$

The open-loop error system of the virtual control design is given as

$$\dot{\mathbf{x}} = \dot{\mathbf{y}}_{\mathbf{c}} \tag{3.12}$$

by utilizing the first time derivative of Equation (3.5).

The virtual control input is designed as

$$\mathbf{u_v} = -\mathbf{G_1 x} \tag{3.13}$$

where $\mathbf{G_1} \in \mathbb{R}^{2\times 2}$ denotes positive definite, constant, and diagonal gain matrix. The closed-loop error system of this part can be obtained as follows by substituting the designed virtual control input with $\dot{\mathbf{y}}_\mathbf{c}$ in Equation (3.12)

$$\dot{\mathbf{x}} = -\mathbf{G_1}\mathbf{x} \tag{3.14}$$

The analysis of the above closed-loop error system is realized via Lyapunov-based arguments. The nonnegative Lyapunov-like function is selected as

$$V_1 \triangleq \frac{1}{2}\mathbf{x}^T\mathbf{x}. \tag{3.15}$$

and its time derivative is taken as follows by utilizing Equation (3.14)

$$\dot{V}_1 = -\mathbf{x}^T\mathbf{G_1}\mathbf{x}. \tag{3.16}$$

According to the Lyapunov stability theorem(Khalil, 2010), semi-global asymptotic stability is provided with the Lyapunov function is non-negative and the time derivative of the Lyapunov function is non-positive. From Equation (3.15) and Equation (3.16) it can be shown that a semi-global asymptotic stability of $\mathbf{x}$ that can mathematically be expressed as

$$\|\mathbf{x}\| \to 0 \text{ as } t \to \infty \tag{3.17}$$

In other words, the given virtual control design is sufficient to reach the control purpose if the zero convergence of an auxiliary error in Equation (3.8) is guaranteed. The subsequent part of the study is proposed for reaching this purpose.

By pre-multiplying the time derivative of Equation (3.8) with $\mathbf{P_1}$ and by utilizing Equation (3.4), Equation (3.11), and the time derivative of Equation (3.13), the open-loop error system of the actual control design is obtained as

$$\mathbf{P_1\dot{e}} = -\left(\widehat{\mathbf{P}}_\mathbf{1} - \widetilde{\mathbf{P}}_\mathbf{1}\right)\mathbf{G_1\dot{y}_C} + \left(\widehat{\mathbf{P}}_\mathbf{2} - \widetilde{\mathbf{P}}_\mathbf{2}\right)\mathbf{f_1} + \left(\widehat{\mathbf{P}}_\mathbf{3} - \widetilde{\mathbf{P}}_\mathbf{3}\right)\mathbf{f_2} - \mathbf{g}u_f \tag{3.18}$$

The following design is proposed as an actual controller

$$u_f = (\mathbf{g^T g})^{-1}\mathbf{g^T}(-\widehat{\mathbf{P}}_\mathbf{1}\mathbf{G_1\dot{y}_c} + \widehat{\mathbf{P}}_\mathbf{2}\mathbf{f_1} + \widehat{\mathbf{P}}_\mathbf{3}\mathbf{f_2} + \mathbf{G_2 e}) \tag{3.19}$$

where $\mathbf{G_2} \in \mathbb{R}^{2\times 2}$ denotes positive definite, constant, and diagonal control gain matrix.

*Remark 3.2***.** As it can be seen from the structure in Figure 3.1 and dynamic model in Equation (3.1) - Equation (3.5) and the control design in Equation (3.19), the single actuator input is used for damping the vibrations on the mass of ATMD system and the top floor simultaneously. According to the authors' best knowledge in all available studies about this subject, the effect of the actuator input on the vibration of the mass of ATMD system was ignored and it was considered that the control system has a single input and single output (i.e., vibration occurred at the top floor). However, for using the designed control in applications without any doubt it should be guaranteed that undesired vibrations that occurred in the mass of ATMD system should also be damped during the control process. By considering this issue, the main motivation is considered as damping the vibrations on the mass of ATMD system and the top floor simultaneously, the controller is designed in Equation (3.19) by considering this motivation and in the subsequent stability analysis, it is mathematically proven that the overall system stability can be protected while both of the mentioned vibrations are damped.

The closed-loop error system can be obtained as follows by substituting the above control design in Equation (3.18)

$$\mathbf{P_1\dot{e}} = -\mathbf{G_2 e} + \widetilde{\mathbf{P}}_\mathbf{1}\mathbf{G_1\dot{y}_c} - \widetilde{\mathbf{P}}_\mathbf{2}\mathbf{f_1} - \widetilde{\mathbf{P}}_\mathbf{3}\mathbf{f_2} \tag{3.20}$$

After that point, the analysis where Lyapunov-based arguments are utilized is conducted to obtain a semi-global asymptotic convergence of $\mathbf{x}$ and $\mathbf{e}$. The following nonnegative Lyapunov function selection is utilized for showing this result

$$V \triangleq V_1 + \frac{1}{2}\left(\mathbf{e}^T\mathbf{P_1}\mathbf{e} + \sum_{\mathbf{k=1}}^{\mathbf{3}}\sum_{\boldsymbol{\ell}\mathbf{=1}}^{\mathbf{2}} \tilde{\mathbf{p}}_{\boldsymbol{kl}}^{\boldsymbol{T}}\tilde{\mathbf{p}}_{k\ell}\right) \tag{3.21}$$

The time derivative of the above function is obtained as

$$\begin{aligned}\dot{V} = &-\mathbf{x}^T\mathbf{G_1}\mathbf{x} - \mathbf{e}^T\mathbf{G_2}\mathbf{e} + \tilde{\mathbf{p}}_{\mathbf{11}}^{\boldsymbol{T}}\left(\dot{\hat{\mathbf{p}}}_{\mathbf{11}} + G_{11}\dot{y}_n\mathbf{e}\right) \\ &+ \tilde{\mathbf{p}}_{\mathbf{12}}^{\boldsymbol{T}}\left(\dot{\hat{\mathbf{p}}}_{\mathbf{12}} + G_{12}\dot{y}_d\mathbf{e}\right) \\ &+\tilde{\mathbf{p}}_{\mathbf{21}}^{\boldsymbol{T}}[\dot{\hat{\mathbf{p}}}_{\mathbf{21}} - (\dot{y}_n - \dot{y}_{n-1})\mathbf{e}] + \tilde{\mathbf{p}}_{\mathbf{22}}^{\boldsymbol{T}}[\dot{\hat{\mathbf{p}}}_{\mathbf{22}} - (\dot{y}_d - \dot{y}_n)\mathbf{e}] \\ &+\tilde{\mathbf{p}}_{\mathbf{31}}^{\boldsymbol{T}}[\dot{\hat{\mathbf{p}}}_{\mathbf{31}} - (y_n - y_{n-1})\mathbf{e}] + \tilde{\mathbf{p}}_{\mathbf{32}}^{\boldsymbol{T}}[\dot{\hat{\mathbf{p}}}_{\mathbf{32}} - (y_d - y_n)\mathbf{e}]\end{aligned} \tag{3.22}$$

where definitions of $\mathbf{f_1}$, $\mathbf{f_2}$ in Equation (3.4), Equation (3.16), and Equation (3.20) are utilized. At this point, it should be noted that G_{11} and $G_{12} \in \mathbb{R}$ denote the first and second diagonal entries of $\mathbf{G_1}$, respectively. From Equation (3.22) it can be seen that if adaptive compensations of uncertain parameters are made according to the following rules

$$\dot{\hat{\mathbf{p}}}_{\mathbf{11}} = -G_{11}\dot{y}_n\boldsymbol{e} \tag{3.23}$$

$$\dot{\hat{\mathbf{p}}}_{\mathbf{12}} = -G_{12}\dot{y}_d\boldsymbol{e} \tag{3.24}$$

$$\dot{\hat{\mathbf{p}}}_{\mathbf{21}} = \mathbf{e}(\dot{y}_n - \dot{y}_{n-1}) \tag{3.25}$$

$$\dot{\hat{\mathbf{p}}}_{\mathbf{22}} = \mathbf{e}(\dot{y}_d - \dot{y}_n) \tag{3.26}$$

$$\dot{\hat{\mathbf{p}}}_{\mathbf{31}} = \mathbf{e}(y_n - y_{n-1}) \tag{3.27}$$

$$\dot{\hat{\mathbf{p}}}_{\mathbf{32}} = \mathbf{e}(y_d - y_n) \tag{3.28}$$

the time derivative of V in Equation (3.22) can be rearranged as

$$\dot{V} = -\mathbf{x}^T\mathbf{G_1}\mathbf{x} - \mathbf{e}^T\mathbf{G_2}\mathbf{e}. \tag{3.29}$$

Remark 3.3. Update rules in Equation (3.23)-(3.28) are considered as finite adaptive compensations of uncertain system parameters. In contrast to the system identification purpose, estimating the numerical values of the uncertain parameters is not the main aim of proposing these update rules. As long as mathematically it can be proven that these adaptive compensations can be used to ensure the system's stability and desired the semi-global asymptotic convergence their numerical values are not crucial for the designed controller.

From Equation (3.24) it is clear that the following bound is obtained for $\dot{V}$

$$\dot{V} \leq -\beta \|\mathbf{z}\|^2 \tag{3.30}$$

where $\mathbf{z} \in \mathbb{R}^4$ denotes the vector of combined errors defined as

$$\mathbf{z} \triangleq [\mathbf{x}^T \quad \mathbf{e}^T]^T \tag{3.31}$$

and $\beta \in \mathbb{R}$ is a positive constant value that equals to the smallest of the diagonal elements of $\mathbf{G_1}$ and $\mathbf{G_2}$ gain matrices.

Boundedness of $\mathbf{z}(t)$ that can be used to show the boundedness of $\mathbf{x}$ and $\mathbf{e}$ is guaranteed via Equation (3.21) and Equation (3.29). Boundedness of the virtual control input $\mathbf{u_v}$ is guaranteed by considering that $\mathbf{x}$ is a bounded variable. Boundedness of the virtual control input and boundedness of $\mathbf{e}$ can be utilized along with Equation (3.8) to show that $\dot{\mathbf{y}}_{\boldsymbol{c}}$ is bounded. When the boundedness of $\dot{\mathbf{y}}_{\mathbf{c}}$ is utilized with Equation (3.5) and the time derivative of Equation (3.14) it can be shown that $\ddot{\mathbf{y}}_{\mathbf{c}}$ is a bounded term and this result can be used to show the boundedness of the time derivative of $\mathbf{u_v}$. Boundedness of $\dot{\mathbf{e}}$ is shown via boundedness of $\dot{\mathbf{u}}_{\mathbf{v}}$ and boundedness of $\ddot{\mathbf{y}}_{\boldsymbol{c}}$ when the time derivative of Equation (3.8) is considered. By utilizing the boundedness of $\ddot{\mathbf{y}}_{\boldsymbol{c}}$ and boundedness of $\dot{\mathbf{e}}$ it can be proven that $\dot{\mathbf{z}}$ is a bounded variable**.**

The following inequality that guarantees that $\mathbf{z}(t) \in \mathcal{L}_2$ can be obtained from the integration of Equation (3.30)

$$\int_0^{\infty} \|\mathbf{z}(\sigma)\|^2 d\sigma \leq \frac{V(0)}{\beta}. \tag{3.32}$$

Boundedness of $\dot{\mathbf{z}}$ is used with $\mathbf{z}(t) \in \mathcal{L}_2 \cap \mathcal{L}_\infty$ and Barbalat's Lemma (Krstic & Smyshlyaev, 2007) to obtain a semi-global asymptotic convergence for $\mathbf{z}(t)$ that can be used to reach the main control aim in the sense that

$$\|\mathbf{x}\|, \|\mathbf{e}\| \to 0 \text{ as } t \to \infty \tag{3.33}$$

3.4 Implementation and Test Results

The numerical parameters of the nine-story building model used in the simulation studies are given in Table 2.1(Hacioglu & Yagiz, 2012). This structure is exposed to the Kocaeli Earthquake that occurred on 17 August 1999 and El Centro Earthquake that occurred on 18 May 1940.

Additive white Gaussian noise (AWGN) was applied to all measurement data to reflect external influences, measurement noise, and any sensor accuracy issues.

The acceleration data of the ground motions measured during these earthquakes are given in Figure 3.2.

The gains are selected as follows and the designed controller is applied from the actuator input of ATMD system

$$\mathbf{G}_1 = diag\{[390 \quad 0.1]\}, \mathbf{G}_2 = diag\{[7500 \quad 950]\} \tag{3.34}$$

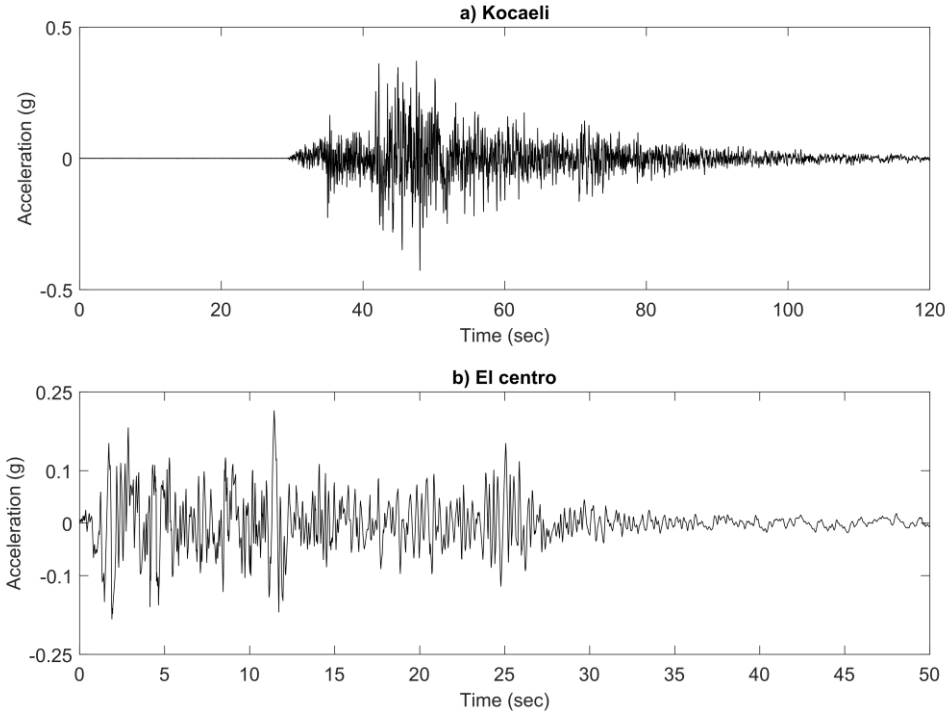

Figure 3.2 Measured acceleration data of earthquakes a) Kocaeli, b) El Centro

Remark 4. At this point it, should be stated that as a result of the trial-and-error process it is observed that then control gain values are increased, ATMD performance improves, but the control effort is also increased. By considering this issue control gain adjustment process is ended at the last point where ATMD performance improves dramatically and these control gains are obtained as in Equation (3.34). After that point, it was observed that control effort increases while the ATMD performance remains similar. In the theoretical analysis presented in the related section, it is proven that the proposed controller can be used to reach the main control purpose in these types of structures as long as control gains are selected as positive definite diagonal matrices. However, the trial-and-error method is the only feasible way for selecting them as optimum numerical values for improving the general control performance.

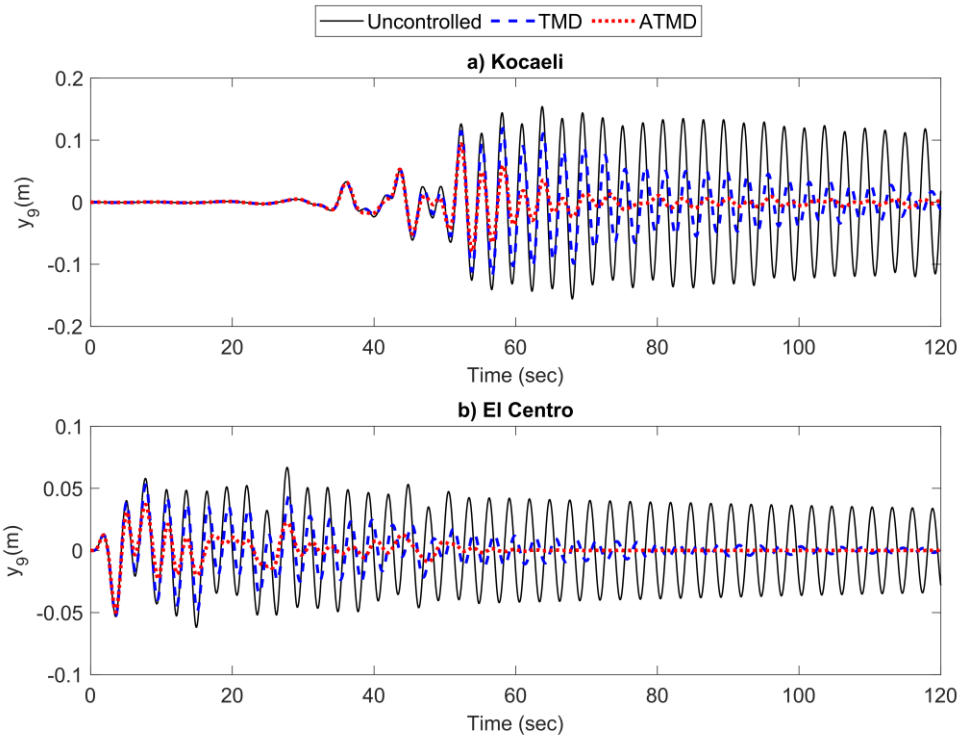

Figure 3.3 Displacement of the ninth floor of the structure

Figure 3.3 shows the vibration of the ninth floor during the earthquake for three different situations: the uncontrolled system, TMD control system, and ATMD control system. From this figure, it is observed that better results than an uncontrolled case can be reached in the case of using the TMD system, but the vibration's amplitude and the time taken to reduce the vibration appeared to be much higher than in the case of using ATMD system. Using the designed controller, ATMD system appears to considerably decrease oscillations occurring on the last floor of the building.

The control force applied to dampen vibrations occurring in the structure is shown in Figure 3.4. The displacement of the controller mass oscillating by the effect of the earthquake and the force applied by the actuator is given in Figure 3.5. From Figure 3.3, Figure 3.4, and Figure 3.5 it can be seen the aim of the control is achieved with an acceptable control force, and the controller mass moves in a reasonable interval.

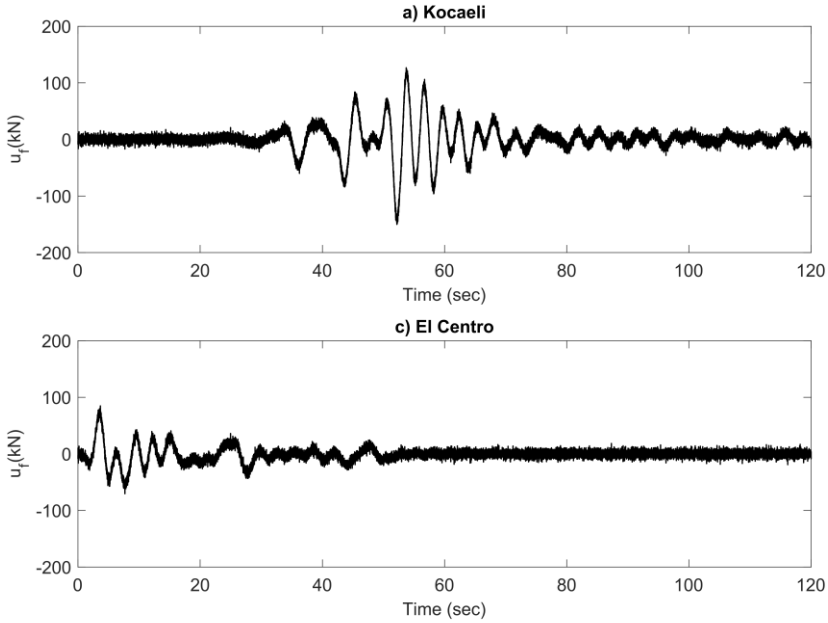

Figure 3.4 Control forces of backstepping controller

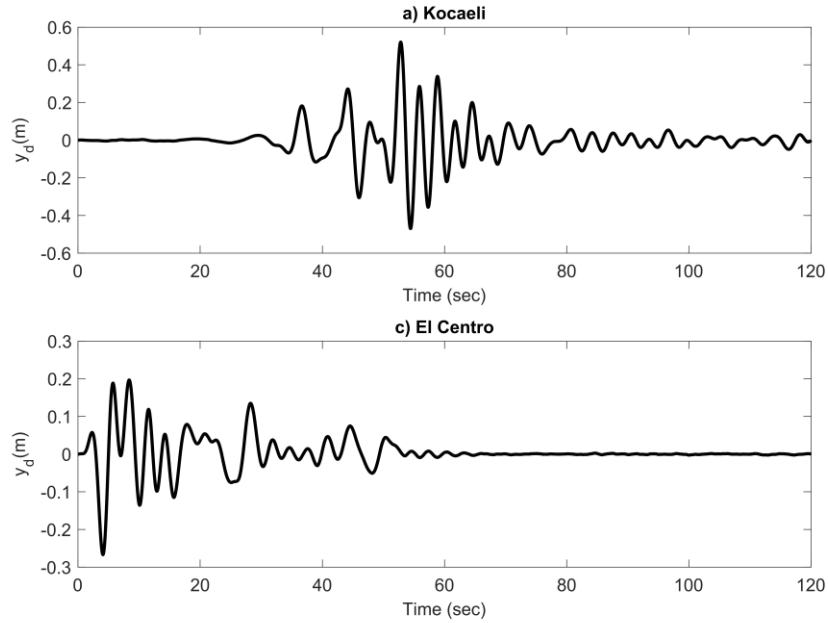

Figure 3.5 Displacement of the active tuned mass damper

Figure 3.6 and Figure 3.7 shows the adaptive compensations of the uncertain parameters $\hat{\mathbf{p}}_{11}, \hat{\mathbf{p}}_{12}, \hat{\mathbf{p}}_{21}, \hat{\mathbf{p}}_{22}, \hat{\mathbf{p}}_{31}$ and $\hat{\mathbf{p}}_{32}$. The first elements of the adaptive compensations are shown with dashed lines while the second elements are shown with straight lines. As stated in Remark 2 before; compensation parameters are utilized to

reach control objectives. Their numerical values are inconsequential provided that they change within a limited range. The change of compensation parameters within a limited range while achieving the control aim is shown in Figure 3.6 and Figure 3.7.

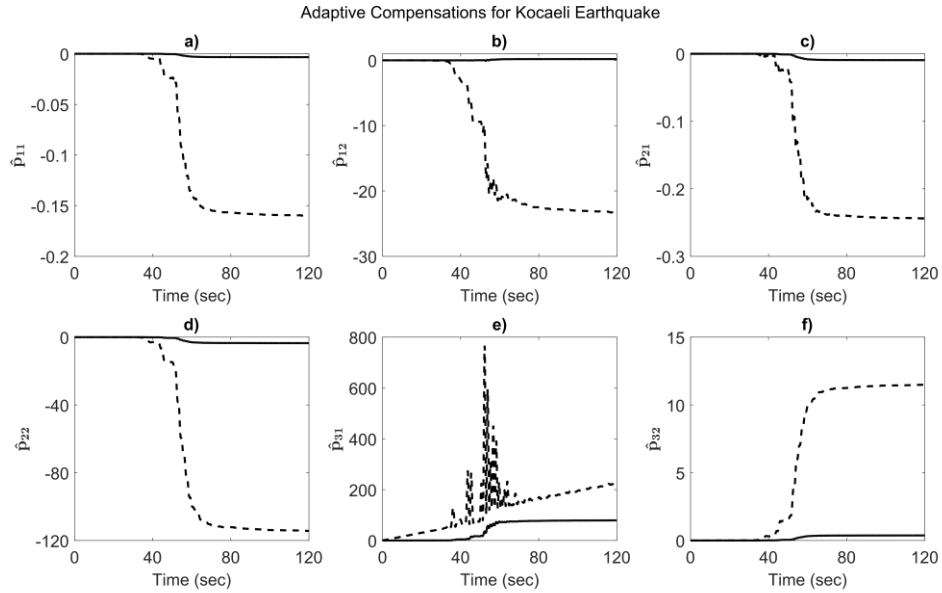

Figure 3.6 Adaptive compensations of uncertain parameters for Kocaeli Earthquake

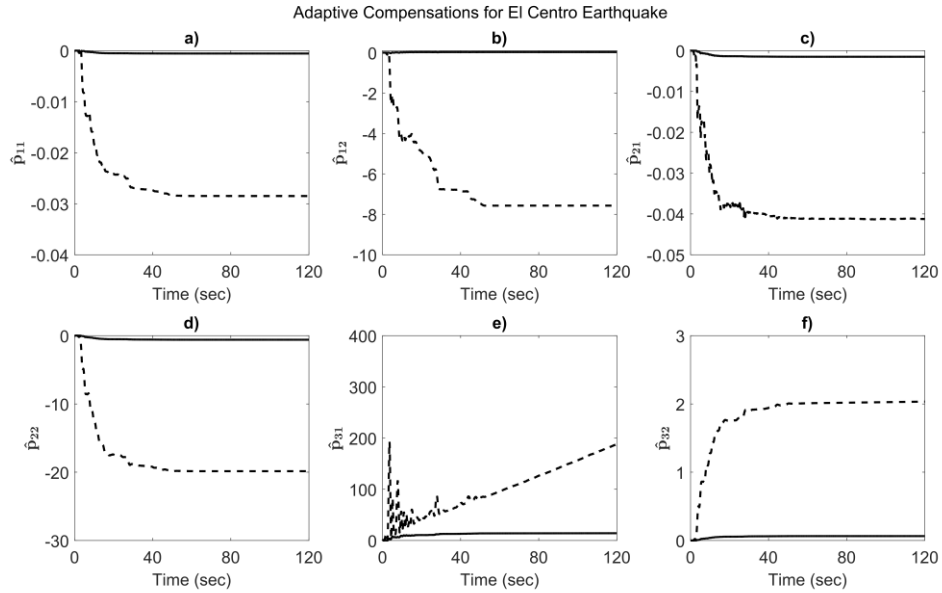

Figure 3.7 Adaptive compensations of uncertain parameters for El Centro Earthquake

3.5 Conclusions

A backstepping adaptive controller is designed in this chapter for use in ATMD systems placed at the top of multi-story buildings. Lyapunov-based arguments are utilized for the analysis of this design where all system parameters are assumed to be uncertain. In the Lyapunov-based stability analysis, it is shown that the proposed controller can be used for maintaining the structure's stability and the controller mass's stability while achieving the main control objective. Different from the related literature, the system, where the stability and zero convergence of two states are guaranteed by using only one actuator, is one of the most crucial contributions of the designed controller. A controller that can be generalized for these types of systems owing to its system parameters' independent structure is designed by utilizing adaptive compensations of uncertain parameters proposed in this chapter. In addition, with its adaptive structure, the designed controller has the potential to achieve control purpose by requiring less control effort than conventional system parameters free controllers. These situations can be noted as other significant developments. The performance of the designed controller is verified via simulation studies conducted in Matlab / Simulink. The finding results of the simulation are also supported by the evaluation criteria. These results show that the designed controller provides an efficient effort in damping earthquake-induced vibrations on the building.

CHAPTER FOUR
A NOVEL LINEAR REGRESSION MODEL BASED CONTROLLER DESIGN FOR THE ATMD SYSTEMS

4.1 Introduction

The sensor precision that may become more difficult to provide as the number of measurements increases is one of the most important things in ATMD systems. More measurements that cannot be obtained from the system precisely may cause a harder control task and worse control results. However, despite these situations, this kind of studies in the literature still assumes that at least all states of the top two floors and the ATMD system are available to use in the feedback information.

In this chapter, it is aimed to design a controller that can be used to absorb the earthquake induced vibrations of multi-story buildings when it is used in accordance with the ATMD system. In this control design, it is assumed that only the states of the last floor are available information about the building and out of these states all other system states and parameters are unknown. Other motivations of this study are: Firstly, obtaining a control design that is able to protect the overall system stability during the control process. Secondly, the designed controller is able to cope with sensor precision problems owing to its structure which requires less measurement than its counterparts in this field of research. Lastly, it can be able to utilized for the control problems of all of these types of systems owing to its system parameters independent and generalized structure. Considering the system requirements, it is seen that all of these motivations can contribute to the research field. However, its structure, which requires the availability of less states, is the main novelty of this controller. According to the authors' best knowledge, there are no similar studies where the main control target was achieved by using such little state feedback. For providing the mentioned structure the designed controller is supported with available states based linear regression (LR) model whose coefficients are adaptively compensated during the control process while modeling error is coped with a bounding term. For the theoretical analysis of the designed controller, a Lyapunov-based stability analysis is conducted and the

numerical simulations are presented for the performance demonstration. In this chapter, the designed controller is tried on two different multi-story buildings under the effect of a major earthquake and it is observed that the control purpose can be reached efficiently for both of these buildings. Comparative studies are also presented to show the efficiency of the designed controller clearly.

4.2 Control System Design for Building Structures

An n-story building with an ATMD system at the top whose structure is shown in Figure 3.1 is represented via a mathematical model having the following form. The model parameters are presented in Table 4.1.

$$m_i\ddot{y}_i + b_i(\dot{y}_i - \dot{y}_{i-1}) - b_{i+1}(\dot{y}_{i+1} - \dot{y}_i) + k_i(y_i - y_{i-1}) - k_{i+1}(y_{i+1} - y_i) = 0 \text{ for } i = 1, \dots, n-1 \quad (4.1)$$

$$m_n\ddot{y}_n + b_n(\dot{y}_n - \dot{y}_{n-1}) - b_d(\dot{y}_d - \dot{y}_n) + k_n(y_n - y_{n-1}) - k_d(y_d - y_n) = u_f \quad (4.2)$$

$$m_d\ddot{y}_d + b_d(\dot{y}_d - \dot{y}_n) + k_d(y_d - y_n) = -u_f \quad (4.3)$$

Table 4.1 Parameters of the generalized structural model

Parameter	Definition
m_i	Mass coefficient of the i^{th} floor.
k_i	Stiffness coefficient of the i^{th} floor.
b_i	Damping coefficient of the i^{th} floor.
m_d	Mass coefficient of the ATMD system.
k_d	Stiffness coefficient of the ATMD system.
b_d	Damping coefficient of the ATMD system.
$y_i, \dot{y}_i, \ddot{y}_i$	Displacement, velocity, and acceleration of the i^{th} floor.
$y_d, \dot{y}_d, \ddot{y}_d$	Displacement, velocity, and acceleration of the ATMD system.
u_f	Control force.

In these types of rigid structures, vibration suppression is realized based on the fact that damping the vibration of the top floor during an earthquake is enough for damping the vibration of the whole building. In such applications, damping systems placed on

the top floor of the building are used to dampen the vibration of the building. Therefore, a control system can be designed by focusing on the displacement of the last floor of the building. In other words, the control problem can mathematically be started from the following equation

$$x = y_n \tag{4.4}$$

From the time derivative of the above equation, it can be observed that if the following condition is satisfied (i.e., the velocity of the top floor is designed as a simple proportional controller) vibration occurred on the last floor can be suppressed.

$$\dot{y}_n = -g_1 x \tag{4.5}$$

In Equation (4.5), $g_1 \in \mathbb{R}^+$ denotes the positive constant control gain. For proving this mathematically, Lyapunov-based arguments can be utilized. As a result of the usage of Equation (4.5) into the time derivative of Equation (4.4) the following expression can be obtained

$$\dot{x} = -g_1 x. \tag{4.6}$$

If the nonnegative Lyapunov function candidate $V_1(x) \in \mathbb{R}^+$ is defined as

$$V_1 \triangleq \frac{1}{2} x^2. \tag{4.7}$$

The time derivative of Equation (4.7) can be obtained as follows by utilizing Equation (4.6)

$$\dot{V}_1 = -g_1 x^2 \tag{4.8}$$

From the viewpoint of Lyapunov based control design Equation (4.7) and its time derivative in Equation (4.8) are enough to show that the semi-global asymptotic

stability result can be provided for x that guarantees the vibration suppression of the last floor mathematically. However, this result is obtained for the design of the system state as in Equation (4.5). Since it is not possible to design the system state, the control input should be designed to get the desired behavior from the system state. Mathematically, it can be stated that if the control force u_f is designed to obtain zero convergence of the term defined as

$$r \triangleq \dot{y}_n + g_1 x. \tag{4.9}$$

main control aim can be reached.

The time derivative of Equation (4.9) is obtained as follows by pre-multiplying it with m_n

$$m_n \dot{r} = f + u_f + g_1 \dot{y}_n m_n \tag{4.10}$$

where f is an auxiliary function of the system states and it is defined as

$$\begin{aligned} f \triangleq & -b_n(\dot{y}_n - \dot{y}_{n-1}) + b_d(\dot{y}_d - \dot{y}_n) - k_n(y_n - y_{n-1}) \\ & + k_d(y_d - y_n) \end{aligned} \tag{4.11}$$

and Equation (4.1) is utilized.

The control design presented in this chapter is based on the assumption that the auxiliary function f can be represented by an LR model having the following form

$$f = \mathbf{c}\boldsymbol{\phi} + \varepsilon \tag{4.12}$$

where $\mathbf{c} \in \mathbb{R}^{1x\ell}$ represents the vector uncertain coefficients, $\boldsymbol{\phi}(\ddot{y}_n) \in \mathbb{R}^{\ell x1}$ denotes the vector of base functions and $\varepsilon \in \mathbb{R}$ represents the modeling error. At this point, it should be stated that owing to the above model the auxiliary function f can approximately be expressed in terms of acceleration of the last floor.

The uncertainty of the system parameters that make the above coefficient matrix an uncertain matrix is coped with via their adaptive compensations. The adaptive compensation errors $\tilde{\mathbf{c}} \in \mathbb{R}^{1\times\ell}$ and $\tilde{m}_n \in \mathbb{R}$ are defined as

$$\tilde{\mathbf{c}} = \mathbf{c} - \hat{\mathbf{c}} \tag{4.13}$$

$$\tilde{m}_n = m_n - \hat{m}_n \tag{4.14}$$

where adaptive compensations are denoted by $\hat{\mathbf{c}} \in \mathbb{R}^{1\times\ell}$ and $\hat{m}_n \in \mathbb{R}$.

The final form of the open-loop error system is obtained as follows by substituting Equation (4.12), Equation (4.13), and Equation (4.14) in Equation (4.10)

$$m_n\dot{r} = (\tilde{\mathbf{c}} + \hat{\mathbf{c}})\boldsymbol{\phi} + \varepsilon + u_f + g_1\dot{y}_n(\tilde{m}_n + \hat{m}_n). \tag{4.15}$$

The control input is designed as

$$u_f = -\hat{\mathbf{c}}\boldsymbol{\phi} - \varepsilon_b sgn(r) - g_1\dot{y}_n\hat{m}_n - g_2 r \tag{4.16}$$

where $g_2 \in \mathbb{R}^+$ is the positive constant control gain and $\epsilon_b \in \mathbb{R}^+$denotes the positive bounding constant of the modeling error defined in Equation (4.12) (i.e., $\epsilon \leq \epsilon_b$). The closed-loop error system is obtained as follows by substituting Equation (4.16) in Equation (4.15).

$$m_n\dot{r} = \tilde{\mathbf{c}}\boldsymbol{\phi} + [\varepsilon - \varepsilon_b sgn(r)] + g_1\dot{y}_n\tilde{m}_n - g_2 r \tag{4.17}$$

After that point, it continues with Lyapunov-based stability analysis. The Lyapunov function candidate is defined as

$$V \triangleq V_1 + \frac{1}{2}m_n r^2 + \frac{1}{2}\tilde{\mathbf{c}}\tilde{\boldsymbol{c}}^{\boldsymbol{T}} + \frac{1}{2}\tilde{m}_n^2 \tag{4.18}$$

The time derivative of Equation (4.21)

$$\begin{aligned}\dot{V} = &-g_1 x^2 - g_2 r^2 + r[\varepsilon - \varepsilon_b sgn(r)] \\ &+\left(\dot{\hat{\mathbf{c}}} + \boldsymbol{\phi}^{\boldsymbol{T}} r\right)\tilde{\mathbf{c}}^{\boldsymbol{T}} + \tilde{m}_{\boldsymbol{n}}(\dot{\hat{m}}_n + g_1 \dot{y}_n r)\end{aligned} \tag{4.19}$$

For the case where adaptive compensations are updated according to the rules given as

$$\dot{\hat{\mathbf{c}}} = -\boldsymbol{\phi}^{\boldsymbol{T}} r \tag{4.20}$$

$$\dot{\hat{m}}_n = -g_1 \dot{y}_n r \tag{4.21}$$

the Lyapunov function in Equation (4.19) can be upper bounded as

$$\dot{V} \leq -\beta_1 \|\mathbf{z}\|^2 \tag{4.22}$$

where $\mathbf{z} \in \mathbb{R}^2$ is an auxiliary vector defined as

$$\mathbf{z} \triangleq [x \quad r]^T \tag{4.23}$$

$\beta_1 \in \mathbb{R}^+$ is a positive constant value equal to the minimum of the constant gains g_1 and g_2. At this point, it should be stated that the bound in Equation (4.22) is obtained by utilizing the negativeness of the term $r[\varepsilon - \varepsilon_b sgn(r)]$.

Lyapunov function in Equation (4.18) and the bound of its time derivative in Equation (4.22) guarantees the boundedness of x, r, and z. From Equation (4.6) it can be seen that the boundedness of x is a necessary and enough condition to show that $\dot{x}$ is a bounded variable. Boundedness of $\dot{x}$ guarantees that $\ddot{y}_n \in \mathcal{L}_\infty$ from the time derivative of Equation (4.5). Boundedness statements of $\dot{x}$ and $\ddot{y}_n$ guarantee the boundedness of $\dot{r}$. From the time derivative of Equation (4.23), it can be seen that boundedness of $\dot{x}$ and $\dot{r}$ guarantees the boundedness of $\dot{\mathbf{z}}(t)$**.**

To show that $\mathbf{z}(t) \in \mathcal{L}_2$, integration of Equation (4.22) that can be obtained as follows is utilized

$$\int_0^\infty \|\mathbf{z}(\sigma)\|^2 d\sigma \leq \frac{V(0)}{\beta}. \tag{4.24}$$

Boundedness statements $\dot{\mathbf{z}}(t) \in \mathcal{L}_\infty$ and $\mathbf{z}(t) \in \mathcal{L}_2 \cap \mathcal{L}_\infty$ are considered in accordance with Barbalat's Lemma (Krstic et al., 1995) to prove semi-global asymptotic stability of $\mathbf{z}(t)$ that guarantees the main purpose of the designed controller stated as

$$x, e \to 0 \text{ as } t \to \infty \tag{4.25}$$

4.3 Numerical Studies and Results

The proposed control design is tested on two different structures in this section. The structures selected for simulation studies are a nine-story building (Hacioglu & Yagiz, 2012) and a fifteen-story building (Guclu & Yazici, 2008). Observing the performance of the designed controller on different building structures for showing that it is efficiency is not affected by the number of floor or system parameters was the main purpose of this choice. The numerical values of the parameters of these buildings are given in Table 4.2. These structures were exposed to the East-West direction component of the 1999 Kocaeli earthquake, which was a major earthquake and caused great loss of life and property. The acceleration, velocity, and displacement data of this earthquake are shown in Figure 4.1.

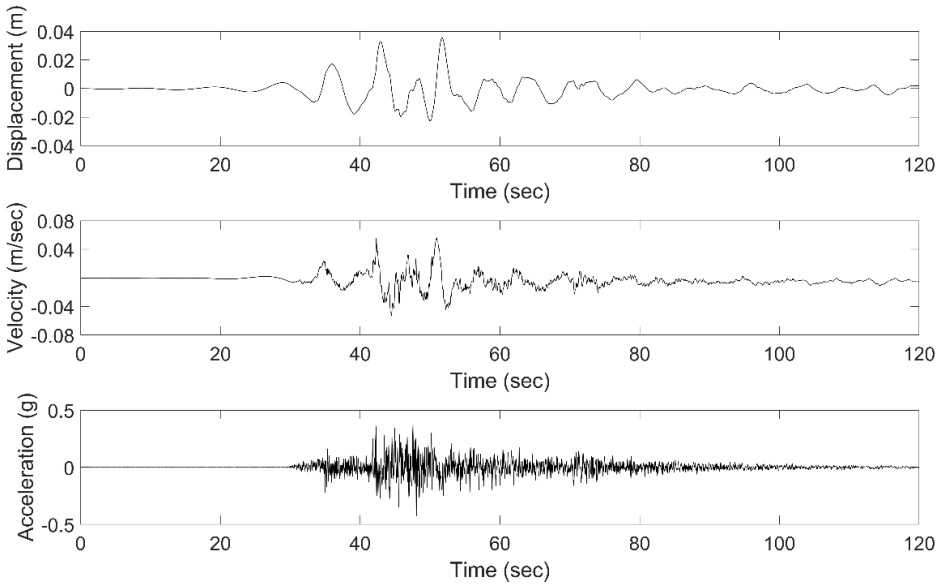

Figure 4.1 Displacement, velocity, and acceleration data of Kocaeli earthquake

The base function is selected as the univariate quadratic polynomial function $\boldsymbol{\phi} = [\ddot{y}_n{}^2 \quad \ddot{y}_n \quad 1\ ]$**.** The values of gains and ε_b are selected as follows.

$$g_1 = 235 \text{ a},\ g_2 = 6250 \text{ and } \varepsilon_b = 10 \tag{4.26}$$

Table 4.2 Parameters of the nine-story and fifteen-story buildings

Parameter	Value $\times 10^3$ (kg)		Parameter	Value $\times 10^6$ (N/m)		Parameter	Value $\times 10^3$ (Ns/m)	
	n=9	n=15		n=9	n=15		n=9	n=15
m_1	450	450	k_1	18.05	18.05	b_1	26.17	26.17
m_2	345	345.6	k_2	340	340.4	b_2	490	293.7
m_3	345	345.6	k_3	326	340.4	b_3	467	293.7
m_4	345	345.6	k_4	285	340.4	b_4	410	293.7
m_5	345	345.6	k_5	269	340.4	b_5	386	293.7
m_6	345	345.6	k_6	243	340.4	b_6	348	293.7
m_7	345	345.6	k_7	207	340.4	b_7	298	293.7
m_8	345	345.6	k_8	169	340.4	b_8	243	293.7
m_9	345	345.6	k_9	137	340.4	b_9	196	293.7
m_{10-15}	-	345.6	k_{10-15}	-	340.4	b_{10-15}	-	293.7
m_d	69	104.918	k_d	0.3365	280	b_d	152.39	597

For two different building models under the effect of earthquakes, vibrations occurring on the last floors of the buildings in uncontrolled, passive, and active control situations are shown in Figure 4.2. In the passive control scenario where TMD is used, there is a serious decrease in vibration amplitudes compared to the uncontrolled situation. In the case of active control, the designed LR model based controller, which needs only the states belonging to the last floor, has absorbed the last floor vibration to a large extent according to TMD.

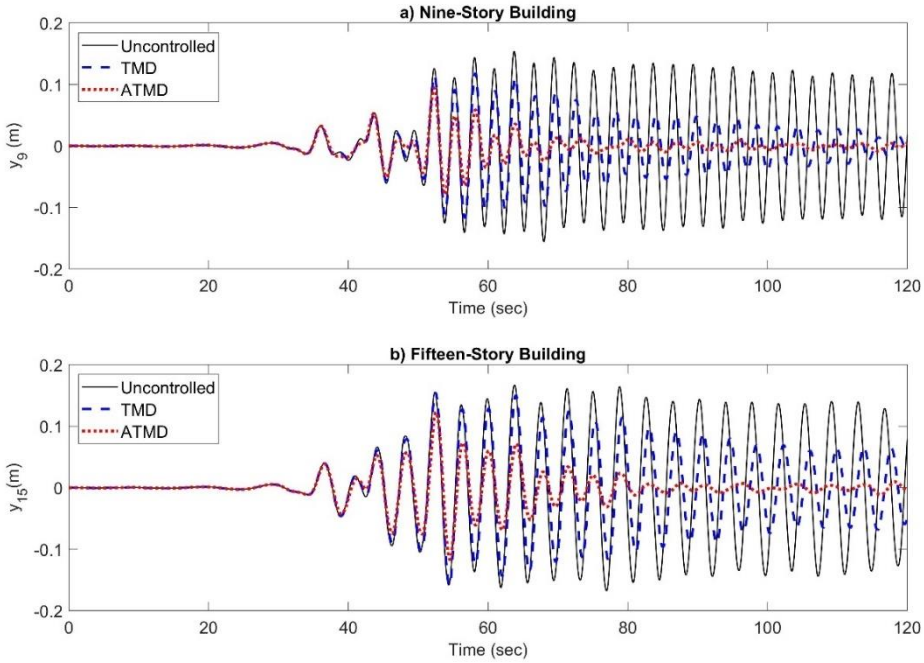

Figure 4.2 The displacements of the last floors of the buildings

Figure 4.3 shows the adaptive compensation of the uncertain parameters of the designed LR model-based adaptive controller tested for two different buildings. The first items of the adaptive compensation $\hat{C}_1$ are shown by solid lines, the second items $\hat{C}_2$ by dashed lines, and the third items $\hat{C}_3$ by dotted lines. Compensation parameters are used to achieve control objectives. It doesn't matter what value it gets, provided its numeric values change within a limited range. Figure 4.3 shows that while achieving the control objective, the compensation parameters, which contain the system parameters and the system states change in a finite range.

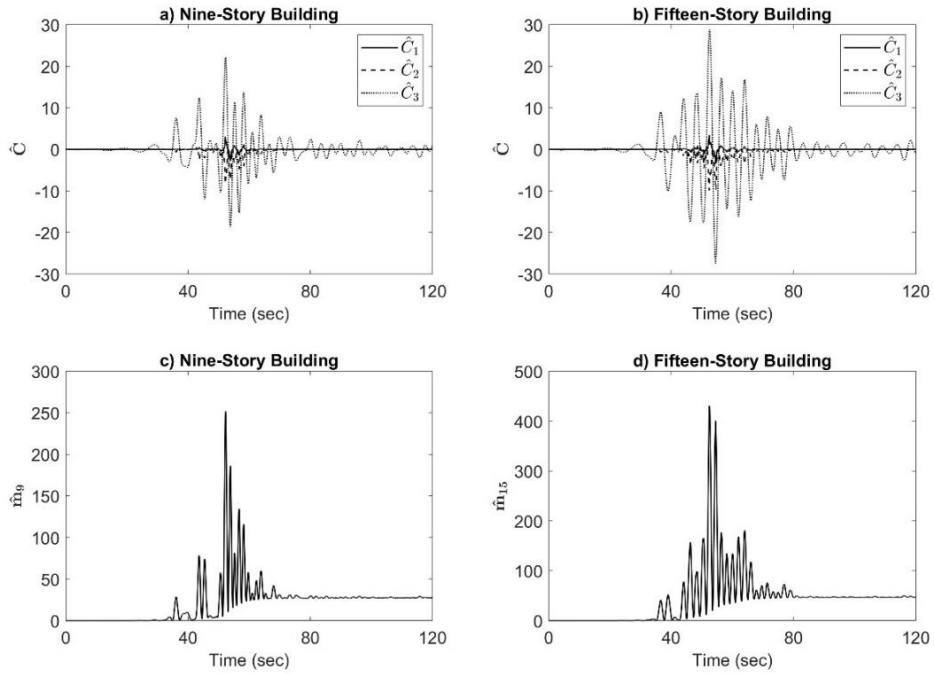

Figure 4.3 The change of values of compensation parameters

The designed LR model-based controller and the robust adaptive controller designed in Ümütlü et al. (Ümütlü et al., 2021) were tested on these two different structures and the results were compared. As seen in Figure 4.4, although the results are almost the same, it is seen that it is possible to design a controller that provides vibration reduction at least as good as the other robust controller, using only the vibration data from the just last floor. Figure 4.5 shows that the designed new LR model based controller requires significantly less control force, especially in the figure for the 15-story building. According to the root mean square values, 0.25% less control force is required for the nine-story building and 0.43% for the fifteen-story building in terms of control effort. Considering the peak-to-peak (PP) values, 4.77% less control force is required for the nine-story building and 9.42% for the fifteen-story building in terms of control effort. Especially the high difference between the two controllers in PP values is important as it will cause a considerable decrease in the maximum power that will be needed. Also, the reduction of the required maximum power is a significant parameter for the reduction of investment costs. In Figure 4.6, the displacements of the control mass moving with the effect of the control force and the earthquake force

is given during the damping of the vibrations caused by the earthquake by the controller force for the two buildings.

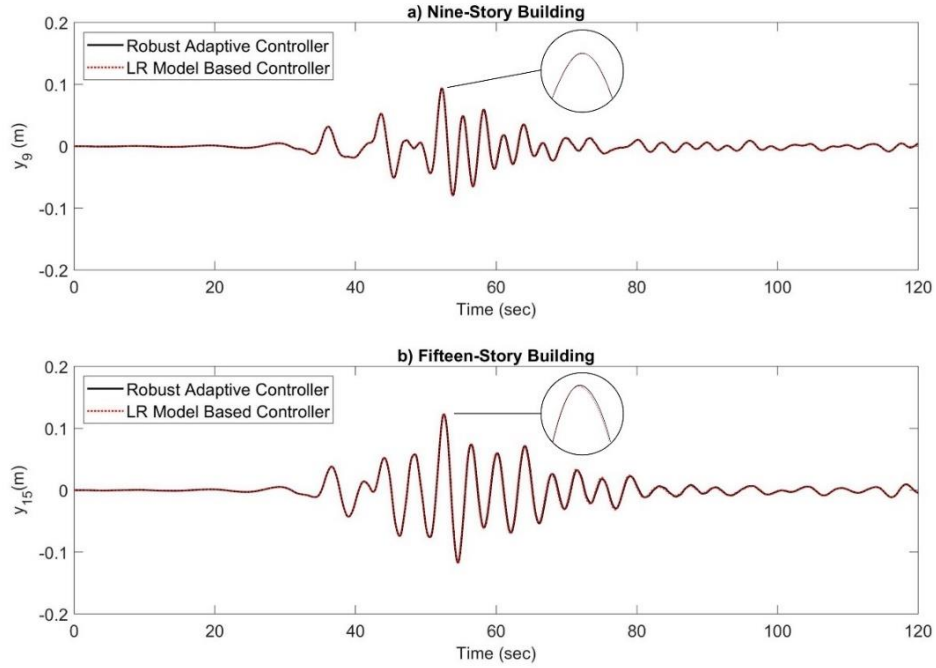

Figure 4.4 Comparison of the displacements of the top floors for the two different controllers

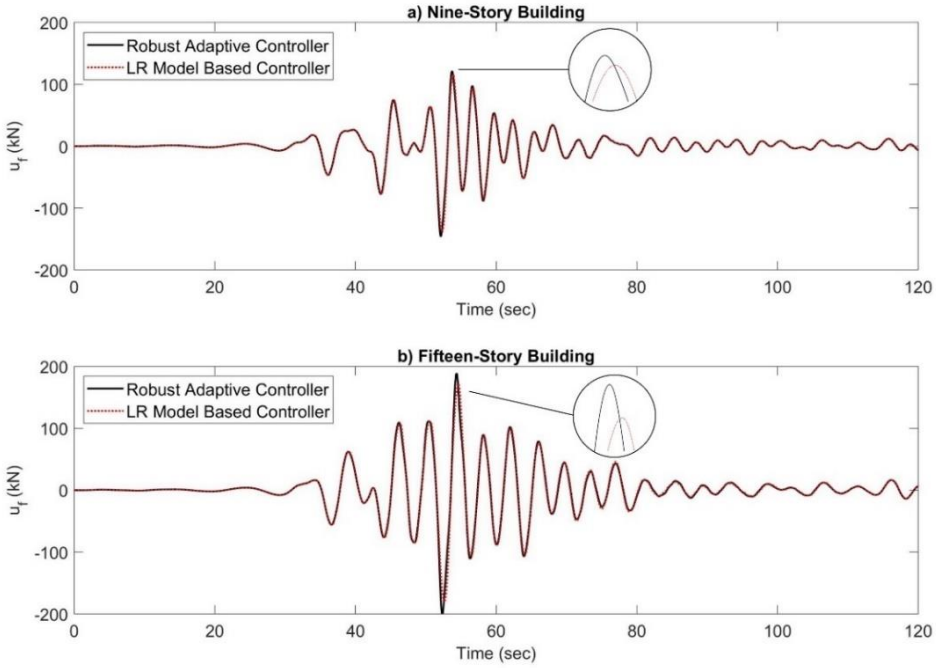

Figure 4.5 Comparison of the control force of the buildings for the two different controllers

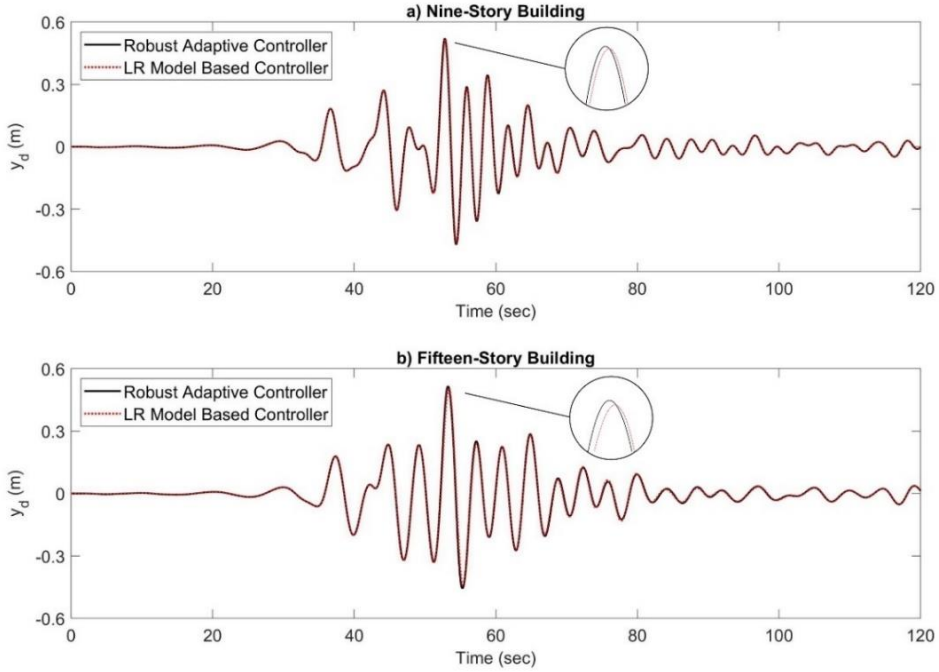

Figure 4.6 Comparison of the displacements of the controller mass of the buildings for the two different controllers

4.4 Conclusions

In this chapter, a novel LR model-based controller was designed to mitigate the vibrations caused by earthquakes in multi-story buildings. Supported by Lyapunov-based stability analysis, the controller generates the response to control the system using only the states of the last floor as feedback information. In addition to the uncertainty of all system parameters of the building, unlike similar studies, a design process was followed in which the states of the other floors were not known. By using adaptive compensation terms, vibration reduction was achieved successfully in the presence of parametric uncertainty, while the protection of the stability of the whole structure was theoretically proven and guaranteed via Lyapunov-based arguments. Owing to its structure that requires less measurement, a control design that can overcome possible sensor precision problems was obtained. Simulation studies performed on nine-story and fifteen-story buildings showed that the designed

controller can be used safely in whole structures with ATMD systems, regardless of the number of story and system parameters.

CHAPTER FIVE
EVALUATION CRITERIA FOR CONTROLLERS OF ATMD SYSTEMS IN LINEAR STRUCTURES

5.1 Introduction

In controller design studies for ATMD systems, various methods are used to measure the success of the designed controller. Comparing results only over time history, without evaluation criteria, sometimes leaves readers with complex graphs. In the literature, many evaluation criteria have been developed for the performance criteria of controllers designed to dampen wind and earthquake-induced vibrations. The general logic of these performance criteria is the same. In order to measure the success of the controller, the acceleration, velocity, displacement data of the structure, and the control mass are compared with the uncontrolled structure. In addition, since the control effort spent is an important parameter, it is often added to the criteria. The performance criteria chosen to test the controllers designed within the scope of this thesis are dimensionless performance criteria (Nagarajaiah & Varadarajan, 2005; J. N. Yang et al., 2001) used in many publications in recent years, in which the RMS and peak values of the acceleration and displacement measurements are used to compare and evaluate the response.

5.2 Evaluation Criteria for Active Tuned Mass Damper Systems

Twelve performance criteria have been defined to evaluate for designed control systems for building structures with ATMD systems by J. N. Yang et al., (2001). These evaluation criteria have been used in many pioneering studies in the literature to test the performance of ATMD systems (Nagarajaiah & Varadarajan, 2005; Varadarajan & Nagarajaiah, 2004). These criteria were developed to test the success of the controller systems designed for the ATMD system, which was placed on the 76-story building model in previous studies, against wind load. In this section, these evaluation criteria are adapted for a nine-story building in accordance with the structures in which these controllers are used to compare three different controllers designed in the

previous three chapters. These evaluation criteria are based on both the peak and root mean square (RMS) responses of the building. Definitions of these criteria are denoted by J_1 - J_{12} are given in below.

$$J_1 = \frac{\max(\sigma_{\ddot{y}n})}{\sigma_{\ddot{y}9o}} \quad \textit{for n=1 to 9} \tag{5.1}$$

In the first criterion J_1, $\sigma_{\ddot{y}n}$ and $\sigma_{\ddot{y}9o}$ represent RMS acceleration of the nth floor and RMS acceleration of the 9th floor for the uncontrolled situation, respectively.

$$J_2 = \frac{1}{6}\sum_{n}\left(\frac{\sigma_{\ddot{y}n}}{\sigma_{\ddot{y}no}}\right) \quad \textit{for n=4,5,6,7,8 and 9} \tag{5.2}$$

In J_2, $\sigma_{\ddot{y}no}$ denotes RMS acceleration of the nth floor for the uncontrolled situation. This performance criterion is the average RMS acceleration performance for the last floors of the building.

$$J_3 = \frac{\sigma_{y9}}{\sigma_{y9o}} \tag{5.3}$$

The J_3 performance criterion gives the rate of RMS displacement of the ninth floor, which is the last floor of the building, for controlled and uncontrolled situations.

$$J_4 = \frac{1}{7}\sum_{n}(\sigma_{yn}/\sigma_{yno}) \quad \textit{for n=3,4,5,6,7,8 and 9} \tag{5.4}$$

In J_4, σ_{yn} and σ_{yno} represent RMS displacements of the nth floor and RMS displacements of the nth floor for the uncontrolled situation, respectively. This

performance criterion is the average RMS displacement performance for the last floors of the building.

$$J_5 = \frac{\sigma_{yd}}{\sigma_{y9o}} \tag{5.5}$$

In criterion five σ_{yd} specify the RMS displacement of controller mass.

$$J_6 = \left\{ \frac{1}{T} \int_0^T \left[\dot{y}_d(t) u_f(t) \right]^2 dt \right\} \tag{5.6}$$

J_6 represents the RMS control power. In Eq. (5.6), $\dot{y}_d(t)$ denotes actuator velocity, T represents the total time of simulation, and $u_f(t)$ denotes actuator force.

$$J_7 = \frac{\max(\ddot{y}_{pn})}{\ddot{y}_{p9o}} \quad \textit{for n=1 to 9} \tag{5.7}$$

Criteria J_7 to J_{11} are calculated similarly to the first five criteria, but peak values are used instead of RMS values. In criterion J_7, $\ddot{y}_{pn}$ and $\ddot{y}_{p9o}$ represent peak acceleration of the nth floor and peak acceleration of the 9th floor for the uncontrolled situation, respectively.

$$J_8 = \frac{1}{6} \sum_n (\ddot{y}_{pn} / \ddot{y}_{pno}) \quad \textit{for n=4,5,6,7,8 and 9} \tag{5.8}$$

In Eq. (5.8), $\ddot{y}_{pno}$ denotes peak acceleration of nth floor for the uncontrolled situation. This performance criterion is the average peak acceleration performance for the last floors of the building.

$$J_9 = \frac{y_{p9}}{y_{p9o}} \tag{5.9}$$

The J_9 performance criterion gives the rate of peak displacement of the ninth floor, which is the last floor of the building, for controlled and uncontrolled situations.

$$J_{10} = \frac{1}{7}\sum_{n}(y_{pn}/y_{pno}) \quad \textit{for n=3,4,5,6,7,8 and 9} \tag{5.10}$$

In J_{10}, y_{pn} and y_{pno} represent peak displacements of the nth floor and peak displacements of the nth floor for the uncontrolled situation, respectively. This performance criterion is the average peak displacement performance for the last floors of the building.

$$J_{11} = \frac{y_{pd}}{y_{p9o}} \tag{5.11}$$

where y_{pd} specify the peak displacement of TMD controller mass.

$$J_{12} = \max_{t}\left|\dot{y}_d(t)u_f(t)\right| \tag{5.12}$$

J_{12} represents the peak control power.

For each criteria of performance values, less than 1.0 implies an improvement in control response compared with the uncontrolled scenario, except for the J_5, J_6, J_{11}, and J_{12} performance indices (Varadarajan & Nagarajaiah, 2004).

5.3 Results of Evaluation Criteria

In this part, evaluation criteria results are given for three different robust adaptive controllers whose stabilities are guaranteed by Lyapunov stability analyzes. The

controllers designed in the Chapter 2 of the thesis are represented by C1 from Table 5.1 to Table 5.12. This controller is guaranteed the stability of the structure throughout the control process of the vibrations caused by earthquakes. The controllers presented in the Chapter 3 of the thesis are denoted by C2. The proposed controller ensures the stability of the structure and the control mass with Lyapunov based stability analysis while achieving the control purpose in an ATMD system. The controller designed in Chapter 4 uses a linear regression-based structure and is represented by C3 in the evaluation criteria tables. The controller uses only the state to be controlled in the controller design, owing to the novel linear regression based design. The designed controllers guarantee the stability of the system regardless of the system parameters using Lyapunov-based stability analysis.

In the simulations in which the results of the evaluation criteria were obtained, a nine-story linear one-dimensional shear structure model equipped with the ATMD system was used. The model of the structure is given in Figure 2.1 and values of the parameters of the structure are given in Table 2.1. This building was exposed to four strong earthquake records to demonstrate the effectiveness of the method against earthquakes of varying intensity and duration. To achieve the said aim, two pulse-like and two non-pulse-like registers shown in Figure 2.2 were chosen. These earthquakes are Kocaeli Earthquake, Kobe Earthquake, El Centro Earthquake, and Imperial Valley-06 Earthquake. Additional white Gaussian noise (AWGN) has been added to all measurement values to represent external influences, measurement noise, and possible sensor sensitivity issues.

In order to show that the designed robust controller is able to cope with the uncertainty in the building parameters, the structure stiffness, which is a widely used method in the literature (Nagarajaiah & Varadarajan, 2005; Varadarajan & Nagarajaiah, 2004; J. N. Yang et al., 2001), has been changed to $\pm 15\%$. The designed controllers are tested with three different types of structures: the original structure, 15% more flex structure, and 15% more rigid structure.

The tables from Table 5.1 to Table 5.12 present the computed performance criteria of the three different controllers which are designed in the previous chapters. In addition to performance criteria, RMS and peak values of control force and controller displacement are given to evaluate controller performance in tables.

Table 5.1 Evaluation criteria results for the Kocaeli Earthquake of three different controllers tested in the structure with original stiffness values

	$C1$	$C2$	$C3$		$C1$	$C2$	$C3$
J_1	0.1939	0.1946	0.1946	J_7	0.5025	0.5083	0.5136
J_2	0.1924	0.1933	0.1934	J_8	0.4910	0.4984	0.5098
J_3	0.2413	0.2402	0.2387	J_9	0.6010	0.6028	0.6044
J_4	0.2437	0.2430	0.2417	J_{10}	0.6048	0.6075	0.6101
J_5	1.4046	1.3808	1.3647	J_{11}	3.3868	3.3427	3.3294
J_6 $(kN\ m/s)$	13.4677	12.9836	12.8483	J_{12} $(kN\ m/s)$	127.2227	117.9163	112.2249
σu_f (kN)	25.1191	24.8629	24.8585	$max\|u_f\|$ (kN)	135.1063	126.6921	125.2096
σ_{yd} (cm)	9.7723	9.6073	9.4951	$max\|y_d\|$ (cm)	52.7470	52.0595	51.8529

Table 5.2 Evaluation criteria results for the Kocaeli Earthquake of three different controllers tested in the structure with flexible stiffness values

	$C1$	$C2$	$C3$		$C1$	$C2$	$C3$
J_1	0.2302	0.2327	0.2334	J_7	0.6130	0.6170	0.6311
J_2	0.2278	0.2305	0.2315	J_8	0.6000	0.6071	0.6185
J_3	0.2854	0.2854	0.2853	J_9	0.7275	0.7316	0.7362
J_4	0.2883	0.2886	0.2887	J_{10}	0.7293	0.7343	0.7391
J_5	1.7872	1.7684	1.7623	J_{11}	4.3519	4.3189	4.3098
J_6 $(kN\ m/s)$	11.8240	11.6090	11.5767	J_{12} $(kN\ m/s)$	115.4594	111.2436	99.8173
σu_f (kN)	24.3331	24.2294	23.8779	$max\|u_f\|$ (kN)	129.0122	125.5741	113.9547
σ_{yd} (cm)	10.1803	10.0733	10.0386	$max\|y_d\|$ (cm)	52.2863	51.8901	51.7816

Table 5.3 Evaluation criteria results for the Kocaeli Earthquake of three different controllers tested in the structure with rigid stiffness values

	$C1$	$C2$	$C3$		$C1$	$C2$	$C3$
J_1	0.2465	0.2445	0.2409	J_7	0.6286	0.6384	0.6358
J_2	0.2426	0.2403	0.2369	J_8	0.6163	0.6190	0.6161
J_3	0.3147	0.3106	0.3072	J_9	0.7875	0.7849	0.7835

Table 5.3 Continues

J_4	0.3183	0.3146	0.3115	J_{10}	0.7756	0.7740	0.7737
J_5	1.7454	1.7016	1.6790	J_{11}	4.2666	4.1761	4.1189
J_6 $(kN\ m/s)$	12.1150	11.4352	11.0737	J_{12} $(kN\ m/s)$	113.2446	102.1283	88.1667
σu_f (kN)	24.1533	23.7169	23.1423	$max\|u_f\|$ (kN)	127.6965	117.8240	105.3206
σ_{yd} (cm)	8.9472	8.7228	8.6071	$max\|y_d\|$ (cm)	50.1134	49.0504	48.3780

In Table 5.1, the results of three different controllers tested for the nine-story structure using the original stiffness values are given for the Kocaeli earthquake. When the results are examined, it is seen that the first controller gives the best results for the J_1, J_2, J_7 and J_8 criteria, which are the building acceleration-based criteria. All three controllers produced similar performance results in original, flex, and rigid structures in criteria related to structure displacement as shown in Table 5.1, Table 5.2, and Table 5.3. As can be seen from the σu_f and $max|u_f|$ results as well as the J_6 and J_{12} parameters that measure the performance in terms of control forces, the third controller has the most successful result. Similarly, the third controller, which is a linear regression-based controller, has the least controller mass displacement as shown in the criteria J_5, J_{11}, σ_{yd}, and $max|y_d|$.

Table 5.4 Evaluation criteria results for the Kobe Earthquake of three different controllers tested in the structure with original stiffness values

	$C1$	$C2$	$C3$		$C1$	$C2$	$C3$
J_1	0.4384	0.4398	0.4317	J_7	0.8569	0.8582	0.8648
J_2	0.4013	0.4016	0.3927	J_8	0.7240	0.7254	0.7329
J_3	0.4145	0.4133	0.4117	J_9	0.6758	0.6758	0.6749
J_4	0.4171	0.4161	0.4146	J_{10}	0.7111	0.7107	0.7097
J_5	2.3642	2.3556	2.3611	J_{11}	4.1706	4.1709	4.1884
J_6 $(kN\ m/s)$	0.8873	0.8841	0.8626	J_{12} $(kN\ m/s)$	7.9411	7.9374	5.9972
σu_f (kN)	8.5343	8.4952	7.1349	$max\|u_f\|$ (kN)	40.9814	41.0433	27.6912
σ_{yd} (cm)	2.7878	2.7776	2.7842	$max\|y_d\|$ (cm)	14.8851	14.8861	14.9487

Table 5.5 Evaluation criteria results for the Kobe Earthquake of three different controllers tested in the structure with flexible stiffness values

	$C1$	$C2$	$C3$		$C1$	$C2$	$C3$
J_1	0.2425	0.2448	0.2429	J_7	0.8733	0.8781	0.8628
J_2	0.2028	0.2040	0.2003	J_8	0.7181	0.7210	0.7195
J_3	0.1876	0.1877	0.1870	J_9	0.5476	0.5477	0.5461
J_5	1.1395	1.1390	1.1409	J_{11}	3.5496	3.5510	3.5755
J_4	0.1890	0.1891	0.1884	J_{10}	0.5812	0.5811	0.5802
J_6 $(kN\ m/s)$	1.0429	1.0435	1.0237	J_{12} $(kN\ m/s)$	10.4205	10.4846	7.6382
σu_f (kN)	8.5806	8.5605	7.2040	$max\|u_f\|$ (kN)	47.0336	47.1016	31.6914
σ_{yd} (cm)	2.9876	2.9862	2.9911	$max\|y_d\|$ (cm)	16.8031	16.8097	16.9255

Table 5.6 Evaluation criteria results for the Kobe Earthquake of three different controllers tested in the structure with rigid stiffness values

	$C1$	$C2$	$C3$		$C1$	$C2$	$C3$
J_1	0.2860	0.2878	0.2869	J_7	0.8971	0.8991	0.9149
J_2	0.2492	0.2501	0.2457	J_8	0.7594	0.7609	0.7527
J_3	0.2556	0.2551	0.2543	J_9	0.7152	0.7148	0.7121
J_4	0.2585	0.2581	0.2572	J_{10}	0.7210	0.7208	0.7180
J_5	1.3692	1.3654	1.3689	J_{11}	4.1482	4.1482	4.1353
J_6 $(kN\ m/s)$	0.7972	0.7973	0.7707	J_{12} $(kN\ m/s)$	8.9020	8.9206	6.7117
σu_f (kN)	8.0386	8.0043	6.5368	$max\|u_f\|$ (kN)	44.4543	44.5471	31.2528
σ_{yd} (cm)	2.3951	2.3885	2.3946	$max\|y_d\|$ (cm)	13.1218	13.1218	13.0809

Table 5.4, Table 5.5, and Table 5.6 give the performance results of the nine-story building with three different stiffness values, which was exposed to the Kobe Earthquake. Controllers give very close results in terms of structure acceleration, structure displacement, and control mass displacement results for three different structures, on the other hand, it is seen that a linear regression-based controller needs less control effort to achieve the control goal.

Table 5.7 Evaluation criteria results for the El Centro Earthquake of three different controllers tested in the structure with original stiffness values

	$C1$	$C2$	$C3$		$C1$	$C2$	$C3$
J_1	0.2057	0.2061	0.2042	J_7	0.6634	0.6660	0.6612

Table 5.7 Continues

J_2	0.1989	0.1991	0.1966	J_8	0.6058	0.6082	0.6056
J_3	0.2731	0.2728	0.2724	J_9	0.7424	0.7428	0.7434
J_4	0.2797	0.2795	0.2791	J_{10}	0.7347	0.7352	0.7361
J_5	1.5482	1.5469	1.5515	J_{11}	3.9888	3.9883	3.9870
J_6 $(kN\ m/s)$	2.4689	2.4643	2.4372	J_{12} $(kN\ m/s)$	23.9200	24.2230	21.1709
σu_f (kN)	12.7441	12.7330	11.9023	$max\|u_f\|$ (kN)	83.9573	84.8736	73.0707
σ_{yd} (cm)	4.6043	4.6003	4.6140	$max\|y_d\|$ (cm)	19.6530	19.6839	19.8749

Table 5.8 Evaluation criteria results for the El Centro Earthquake of three different controllers tested in the structure with flexible stiffness values

	$C1$	$C2$	$C3$		$C1$	$C2$	$C3$
J_1	0.2595	0.2601	0.2562	J_7	0.6961	0.6991	0.6998
J_2	0.2521	0.2525	0.2477	J_8	0.6595	0.6616	0.6434
J_3	0.3358	0.3355	0.3349	J_9	0.7947	0.7951	0.7957
J_4	0.3432	0.3429	0.3423	J_{10}	0.7976	0.7981	0.7987
J_5	2.0771	2.0766	2.0830	J_{11}	4.6167	4.6196	4.6174
J_6 $(kN\ m/s)$	2.5819	2.5798	2.5515	J_{12} $(kN\ m/s)$	27.8284	27.5442	22.5587
σu_f (kN)	12.9682	12.9626	12.1510	$max\|u_f\|$ (kN)	88.5336	88.2981	73.4898
σ_{yd} (cm)	5.1298	5.1285	5.1445	$max\|y_d\|$ (cm)	21.5504	21.5073	21.5106

Table 5.9 Evaluation criteria results for the El Centro Earthquake of three different controllers tested in the structure with rigid stiffness values

	$C1$	$C2$	$C3$		$C1$	$C2$	$C3$
J_1	0.2549	0.2554	0.2495	J_7	0.7769	0.7805	0.7707
J_2	0.2442	0.2444	0.2393	J_8	0.7426	0.7442	0.7343
J_3	0.3415	0.3410	0.3407	J_9	0.8083	0.8086	0.8098
J_4	0.3502	0.3497	0.3495	J_{10}	0.7987	0.7991	0.8003
J_5	1.7987	1.7962	1.8028	J_{11}	4.0642	4.0617	4.0588
J_6 $(kN\ m/s)$	2.2519	2.2448	2.2307	J_{12} $(kN\ m/s)$	22.5288	22.4815	19.2300
σu_f (kN)	12.2714	12.2584	11.3959	$max\|u_f\|$ (kN)	81.2324	79.9121	71.5882
σ_{yd} (cm)	4.0949	4.0894	4.1042	$max\|y_d\|$ (cm)	20.5040	20.5091	20.7048

Table 5.10 Evaluation criteria results for the Imperial Valley-06 Earthquake of three different controllers tested in the structure with original stiffness values

	$C1$	$C2$	$C3$		$C1$	$C2$	$C3$
J_1	0.2081	0.2096	0.2090	J_7	0.4427	0.4453	0.4534
J_2	0.1893	0.1900	0.1888	J_8	0.4820	0.4838	0.4845
J_3	0.1811	0.1807	0.1798	J_9	0.4513	0.4514	0.4495
J_4	0.1804	0.1801	0.1793	J_{10}	0.4423	0.4423	0.4406
J_5	1.0057	1.0013	1.0007	J_{11}	2.3866	2.3812	2.3739
J_6 $(kN\ m/s)$	3.5903	3.5825	3.5573	J_{12} $(kN\ m/s)$	27.8939	27.8250	24.1119
σu_f (kN)	13.1071	13.0656	12.2271	$max\|u_f\|$ (kN)	64.1600	64.2026	56.1255
σ_{yd} (cm)	4.6544	4.6338	4.6314	$max\|y_d\|$ (cm)	19.5052	19.4171	19.3037

Table 5.11 Evaluation criteria results for the Imperial Valley-06 Earthquake of three different controllers tested in the structure with flexible stiffness values

	$C1$	$C2$	$C3$		$C1$	$C2$	$C3$
J_1	0.1666	0.1669	0.1652	J_7	0.4992	0.5003	0.4954
J_2	0.1570	0.1573	0.1555	J_8	0.5001	0.5011	0.4986
J_3	0.1437	0.1437	0.1427	J_9	0.3426	0.3427	0.3391
J_4	0.1429	0.1429	0.1419	J_{10}	0.3355	0.3357	0.3330
J_5	0.8173	0.8158	0.8149	J_{11}	1.9025	1.9030	1.8972
J_6 $(kN\ m/s)$	2.6077	2.6125	2.5865	J_{12} $(kN\ m/s)$	17.9050	17.9494	14.6756
σu_f (kN)	12.0282	12.0081	11.0777	$max\|u_f\|$ (kN)	55.6723	55.3295	43.8873
σ_{yd} (cm)	4.3181	4.3099	4.3056	$max\|y_d\|$ (cm)	16.3124	16.3091	16.1434

Table 5.12 Evaluation criteria results for the Imperial Valley-06 Earthquake of three different controllers tested in the structure with rigid stiffness values

	$C1$	$C2$	$C3$		$C1$	$C2$	$C3$
J_1	0.1908	0.1909	0.1887	J_7	0.5325	0.5322	0.5184
J_2	0.1812	0.1811	0.1791	J_8	0.5583	0.5592	0.5480
J_3	0.1885	0.1878	0.1870	J_9	0.4891	0.4893	0.4883
J_4	0.1883	0.1877	0.1869	J_{10}	0.4860	0.4862	0.4857
J_5	1.0210	1.0150	1.0166	J_{11}	2.4749	2.4602	2.4524
J_6 $(kN\ m/s)$	3.5311	3.5107	3.4968	J_{12} $(kN\ m/s)$	27.1006	27.0406	23.0268
σu_f (kN)	12.9441	12.8855	12.0604	$max\|u_f\|$ (kN)	67.2066	67.2423	57.0429
σ_{yd} (cm)	4.4819	4.4557	4.4625	$max\|y_d\|$ (cm)	18.6323	18.6048	18.7811

The evaluation results of three different structures and three different controllers for the El Centro and Imperial Valley-06 earthquakes are given in Table 5.7 to Table 5.12. The performance criteria of the controllers, whose performance is quite high, are obtained very close to each other, especially in the performance criteria of construction acceleration and construction displacement. In addition, the tests for El Centro and Imperial Valley-06 earthquakes, as well as the Kocaeli and Kobe earthquakes, the third controller, which has a robust adaptive controller design supported by linear regression, can produce performances close to other controllers with less control effort and achieve the control purpose. The reason for this is the first and second controllers require displacement and velocity measurements from three masses, the top floor, the penultimate floor, and the controller mass, to generate the control signal. The third controller only uses the states of the structure's last floor for controller design. Its controller architecture, unlike that of other controllers, incorporates the acceleration state as well as velocity and displacement states. Signal to noise ratio (SNR) of additive white gaussian noise selected the same value to add to all measurements in order to make an evaluation under equal conditions in these evaluation criteria. The first two controllers need six signals by nature, but the third controller only requires three measurements, therefore the amount of noise it is exposed to is less. This is the reason for the relatively low control effort of the third controller compared to the other two controllers among the three robust adaptive controllers based on the Lyapunov stability analysis.

The control gain values of the controllers whose performance was tested for three different structures and with four different earthquakes were used at the values presented in the relevant chapters throughout all the tests. It has been proven that the proposed controllers will achieve the control purpose by producing satisfactory results while guaranteeing the system stability for different structures and different earthquakes.

5.4 Conclusions

Considering the displacement-based evaluation criteria J_3, J_4, J_9 and J_{10}, although the results are extremely close, it is seen that the Lineer regression model-based controller performs better. In the J_1, J_2, J_7 and J_8 criteria, which are acceleration-based evaluation criteria, the control design designed in Chapter 2 and which only guarantees the stability of the structure is more successful. In the evaluation criteria of control effort and control mass displacement, it is clearly seen that the LR model-based controller design is more successful. Unlike the other two controllers, it has a stronger structure against disturbance effects such as measurement error and sensor noise, as it compensates the states of the penultimate floor and controller mass with the help of linear regression using only the sensor data to the last floor.

CHAPTER SIX
AN ADAPTIVE CONTROLLER DESIGN FOR ATMD SYSTEM USED IN STRUCTURES UNDER THE EFFECT OF UNKNOWN NONLINEAR EFFECTS

6.1 Introduction

The building structures have been modeled linearly in the majority of studies so far in the literature. As a result, the controls in these researches are linear as well. Only a few studies have considered the nonlinear dynamics of multi-story structures, however, in these works, linear control schemes employing various linearization approaches are provided. Nonlinear behavior is the inherent behavior of multi-story buildings with ATMD systems. As a consequence, studying nonlinear dynamics while designing a nonlinear controller is regarded to be a more realistic approach. Furthermore, numerous unpredictable external factors should be considered during control design to guarantee that the control systems are able to operate securely in any environment. In this chapter, the linear model of the multi-story building is reconfigured by adding nonlinear ambiguous functions to create a more realistic approach. It is assumed in this chapter that the structural parameters were unknown at the time of controller design. Band-limited white noise has been added to the system equation of the structure as a f_n function. This function is used in this chapter, taking into account the nonlinear parameters, measurement noise, and uncertain dynamics. A completely robust control strategy is proposed to provide robustness against these uncertain and nonlinear dynamics of the structure. The controller designed with a robust adaptive structure can be applied to different buildings with different structural parameters. The designed controller also compensates for the unknown system parameters with the term compensation and overcomes the system nonlinearities owing to its nonlinear structure. Theoretically, Lyapunov-based arguments are used to show that the developed controller can keep the structure stable while attaining the main control aim. Matlab-Simulink is used to analyze the performance of the developed controllers.

6.2 Structure Model and Controller Design

The nine-story building structure is selected the use in this chapter as a model. The ATMD system is placed on the top floor, as seen in Figure 6.1. m_i, k_i and b_i represent mass, stiffness, and damping coefficients of stories of the structure, respectively. In addition to m_d, k_d and b_d represent mass, stiffness, and damping coefficients of ATMD systems, respectively.

In these types of rigid structures, vibration suppression is realized based on the fact that damping the vibration of the top floor during an earthquake is enough for damping the vibration of the whole building. In such applications, damping systems placed on the top floor of the building are used to reduce the vibration of the building. Therefore, a control system can be designed by focusing on the displacement of the last floor of the building. In other words, the control problem can mathematically be started from the following equation.

Equations of motion of a nine-story building under earthquake excitation with the ATMD are given below;

$$m_i\ddot{y}_i + b_i(\dot{y}_i - \dot{y}_{i-1}) - b_{i+1}(\dot{y}_{i+1} - \dot{y}_i) + k_i(y_i - y_{i-1}) - k_{i+1}(y_{i+1} - y_i) = 0 \text{ for } i = 1, \dots, n-1 \quad (6.1)$$

$$m_n\ddot{y}_n + b_n(\dot{y}_n - \dot{y}_{n-1}) - b_d(\dot{y}_d - \dot{y}_n) + k_n(y_n - y_{n-1}) - k_d(y_d - y_n) + f_n = u_f \quad (6.2)$$

$$m_d\ddot{y}_d + b_d(\dot{y}_d - \dot{y}_n) + k_d(y_d - y_n) = -u_f \quad (6.3)$$

In Equation (6.1), For the case where i = 1, y_0 and $\dot{y}_0$ represents the displacement and velocity of ground motion.

In Equation (6.2) f_n represents nonlinearity, noise, and other uncertainties. In Equation (6.2) and Equation (6.3),u_f symbolize the force applied to the control mass to mitigate the vibration of the building.

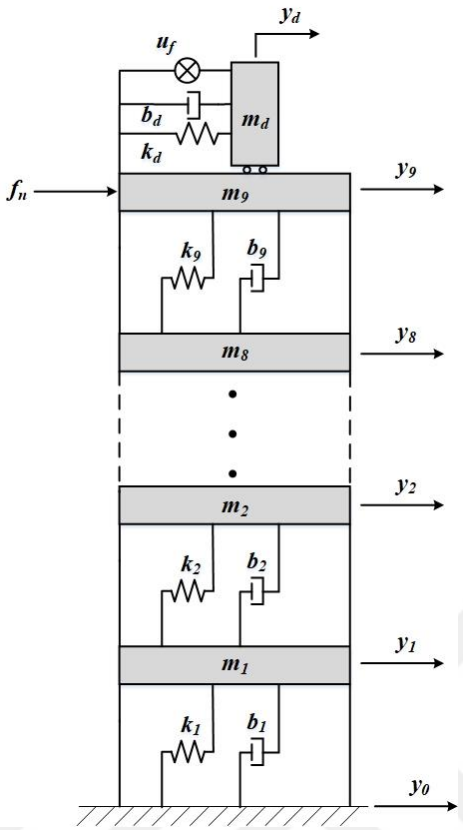

Figure 6.1 Building structure model under earthquake excitation ATMD systems on the top floor.

The Equation (6.2) can be rearranged as

$$m_9\ddot{y}_9 + f_m(\dot{y}_8, \dot{y}_9, \dot{y}_d, y_8, y_9, y_d) + f_n = u_f \tag{6.4}$$

where f_m represents a remaining function, which includes system states and system parameters. Equation (6.5), it is aimed to assign the state to be controlled in Equation (6.4) to a variable and make it proper for the control design.

$$x = y_9 \tag{6.5}$$

The auxiliary error term $e \in \mathbb{R}$ is defined as

$$e \triangleq u_v - \dot{y}_9 \tag{6.6}$$

Time Derivative of Equation (6.6) multiplied by m_9

$$m_9\dot{e} = m_9\dot{u}_v - m_9\ddot{y}_9 \tag{6.7}$$

Design virtual controller

$$u_v \triangleq -g_1 x \tag{6.8}$$

where $g_1 \in \mathbb{R}^+$ denotes the positive constant control gain.

The time derivative of Equation (6.8) is used in Equation (6.7). The Equation (6.7) is rearranged utilizing Equation (6.4) and is obtained Equation (6.9).

$$m_9\dot{e} = -m_9 g_1 \dot{y}_9 - u_f + f_m + f_n. \tag{6.9}$$

In Equation (6.9), $(f_m - m_9 g_1 \dot{y}_9)$ terms are defined as

$$(f_m - m_9 g_1 \dot{y}_9) \triangleq \mathbf{C}\boldsymbol{\phi} \tag{6.10}$$

where $\mathbf{C} \in \mathbb{R}^{1x6}$ represents the vector of uncertain coefficients, $\boldsymbol{\phi}(\dot{y}_8, \dot{y}_9, \dot{y}_d, y_8, y_9, y_d) \in \mathbb{R}^{6x1}$ represents the certain vector of base functions. Rearranging Equation (6.9) by using Equation (6.10)

$$m_9\dot{e} = -u_f + \mathbf{C}\boldsymbol{\phi} + f_n \tag{6.11}$$

Uncertain coefficients vector $\mathbf{C}$ is adaptively compensated using compensator error $\tilde{\mathbf{c}} \in \mathbb{R}^{1\times6}$ and compensator vector $\hat{\mathbf{C}} \in \mathbb{R}^{1\times6}$defined as

$$\tilde{\mathbf{C}} = \mathbf{C} - \hat{\mathbf{C}} \tag{6.12}$$

Design the controller

$$u_f = \hat{\mathbf{C}}\boldsymbol{\phi} + \rho_b tanh(e) + g_2 e. \tag{6.13}$$

where $g_2 \in \mathbb{R}^+$ denotes the positive constant control gain. and $\rho_b \in \mathbb{R}^+$denotes the positive bounding constant of the modeling error and ρ_b is selected as

$$|f_n| \leq \rho_b. \tag{6.14}$$

The Lyapunov function is defined as

$$V \triangleq \frac{1}{2} y_9^2 + \frac{1}{2} m_9 e^2 + \frac{1}{2} \tilde{\mathbf{C}}^{\boldsymbol{T}} \hat{\mathbf{C}}. \tag{6.15}$$

The time derivative of Equation (6.15)

$$\dot{V} = -g_1 y_9^2 - g_2 e^2 + \tilde{\mathbf{C}}^{\boldsymbol{T}} \left(\dot{\hat{\mathbf{C}}} + \boldsymbol{\phi}^{\boldsymbol{T}} \boldsymbol{e} \right) + e[f_n - \rho_b tanh(e)] \tag{6.16}$$

The adaptive compensation rules are determined from Equation (6.17)

$$\dot{\hat{\mathbf{C}}} = -\boldsymbol{\phi}^{\boldsymbol{T}} r \tag{6.17}$$

In Equation (6.16), $\dot{V}$ is nonpositive and that provides the Lyapunov stability criterion.

$$\dot{V} \leq -\beta \|\mathbf{z}\|^2 \tag{6.18}$$

where $\mathbf{z} \in \mathbb{R}^2$ is a vector defined as

$$\mathbf{z} \triangleq [x \quad e]^T \tag{6.19}$$

and $\beta \in \mathbb{R}^+$ denotes a positive constant selected as

$$\beta = \min \{g_1, g_2\} \tag{6.20}$$

From Equation (6.15) and the bound of its time derivative Equation (6.18), it is seen that $\mathbf{z}(t) \in \mathcal{L}_\infty$. Boundedness of this term guarantees the boundedness of x and e. From its design in Equation (6.8), it is seen that boundedness of x guarantees the boundedness of u_v. Boundedness of the virtual control input can be utilized along with the boundedness of e and its definition in Equation (6.6) to show that $\dot{y}_9 \in \mathcal{L}_\infty$. Boundedness of $\dot{y}_9$ is utilized along with Equation (6.5) and can be utilized with the time derivative of Equation (6.7) to show that $\dot{u}_v \in \mathcal{L}_\infty$. Boundedness of $\dot{u}_v$ can be used with the time derivative of Equation (6.6) to show that $\dot{e} \in \mathcal{L}_\infty$. Boundedness of $\dot{y}_9$ and $\dot{e}$ guarantees the boundedness of $\dot{\mathbf{z}}(t)$. All of the remaining signals under the closed-loop operation can be shown via standard signal chasing arguments.

The following equation guarantees that $\mathbf{z}(t) \in \mathcal{L}_2$, integration of Equation (6.18) that can be obtained as follows is utilized

$$\int_0^\infty \|\mathbf{z}(\sigma)\|^2 d\sigma \leq \frac{V(0)}{\beta} \tag{6.21}$$

Boundedness of $\dot{\mathbf{z}}(t)$ can be utilized with $\mathbf{z}(t) \in \mathcal{L}_2 \cap \mathcal{L}_\infty$ and Barbalat's Lemma (Krstic & Smyshlyaev, 2007) to prove semi-global asymptotic stability of $\mathbf{z}(t)$ that guarantees the main purpose of the control design in the sense that

$$x, e \to 0 \text{ as } t \to \infty. \tag{6.22}$$

6.3 Simulation Studies

The numerical parameters of the nine-story building model used in the simulation studies are given in Table 2.1(Hacioglu & Yagiz, 2012). The determined structure is exposed to the Kocaeli earthquake in Turkey on 17 August 1999. Acceleration, velocity, and displacement of ground motion are shown in Figure 4.1.

One of the most significant benefits of Lyapunov-based control design techniques is that the theoretical limits of control gains that preserve overall system stability can be found in the stability analysis. Control gains can then be chosen from stated rules through trial and error, as long as the system's overall stability is assured. According to the stability analysis described in the article, choosing positive defined control gains is sufficient to guarantee the stability of the system.

The control design in Equation (6.13) is applied from the actuator input and the control gains are selected as follows via trial and error method

$$g_1 = 360,\ g_2 = 4700, \rho_b = 1 \tag{6.23}$$

Uncontrolled system, TMD control system, and ATMD control system were examined. Figure 6.2 shows the vibration of the ninth floor during the earthquake for these three different situations. The TMD system reduces the vibration response compared to an uncontrolled situation, but it has been observed that the amplitude of the vibration and the time taken to reduce the vibration is much higher than the ATMD system. The root mean square (RMS) and peak values of three different cases are given in Table 6.1. In RMS values, TMD showed 51.44% vibration reduction compared to uncontrolled conditions, while ATMD achieved 56.76% improvement in vibration response compared to TMD. According to peak values, the ATMD system reached a 25% better result than the TMD controller. It is seen that the designed controller is used together with ATMD systems to significantly reduce vibrations caused by earthquakes in structures containing nonlinear parameters.

As can be seen in Figure 6.3, the controller mass displacement remained within a reasonable range. Figure 6.4 shows the variation of the force required to be applied to the controller mass during the earthquake to dampen vibrations caused by the earthquake.

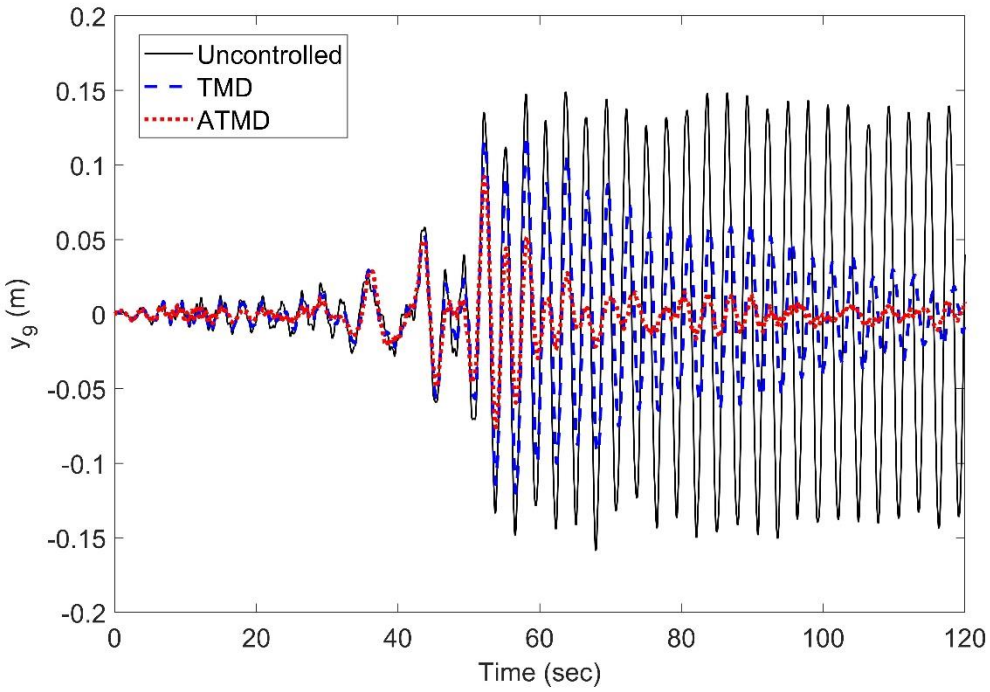

Figure 6.2 Displacement of nineth story of building for three different case

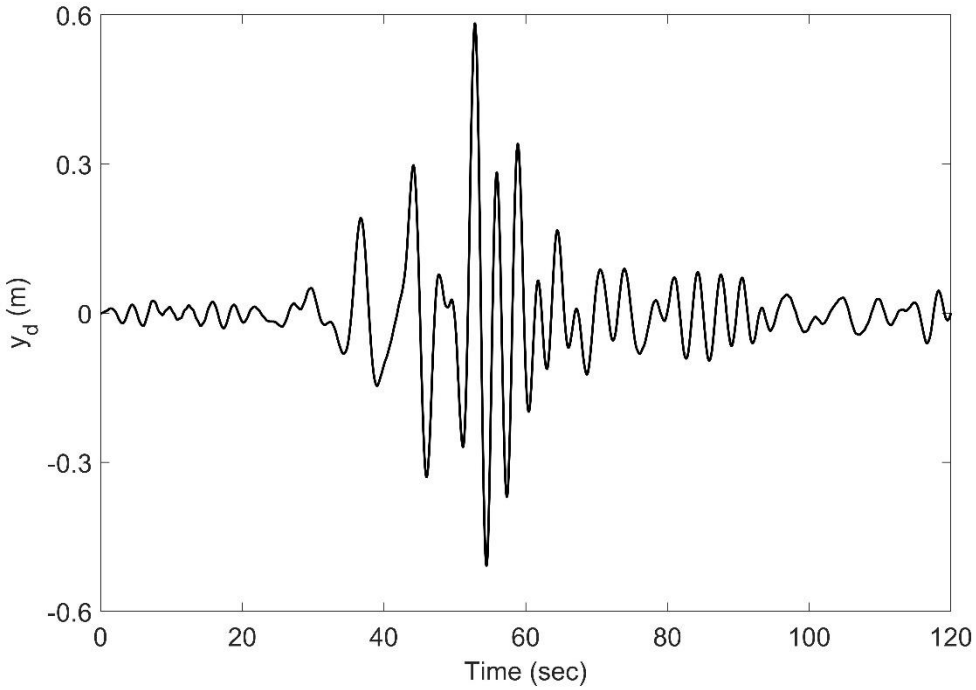

Figure 6.3 Displacement of ATMD mass

Table 6.1 Statistical values of last story displacement

	Uncontrolled (m)	TMD (m)	ATMD (m)
RMS	0.0745	0.0370	0.0160
Peak	0.1587	0.1199	0.0920

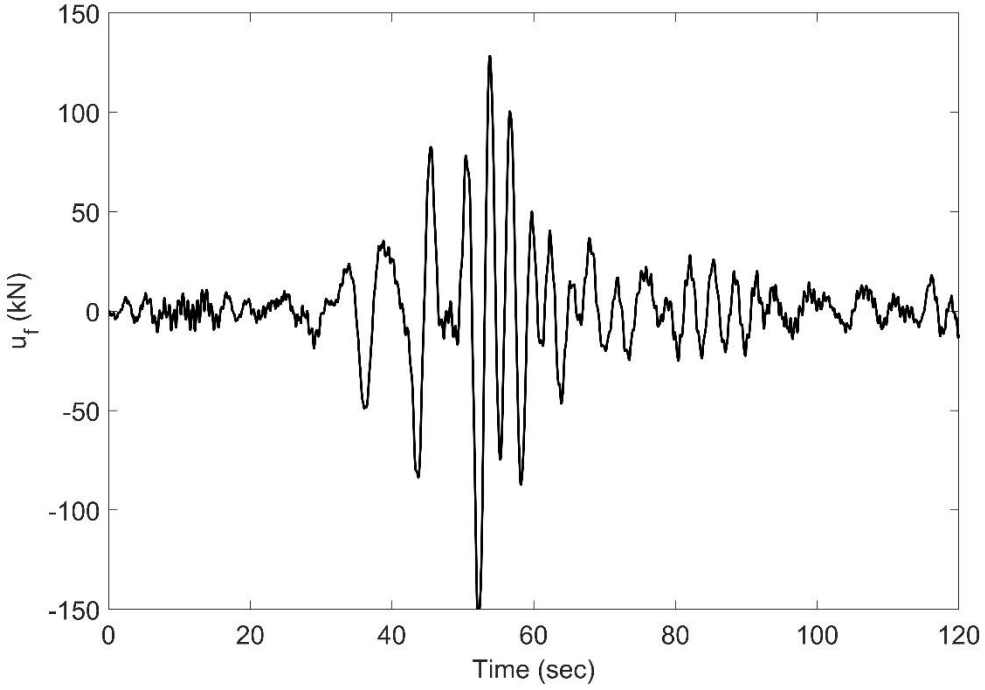

Figure 6.4 Controller force applied to the ATMD for vibration attenuation of structure

Figure 6.5(a), 6.5(b), 6.5(c), 6.5(d), 6.5(e), and 6.5(f) shows the adaptive compensations of the uncertain parameters $\hat{\mathbf{C}}_1, \hat{\mathbf{C}}_2, \hat{\mathbf{C}}_3, \hat{\mathbf{C}}_4, \hat{\mathbf{C}}_5$ and $\hat{\mathbf{C}}_6$, respectively. The term compensation is used to achieve the control objective. The numerical values of these terms are irrelevant provided they change within a limited range. The variation of compensation parameters in a limited range while vibration control is taking place during an earthquake as shown in Figure 6.5.

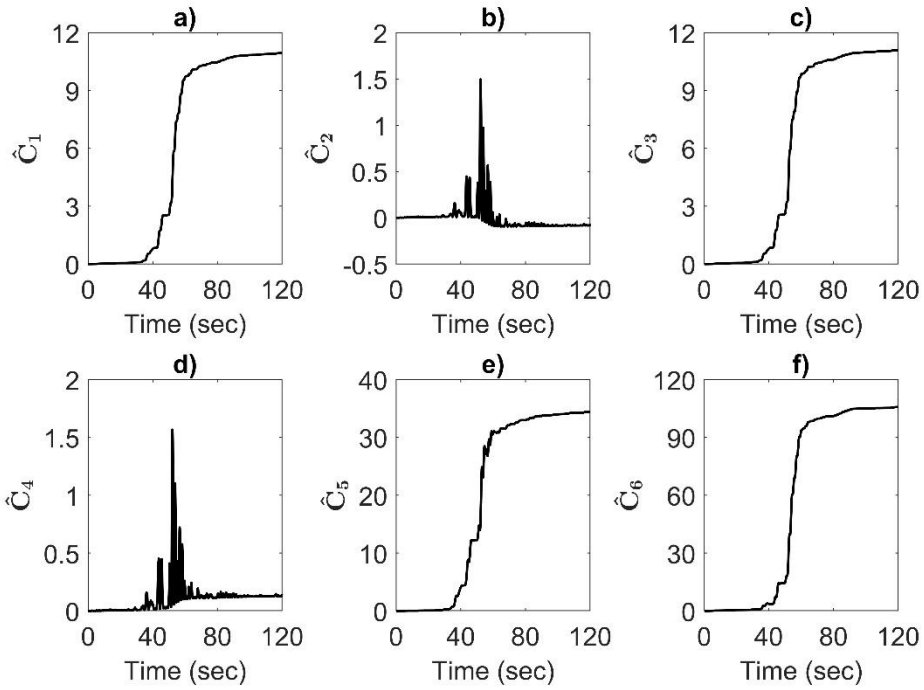

Figure 6.5 Changing values of compensation parameters during the earthquake

6.4 Conclusions

In this chapter, a Lyapunov based adaptive controller is designed to reduce the vibration of a nine-story building under earthquake effect. In order to get a more realistic approach, the linear model of the multi-story building has been rearranged by adding a nonlinear function f_n. This function represents the nonlinear parameters, measurement noise, and uncertain dynamics in the mathematical model. Band limited white noise is used instead of defined nonlinear uncertain function in this chapter. The main purpose of controller design is to reduce vibrations of building structure stories under earthquake excitation with ATMD placed on the top floor. A completely robust control strategy is proposed to ensure the robustness of the designed structure against uncertain and nonlinear dynamics. The designed controller can compensate for the coefficient of the remaining function that includes system parameters independently of the system model. Top floor displacements have been compared for three different situations, uncontrolled, TMD and ATMD, and the damping effect of the ATMD system driven by the designed controller is quite successful. It is theoretically proved

by using Lyapunov-based arguments that the designed controller can maintain the stability of the structure while achieving this main control goal.

CHAPTER SEVEN
ADAPTIVE BACKSTEPPING CONTROL DESIGN FOR ATMD SYSTEMS IN NONLINEAR STRUCTURES WITH NONLINEAR DISTURBANCE AND PARAMETRIC UNCERTAINTIES

7.1 Introduction

Building structures are commonly modeled linearly in structural vibration control studies with ATMD in the literature. In Chapter 6, an auxiliary function has been added to the system as a disturbing input and the nonlinearity of the system has been tried to be simulated. In this section, a Lyapunov-based adaptive controller is designed for a nonlinear structure and a nonlinear ATMD system by taking the previous design one step further.

Physical system models typically incorporate various kinds of uncertainty. These uncertainties generally arise from material and geometric nonlinearities, but also possible uncertain external effects like measurement noise, unmodeled dynamics, etc. Nonlinear behavior is the natural behavior of multi-story buildings with ATMD systems. Therefore, studying nonlinearity in structural systems has been a necessary area of research in recent years. Along with these studies, vibration reduction and performance improvement of nonlinear systems under major earthquakes have recently attracted the attention of researchers (Aghabalaei Baghaei et al., 2019). For this reason, a large number of controllers have been designed to be used with various vibration dampening systems in models containing various nonlinearities. However, in buildings where nonlinear models are used, which have increased in recent years, linear building models placed on a nonlinear base isolator are often preferred instead of using a completely nonlinear structure.

Nonlinear systems have complex behavior when compared to linear systems. Numerous nonlinear models have been developed by researchers to model these complex behaviors. The Duffing oscillator, which is a second-order differential equation with nonlinear cubic stiffness, is often preferred in nonlinear problems

(Ghandchi Tehrani & Elliott, 2014; Mañosa et al., 2005). One of the characteristic features of a Duffing oscillator is its chaotic behavior tendency when forced by a periodic force (Fang et al., 2001; Ghandchi-Tehrani et al., 2015; Novak & Frehlich, 1982). In addition to the difficulty of dealing mathematically with typical nonlinear systems, these types of systems are equally challenging to control. To overcome this difficulty, various linearization approaches such as feedback linearization, linearization around equilibrium points, etc. have been used in vibration control studies for nonlinear modeled structures(Anh & Nguyen, 2012; Ghaffarzadeh et al., 2020; Socha & Blachuta, 2000). To improve the performance of nonlinear duffing systems exposed to nonstationary random excitations, Aghabalaei Baghaei et al., (2019) applied equivalent linearization (EL) and SMC techniques. As a result of this linearization, linear control strategies are used for ATMD systems. However, while designing controllers for a structure with nonlinear dynamics, it is seen as a more realistic approach to design a nonlinear controller.

In controller design for ATMD systems, it is a critical strategy to create a controller that just requires system states. Because a controller design based on the assumption that the system parameters are completely or partially known is not a practical approach when it comes to a construction system. ATMD systems, which are used for damping structural vibrations, are very useful systems not only for new structures but also for existing structures. In particular, it is not possible to estimate the system parameters of existing structures with absolute accuracy. A controller design that includes system parameters is very inefficient when these values cannot be used correctly. It even has the potential to be dangerous by increasing vibration and producing control responses that can cause resonance. In addition, a control design free from system parameters will be in a generalized form that can be used not only for a single structure but also for all structures with the same mathematical model. Considering the aforementioned cases, it seems that system parameters free control design is appropriate for this type of system.

A vital point that should not be neglected in the design of the controller for ATMD systems is to support the controller with a stability analysis that guarantees the stability

of the system. When controller designs whose stability is not mathematically guaranteed are used in such ATMD systems, the system may be unstable due to the control input effect. This situation can be more harmful to the structure than an earthquake. In this case, it should theoretically be assured that the proposed controller can achieve zero convergence of all structural states and ensure the overall system's stability during the control process.

The major aim of this chapter is to develop a controller that can mitigate earthquake-induced vibrations on a nonlinear structure using ATMD systems without relying on system characteristics. It is aimed to eliminate parametric uncertainties by employing compensation terms that are recommended based on the existing system circumstances. Another motivation for this approach is that controllers equipped with such compensation rules require much less control effort than traditional robust controller designs for nonlinear structures, as evidenced many times in the control literature to control various linear systems. Considering its appropriateness for these types of vibration control work, a backstepping control method was used in the controller design. It is theoretically supported by Lyapunov-based arguments to show that the developed controller can achieve zero convergence of all fundamental displacements and maintain system stability throughout the control process. A nonlinear nine-story building model that was subjected to a severe earthquake was utilized for the simulation studies of the proposed controller. Matlab/Simulink was used to conduct the simulation studies required for this research.

7.2 Optimal TMD Design for SDOF Structures

Calculations for optimal TMD are taken from Krenk, (2005). The optimal TMD calculations for the generalized SDOF system are given below.

The TMD is placed at the top of the structure as shown in Figure 7.1. It is characterized by the mass m_d the stiffness k_d and the viscous damping c_d. The equation of motion of the SDOF system with TMD is given Equation (7.1) and Equation (7.2).

$$m_s\ddot{y}_s + b_s(\dot{y}_s - \dot{y}_0) - b_d(\dot{y}_d - \dot{y}_s) + k_s(y_s - y_0) - k_d(y_d - y_s) = 0 \quad (7.1)$$

$$m_d\ddot{y}_d + b_d(\dot{y}_d - \dot{y}_s) + k_d(y_d - y_s) = 0 \quad (7.2)$$

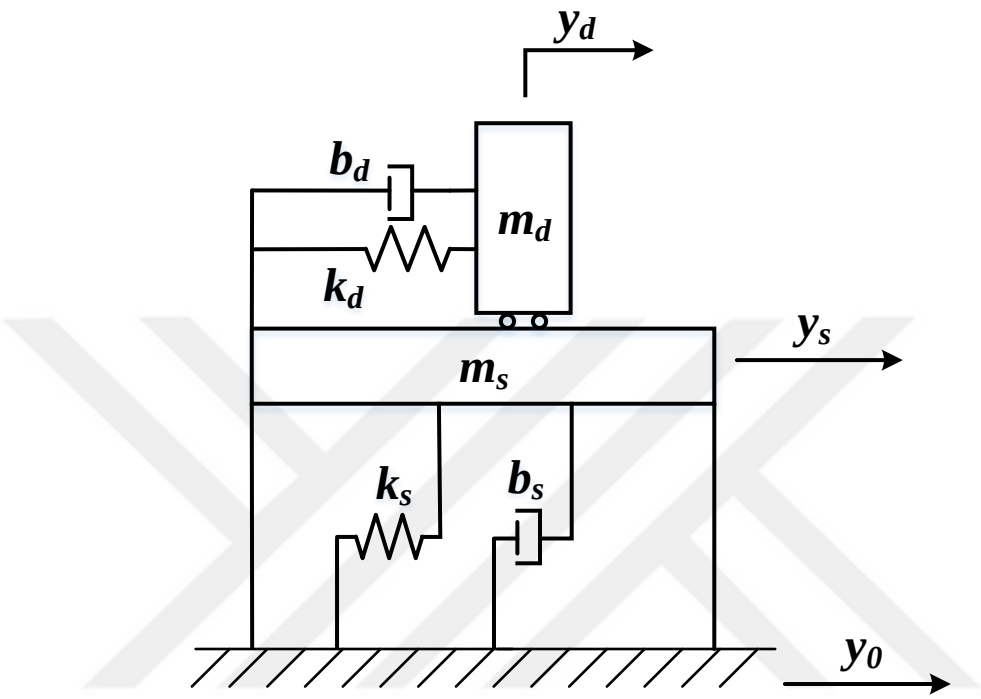

Figure 7.1 Model of a SDOF structure with a TMD.

The natural frequency of TMD ω_d is calculated as follows:

$$\omega_d = \frac{\omega_s}{1+\mu} \quad (7.3)$$

Where μ represents the mass ratio, and damping ratio of TMD ξ_d as

$$\xi_d = \sqrt{\frac{1}{2}\frac{\mu}{1+\mu}} \quad (7.4)$$

The TMD structure in the nine-story structure used for simulation in Chapters 2, 3, 4, and 6 is developed by applying Equation (7.3) and Equation (7.4) given for an SDOF system. For this, firstly, the modal mass was calculated and the mass ratio was found.

Then, the TMD natural frequency was found and the stiffness value of the optimal TMD was determined. Then, the damping coefficient was determined by finding the TMD damping ratio from Equation (7.4). Table 7.1 shows the natural frequencies of the nine-story building.

Table 7.1 Computed Natural Frequencies of nine-DOF Structure without TMD

Mode No.	Frequency (Hz)
1.	0.35149
2.	1.4826
3.	2.7550
4.	4.0123
5.	5.1314
6.	6.1034
7.	7.0309
8.	8.0292
9.	9.0475

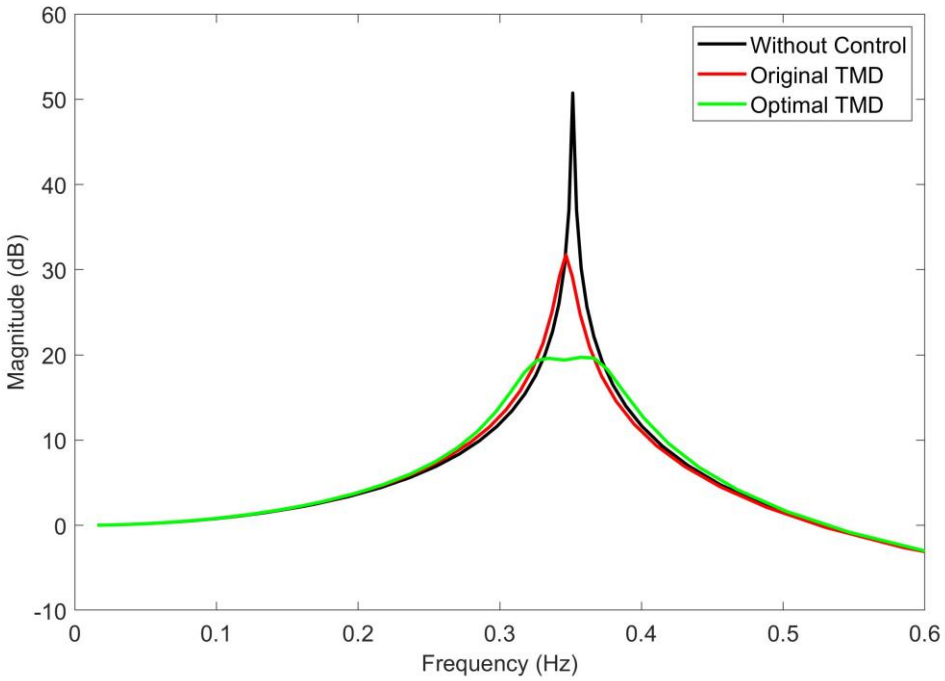

Figure 7.2 Frequency response of first natural frequency of nine-story structure for original and optimal TMD systems

During the optimal TMD design process for the nine DOF structure, initially, the modal mass was calculated. In this chapter, since an optimal TMD design with the same mass as the original TMD is desired, necessary calculations have been made on the condition that the original mass remains the same. After this stage, optimal TMD design is applied for the structure converted into an SDOF system. According to the calculations made according to Equation (7.3) and Equation (7.4), the stiffness constant for optimal TMD was calculated as $k_d = 319543.49\ \mathrm{N/m}$ and damping constant as $b_d = 33553.42\ \mathrm{Ns/m}$. The frequency response of the original and optimal TMD systems is given in Figure 7.2. As can be seen, as a result of the rearrangement of the TMD according to the optimal TMD equations, the peak at the first natural frequency of the structure in frequency response decreased by about 10dB compared to the original TMD. Both TMD systems are simulated by the 1999 Kocaeli earthquake as given in Figure 7.4. Table 7.2 shows the natural frequencies of the nine-story structure using optimal TMD.

Table 7.2 Computed Natural Frequencies of Structure with optimal TMD

Mode No.	Frequency (Hz)
1.	0.32689
2.	0.36753
3.	1.4848
4.	2.756
5.	4.0128
6.	5.1317
7.	6.1034
8.	7.0309
9.	8.0292
10.	9.0475

7.3 MDOF Duffing Structure System

The mathematical model of N story shear type duffing structure is given below,

$$\mathbf{M}\ddot{\mathbf{y}}(t) + \mathbf{C}\dot{\mathbf{y}}(t) + \mathbf{K}\mathbf{y}(t) + \mathbf{G}(t) + \boldsymbol{\psi} F_d = 0 \qquad (7.5)$$

where $\mathbf{M} \in \mathbb{R}^{n\times n}, \mathbf{C} \in \mathbb{R}^{n\times n}$ and $\mathbf{K} \in \mathbb{R}^{n\times n}$ represent mass, damping, and stiffness coefficient matrixes, respectively. F_d is the nonlinear disturbance term and $\boldsymbol{\psi} = [\mathbf{0}\ \mathbf{0} \dots \mathbf{0}\ \mathbf{1}]^{\boldsymbol{T}}$ is the (nxn) orientation vector for the nonlinear disturbance. $\mathbf{G}(t) \in \mathbb{R}^{n\times n}$ is the nonlinear term vector. $\mathbf{y}(t) = [\boldsymbol{y_0}\ \boldsymbol{y_1} \dots\ \boldsymbol{y_{n-1}}\ \boldsymbol{y_n}]^{\boldsymbol{T}}$ is the displacement vector and each element of this vector represents the related floor displacement. $\dot{\mathbf{y}}(t)$ and $\ddot{\mathbf{y}}(t)$ are first and second-time derivatives of the displacement vector. They represent the velocity vector and acceleration vector, respectively. The earthquake-induced ground motion is indicated by $y_0 \in \mathbb{R}$, and its first time derivative is the velocity of the ground motion is represented by $\dot{y}_0 \in \mathbb{R}$.

$$\mathbf{G}(t) = \begin{bmatrix} \alpha_1 k_1 x_1^3 - \alpha_2 k_2 x_2^3 \\ \alpha_2 k_2 x_2^3 - \alpha_3 k_3 x_3^3 \\ \alpha_3 k_3 x_3^3 - \alpha_4 k_4 x_4^3 \\ \vdots \\ \alpha_{n-1} k_{n-1} x_{n-1}^3 - \alpha_n k_n x_n^3 \\ \alpha_n k_n x_n^3 \end{bmatrix}; \begin{bmatrix} x_1 \\ x_2 \\ x_3 \\ \vdots \\ x_{n-1} \\ x_n \end{bmatrix} = \begin{bmatrix} y_1 - y_0 \\ y_2 - y_1 \\ y_3 - y_2 \\ \vdots \\ y_{n-1} - y_{n-2} \\ y_n - y_{n-1} \end{bmatrix} \tag{7.6}$$

The extended mathematical model of the top floor and control mass when a nonlinear optimum ATMD is installed on the top floor of the NDOF shear nonlinear building structure, described in Equation (7.5) and Equation (7.6), for vibration control purposes is as follows.

$$\begin{aligned} m_n\ddot{y}_n + b_n(\dot{y}_n - \dot{y}_{n-1}) - b_d(\dot{y}_d - \dot{y}_n) + k_n\alpha_n(y_n - y_{n-1}) \\ + k_n(1-\alpha_n)(y_n - y_{n-1})^3 - k_d\alpha_d(y_d - y_n) \\ - k_d(1-\alpha_d)(y_d - y_n)^3 + F_d = u_f \end{aligned} \tag{7.7}$$

$$m_d\ddot{y}_d + b_d(\dot{y}_d - \dot{y}_n) + k_d\alpha_d(y_d - y_n) + k_d(1-\alpha_d)(y_d - y_n)^3 = -u_f \tag{7.8}$$

where $m_d \in \mathbb{R}$ represents mass coefficient, $k_d \in \mathbb{R}$ represents stiffness coefficient and $b_d \in \mathbb{R}$ represents the damping coefficient for the ATMD system.

In Equation (7.7) and Equation (7.8) $m_n \in \mathbb{R}$ represents mass coefficient, $k_n \in \mathbb{R}$ represents stiffness coefficient, $b_n \in \mathbb{R}$ represents the damping coefficient, and $\alpha_n \in \mathbb{R}$ represents the nonlinearity coefficient for the last floor. $y_j \in \mathbb{R}$ and first and second-

time derivatives of the displacement represent the related floor's velocity and acceleration. As shown in Figure 7.3, the ATMD system features a tuned moveable mass whose movement is controlled by force input denoted by $u_f \in \mathbb{R}$. The specified controller mass moves in the horizontal axis as a consequence of the common action of spring and damping components and the applied force, and this movement is represented by displacement denoted by $y_d \in \mathbb{R}$.

In the aforementioned model, the mass coefficient $m_d \in \mathbb{R}$, stiffness coefficient $k_d \in \mathbb{R}$, damping coefficient $b_d \in \mathbb{R}$, and nonlinearity coefficient $\alpha_d \in \mathbb{R}$ are used to represent this movement mathematically. The ground motion caused by an earthquake is indicated by $y_0 \in \mathbb{R}$, and the velocity is represented by its first time derivative.

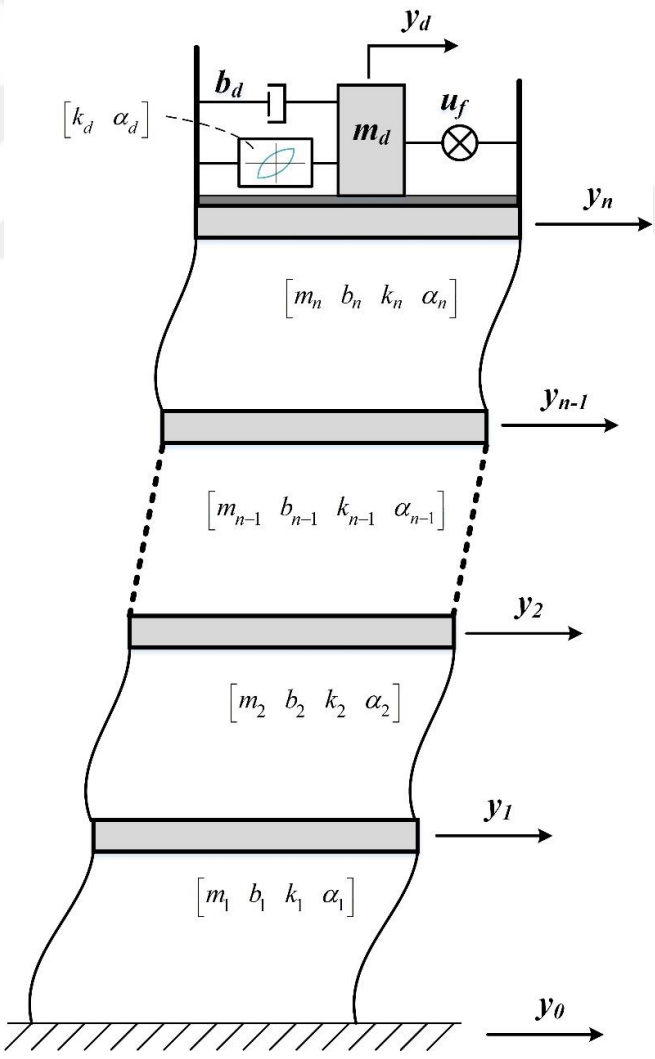

Figure 7.3 Model of nonlinear structure with nonlinear ATMD

7.4 Controller Design for nonlinear ATMD systems used in Nonlinear Structures

The control design and Lyapunov based stability analysis of closed loop system proposed in this section are based on the representation of multi-story nonlinear buildings controlled by the ATMD system against seismic vibrations with a generalized model similar to the system model.

$$\dot{x} = \dot{\xi}_n \tag{7.9}$$

$$p_1\ddot{\xi}_n = f\left(\xi_{n-1}, \xi_n, \xi_{n+1}, \dot{\xi}_{n-1}, \dot{\xi}_n, \dot{\xi}_{n+1}\right) + f_d - u_f \tag{7.10}$$

where $x, \xi_{n+1}, \xi_n, \xi_{n-1} \in \mathbb{R}$ and their first and second time derivatives denote the system states, n denotes the degree-of-freedom of the system, f is a nonlinear auxiliary function that consists of system states, $p \in \mathbb{R}$ denotes the constant system parameters.

$$f = Y_d\phi \tag{7.11}$$

In Equation (7.11), $Y_d\left(\xi_{n-1}, \xi_n, \xi_{n+1}, \dot{\xi}_{n-1}, \dot{\xi}_n, \dot{\xi}_{n+1}\right) \in \mathbb{R}^{1xl}$ is the system state vector and $\phi \in \mathbb{R}^{lx1}$ is the represents unknown parameter vector of the system.

Property 1. All elements of vector Y_d are available.

The adaptive compensation term represented by $\hat{\phi} \in \mathbb{R}$ ensure the robustness of the designed controller. A Compensation error term is needed to show the difference between the system parameters and the adaptive compensation term. The compensation error is defined as follows

$$\tilde{\phi} \triangleq \hat{\phi} - \phi \tag{7.12}$$

The auxiliary error is defined as

$$e \triangleq u_v - \dot{\xi}_n \tag{7.13}$$

Virtual controller designed as

$$u_v \triangleq -G_1 x \tag{7.14}$$

where $G_1 \in \mathbb{R}^+$ represents the constant positive definite gain of the virtual controller. The first close loop system is completed by the virtual controller substituting for the system state to be controlled in Equation (7.9).

$$\dot{x} = -G_1 x \tag{7.15}$$

The time derivative of Equation (7.9) is multiplied by p_1. Substituting Equation (7.10) and Equation (7.11) in the obtained equation, the following equation is obtained.

$$p_1 \dot{e} = -p_1 G_1 \dot{\xi}_n + Y_d \phi + f_d - u_f \tag{7.16}$$

Adaptive compensations of uncertain system parameters are used to deal with parametric uncertainty. The adaptive compensation errors $\tilde{p}_1$ and $\tilde{\phi}$ show the errors between adaptive compensation terms $\hat{p}_1$and $\hat{\phi}$ uncertain system parameters $p_1$and ϕ.

$$\tilde{p}_1 = \hat{p}_1 - p_1 \tag{7.17}$$

$$\tilde{\phi} = \hat{\phi} - \phi \tag{7.18}$$

Equation (7.17) and Equation (7.18) are substituted in Equation (7.19).

$$p_1 \dot{e} = (\tilde{p}_1 - \hat{p}_1) G_1 \dot{\xi}_n + Y_d(\hat{\phi} - \tilde{\phi}) + f_d - u_f \tag{7.19}$$

The control function is designed according to Equation (7.19).

$$u_f = -\hat{p}_1 G_1 \dot{\xi}_n + Y_d \hat{\phi} + \rho_e tan\, h(e) + G_2 e \tag{7.20}$$

where $G_2 \in \mathbb{R}^+$ is constant positive definite control gain. Equation (7.20) is substituted in Equation (7.21).

$$p_1\dot{e} = \tilde{p}_1 G_1 \dot{\xi}_n - Y_d\tilde{\phi} + f_d - \rho_e tanh\,(e) - G_2 e \tag{7.21}$$

Lyapunov-based stability analysis is performed to obtain semi-global asymptotic convergence of the error terms defined in the closed-loop system. The nonnegative Lyapunov function $V(x, e, \tilde{p}_1, \tilde{\phi})$ is defined as

$$V \triangleq \frac{1}{2}x^2 + \frac{1}{2}p_1 e^2 + \frac{1}{2}\tilde{\phi}^T\tilde{\phi} + \frac{1}{2}\tilde{p}_1{}^2 \tag{7.22}$$

The time derivative of Equation (7.19) is obtained in the following form when Equation (7.8), Equation (7.13), and Equation (7.18) are utilized

$$\begin{aligned}\dot{V} = -G_1 x^2 - G_2 e^2 + \tilde{\phi}^T\left(\dot{\hat{\phi}} - Y_d^T e\right) \\ + \tilde{p}_1\left(\dot{\hat{p}}_1 + eG_1\dot{\xi}_n\right) + e(f_d \\ - \rho_e tanh\,(e))\end{aligned} \tag{7.23}$$

If adaptive compensations of uncertain parameters are made according to the following rules, the Lyapunov stability criterion in Equation (7.23) is guaranteed.

$$\dot{\hat{\phi}} = Y_d^T e \tag{7.24}$$

$$\dot{\hat{p}}_1 = -eG_1\dot{\xi}_n \tag{7.25}$$

$$\rho_e \geq max(f_d) \tag{7.26}$$

Using Equation (7.24), Equation (7.25), and Equation (7.26), the time derivative of the Lyapunov function in Equation (7.23) can be rearranged as shown in Equation (7.27).

$$\dot{V} = -G_1 x^2 - G_2 e^2 \tag{7.27}$$

From the Equation (7.27), it can be demonstrated that the time derivative of the Lyapunov function can be upper bounded as

$$\dot{V} \leq -\beta \|\mathbf{z}\|^2 \tag{7.28}$$

where $\mathbf{z} \in \mathbb{R}^2$ is a vector defined as

$$\mathbf{z} \triangleq [x \quad e]^T \tag{7.29}$$

and $\beta \in \mathbb{R}^+$ denotes a positive constant selected as

$$\beta = \min\{g_1, g_2\}. \tag{7.30}$$

Lyapunov function Equation (7.22) and the bound of the time derivative of Lyapunov function Equation (7.28) it is seen that $\mathbf{z}(t) \in \mathcal{L}_\infty$. Boundedness of this term guarantees the boundedness of x and e. From virtual controller design in Equation (7.14), it is seen that boundedness of x guarantees the boundedness of u_v. The virtual control input's boundedness, as well as the boundedness of e and its definition in Equation (7.13), can be used together to show that $\dot{\xi}_n \in \mathcal{L}_\infty$. When boundedness of $\dot{\xi}_n$ is utilized along with Equation (7.9) and the time derivative of Equation (7.15) to show that $\ddot{\xi}_n \in \mathcal{L}_\infty$ and can be utilized with the time derivative of Equation (7.14) to show that $\dot{u}_v \in \mathcal{L}_\infty$. Boundedness of time derivative of virtual controller and boundedness of $\ddot{\xi}_n$ can be used along with the time derivative of the error function to show that $\dot{e} \in \mathcal{L}_\infty$. Boundedness of $\dot{\xi}_n$ and $\dot{e}$ ensures that $\dot{\mathbf{z}}(t)$ is also bounded.

$$\int_0^\infty \|\mathbf{z}(\sigma)\|^2 d\sigma \leq \frac{V(0)}{\beta}. \tag{7.31}$$

The boundedness of the $\dot{\mathbf{z}}(t) \in \mathcal{L}_\infty$, together with $\mathbf{z}(t) \in \mathcal{L}_2 \cap \mathcal{L}_\infty$ and Barbalat's Lemma (Krstic et al., 1995), can be used to show semi-global asymptotic stability of z(t), which assures the main aim of the control design defined as

$$x, e \to 0 \text{ as } t \to \infty \tag{7.32}$$

7.5 Numerical Studies

The numerical parameters of the nine-story building model used in the simulation studies were taken from a transparent type linear structure used in the literature. This structure is not linearized according to the duffing nonlinearity rules, and this nonlinearity is explained in Equation (7.5) to Equation (7.8). In the non-linear structure, instead of the TMD damper used in the literature, Optimal TMD with the same mass as the original TMD (Hacioglu & Yagiz, 2012; Ümütlü et al., 2022) and much better performance is used. Calculations for optimal TMD are taken from Krenk, (2005). The original TMD and optimal TMD results are compared in Figure 7.5. Optimal TMD, which has a much better performance than the original TMD, was activated and used as ATMD in the chapter.

Table 7.3 Parameters of the nonlinear building model and the nonlinear ATMD

Parameter	Value $\times 10^3$ (kg)	Parameter	Value $\times 10^6$ (N/m)	Parameter	Value $\times 10^3$ (Ns/m)	Parameter	Value
m_1	450	k_1	18.05	b_1	26.17	α_1	0.6
m_2	345	k_2	340	b_2	490	α_2	0.5
m_3	345	k_3	326	b_3	467	α_3	0.5
m_4	345	k_4	285	b_4	410	α_4	0.5
m_5	345	k_5	269	b_5	386	α_5	0.5
m_6	345	k_6	243	b_6	348	α_6	0.5
m_7	345	k_7	207	b_7	298	α_7	0.5
m_8	345	k_8	169	b_8	243	α_8	0.5
m_9	345	k_9	137	b_9	196	α_9	0.5
m_d	69	k_d	0.31954	b_d	33.553	α_d	0.5

The nonlinear structure and the nonlinear optimal TMD parameters are given in Table 7.3. The determined structure was exposed to the 17 August 1999 Kocaeli

earthquake in Turkey. The acceleration, velocity, and displacement of the ground motion are shown in Figure 4.1.

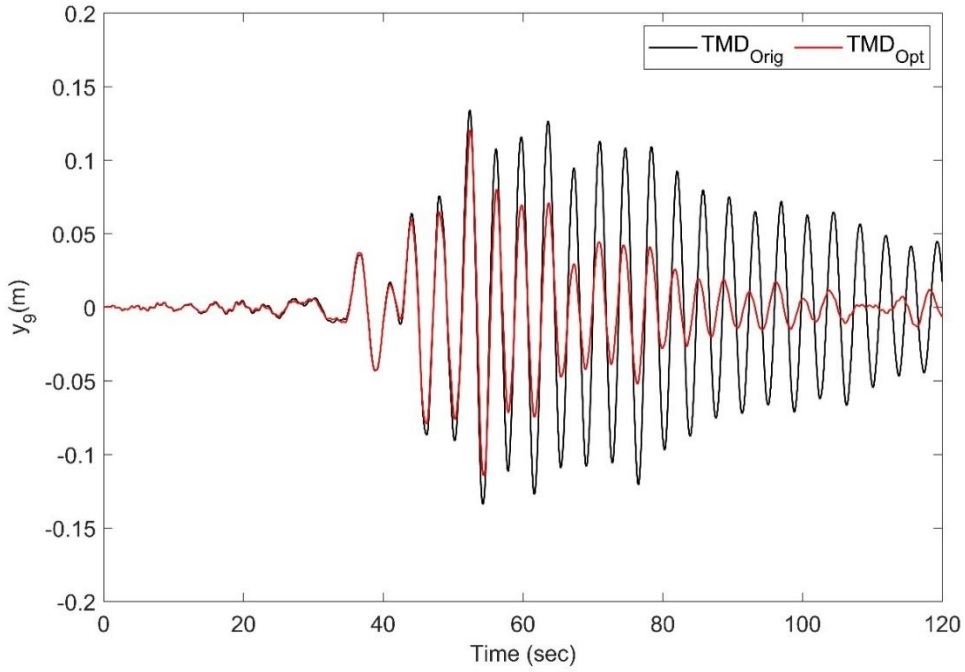

Figure 7.4 Comparison of original TMD and optimal TMD against the Kocaeli earthquake

The optimal TMD design with the same mass as the original TMD design showed a great performance improvement as shown in Figure 7.4. The passive controller, to which the robust adaptive controller designed within the scope of this chapter will be compared, has reached the best point it can be reached with the optimal TMD design. The point that should not be forgotten here is that due to the structure of optimal TMD design, gives these types of successful results only for the proposed structure. When the structural parameters are changed, its performance will be adversely affected. However, it would be more accurate to compare the controller designed to reduce vibration in nonlinear structures with the optimal TMD, in order to ensure adequate comparison.

The gains are selected as follows via trial and error method and the designed controller in Equation (7.20) is applied from the actuator input of the ATMD system

$$G_1 = 100, G_2 = 1000, \rho_e = 50000 \tag{7.33}$$

It should be mentioned at this time that as the control gains values are increased while determining the gains, the ATMD performance improves, but the control effort and stroke of the control mass also increased. In light of this, the control gain adjustment procedure was stopped at the final position when ATMD performance greatly improved, and the control gains were acquired as shown in Equation (7.29). Following this point, the control effort and displacement of the control mass increased as the control gains increased, while the ATMD performance remained similar. It has been demonstrated that the suggested controller may be used in such structures if the control gains are chosen to be positive definite in order to meet the main control goal.

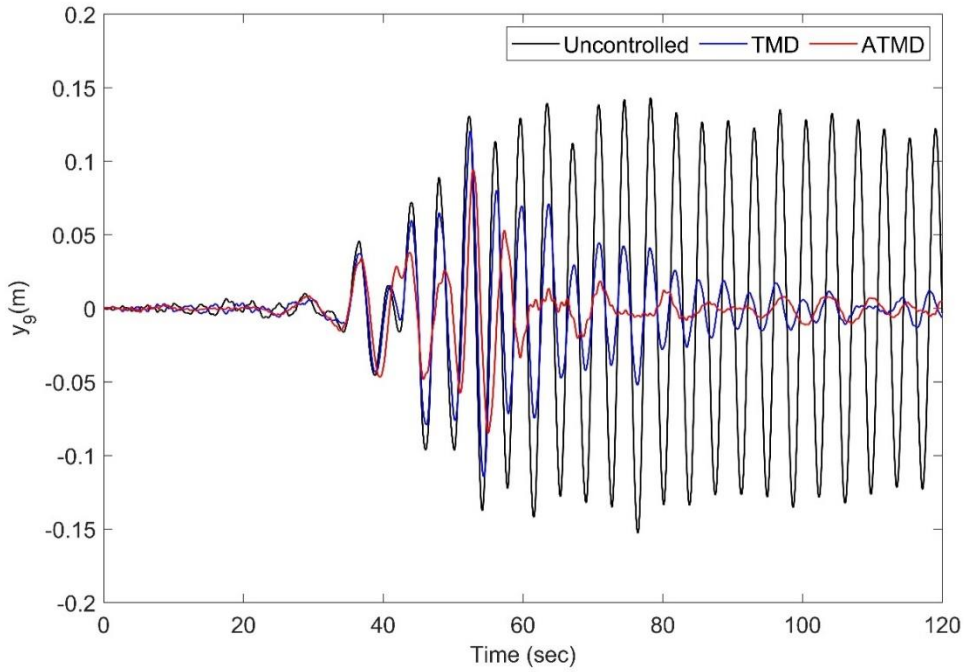

Figure 7.5 Displacement of the last floor of the structure for three different situations

Figure 7.5 shows the displacement of the last floor of a nine-story nonlinear structure for three different control situations during the Kocaeli earthquake. These situations are referred uncontrolled, optimal TMD control, and ATMD control situations. Optimal TMD is used in the ATMD system by activating it with an actuator. As can be easily understood from the figure, it has been observed that better results can be obtained in the final floor displacements of the building compared to an

uncontrolled situation by using the TMD system. However, the amplitude of the displacement in each period during the earthquake and the time it takes to reduce the residual vibrations are considerably lower when the ATMD system is used with the designed controller compared to the case when TMD is used. It is seen that the designed controller, a nonlinear ATMD system, significantly reduces earthquake-induced oscillations occurring on the top floor of a nonlinear structure.

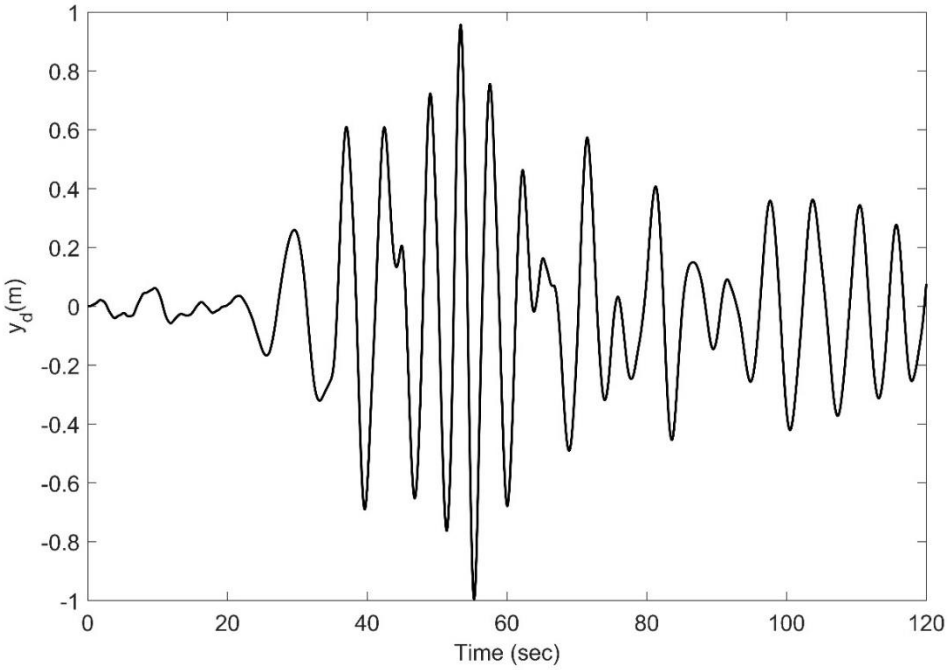

Figure 7.6 Displacement of controller mass while reaching the control aim

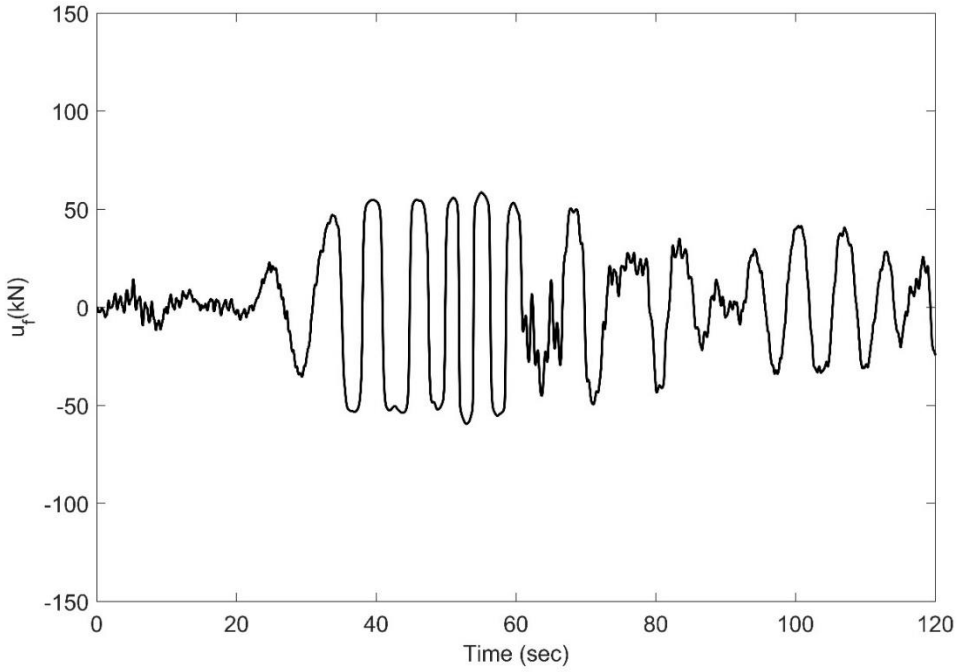

Figure 7.7 Change of control force needed while reaching control objective

The displacement of the oscillating controller mass due to the force applied by the earthquake and the actuator is given in Figure 7.6. The control mass moves at a range of 2 meters, which is an acceptable stroke for such systems. The control force applied to reduce earthquake-induced vibrations in the building is shown in Figure 7.7.

Figure 7.8(a), 7.8(b), 7.8(c), 7.8(d), 7.8(e), 7.8(f) and 7.8(g) show adaptive compensations for uncertain parameters $\hat{\phi}_1, \hat{\phi}_2, \hat{\phi}_3, \hat{\phi}_4, \hat{\phi}_5, \hat{\phi}_6$ and $\hat{p}_1$, respectively. Compensation terms are used to achieve the overall control purpose. The numerical values that these terms have in the process are unimportant, provided they change within a limited range. As shown in Figure 7.7, while the structural vibrations caused by an earthquake are reduced by using the designed controller in the ATMD system, the variation of compensation parameters in a limited range is observed.

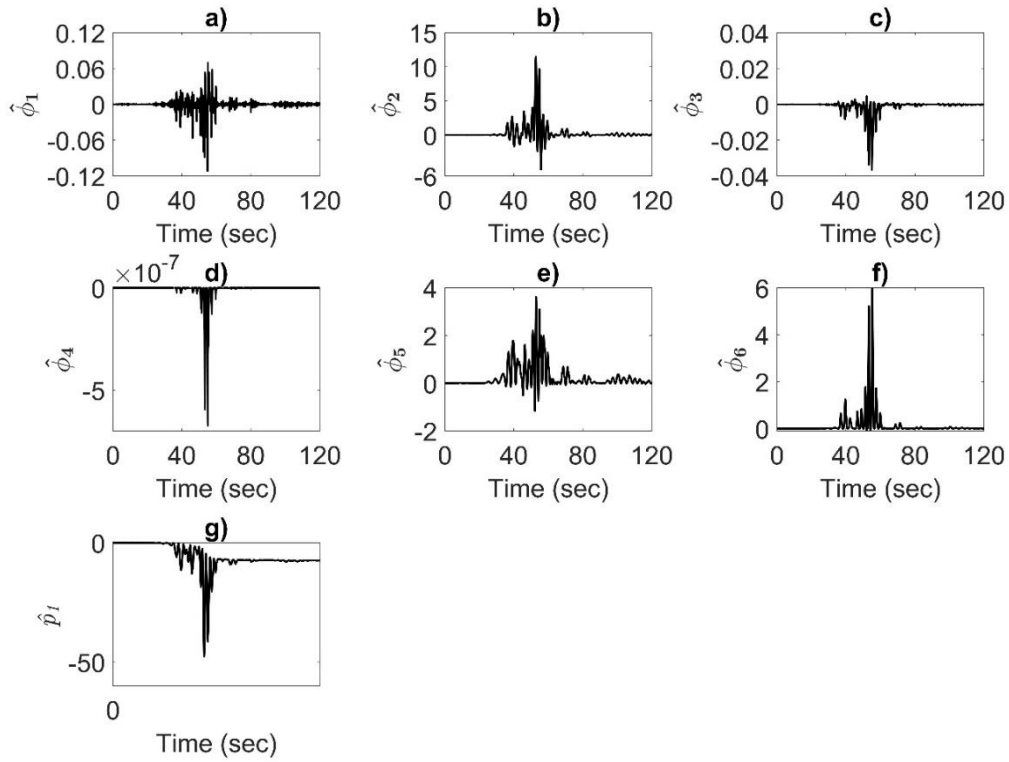

Figure 7.8 Adaptive compensations of uncertain parameters for Kocaeli Earthquake

7.6 Conclusions

In this chapter, a controller is designed to mitigate earthquake-induced vibrations of a non-linear multi-story building using ATMD. In addition to structural nonlinearities, band-limited white noise has been applied as a disturbance input on the last floor of the building to represent unknown nonlinear situations such as measurement noise and uncertain dynamics. Adaptive compensation terms are used to design a robust controller independent of structural parameters. Stability of the structure while reaching the control target is guaranteed by a Lyapunov-based stability criterion that handles all nonlinear and unknown situations. With the Lyapunov-based stability analysis described in the paper, it is theoretically guaranteed that the proposed controller will keep the system stable while attaining the main control goal, as long as the constant control gains are chosen as positive numerical values. Owing to the robust structure of the designed controller and the adaptive compensation rules proposed in the chapter, a general controller structure that can be used in all systems with a similar

mathematical model aiming at vibration damping with ATMD systems has been obtained. Simulation experiments in Matlab/Simulink were used to verify the performance of the developed controller.

CHAPTER EIGHT
THE α-CONTROLLER DESIGN WITH NONLINEAR DAMPING APPROACH

8.1 Introduction

In this chapter, studies focus on the controller design for ATMD systems in order to mitigate wind-induced vibrations in skyscrapers. Since tall buildings such as skyscrapers oscillating under the effect of the wind show a tendency to move in the first mode, in this chapter, the SDOF structure model is used during the controller design in parallel with similar studies in the literature. This controller design is aimed to reduce these wind-induced vibrations by using a control method that using with velocity feedback. In this context, an α-controller (Collette & Chesné, 2016) designed according to the natural frequency of the structure is used to prevent velocity feedback systems from showing unstable behavior at high control gain values. This proposed controller is developed with a nonlinear damping approach called NLD (Venanzi et al., 2015; Venanzi & Ubertini, 2014) designed to avoid high ATMD displacements. In order to preserve the structural integrity of the thesis, the NLD-supported α controller designed in this chapter is tested in a nine-story building to dampen earthquake-induced vibrations. Throughout this thesis, various Lyapunov-based controllers have also been simulated with this structure. The performance criteria in Chapter 5 are used to evaluate the findings and the results obtained are compared with the innovative Linear Regression (LR) model-based controller introduced in Chapter 4.

8.2 Controller Design

8.2.1 The α-Controller Design for SDOF Structures

The primary purpose of the development of the α controller is to find a solution to the stability problem of proportional velocity feedback controls, which are the most basic controllers and are frequently used in vibration damping studies with this type of ATMD system. The classical velocity feedback-based controller design is preferred so

often because of its basic structure, which is roughly based on the logic of increasing the system damping. In classical proportional controllers designed for ATMD systems, the system shows unstable behavior for high gain values. Since the stability of the structure is not guaranteed for all control gain values, the control force applied by the ATMD system may cause resonance, causing a situation that is even more dangerous than the vibration desired to be damped. The α controller was designed by Collette and Chesne (Collette & Chesné, 2016) in order to prevent this shortcoming of classical proportional velocity feedback systems.

An SDOF structure has been chosen to illustrate the working principle of the α controller. The TMD is placed at the top of the structure as shown in Figure 8.1. The mathematical model of the structure and TMD system is given in Equation (8.1).

$$\mathbf{M}\ddot{\mathbf{X}} + \boldsymbol{C}\dot{\mathbf{X}} + \mathbf{K}\mathbf{X} = \mathbf{r}F_{wind} \tag{8.1}$$

$$\begin{bmatrix} m_s & 0 \\ 0 & m_d \end{bmatrix}\begin{bmatrix} \ddot{x}_s \\ \ddot{x}_d \end{bmatrix} + \begin{bmatrix} c_s + c_d & -c_d \\ -c_d & c_d \end{bmatrix}\begin{bmatrix} \dot{x}_s \\ \dot{x}_d \end{bmatrix} + \begin{bmatrix} k_s + k_d & -k_d \\ -k_d & k_d \end{bmatrix}\begin{bmatrix} x_s \\ x_d \end{bmatrix} = \begin{bmatrix} 1 \\ 0 \end{bmatrix} F_{wind} + \begin{bmatrix} -1 \\ 1 \end{bmatrix} u_f \tag{8.2}$$

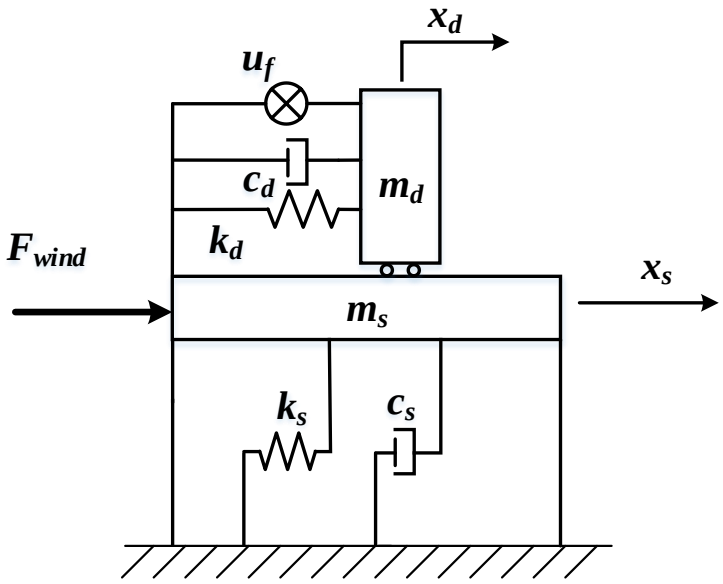

Figure 8.1 Model of an SDOF structure with a TMD.

In Equation (8.2) m_s, k_s and $c_s \in \mathbb{R}$ represents mass, stiffness coefficients, and damping coefficient of structure, respectively while $x_s \in \mathbb{R}$ represents the

displacement of the structure. At this point, it is noted that $\dot{x}_s$ and $\ddot{x}_s \in \mathbb{R}$ indicates velocity and acceleration of the structural system, respectively. It is characterized by the mass m_d , and the stiffness k_d. At this part, for a clearer representation of the stability analysis of the α controller, the system is selected as undamped with roots on the imaginary axis.

The behavior of the ATMD system, which is obtained by adding an actuator to the optimal TMD, is managed by the controller input signal. Such systems, which are controlled with a fixed gain value in the classical proportional velocity feedback controller design, show unstable behavior for high gain values, as seen in Figure 8.2. The limits of this control design, which cannot guarantee system stability for high control gains, are clearly shown by the stability analysis.

The main reason why the proportional controller leads the system to instability for high control gain values is that there is no zero between the pole of the TMD and the pole of the structure (Chesné & Collette, 2018). In order to avoid this boundary for high control gain, a zero is added between the structure and TMD poles with the α controller, which is actually a filter for the classical velocity feedback controller system, designed by (Collette & Chesné, 2016).

$$u_0 = \mathrm{H}_a(s) H_{HP}(s) \dot{x}_s \tag{8.3}$$

where $H_{HP}(s)$ represents high pass filter and cut-off frequency equals to $\omega_0/10$. ω_0 represents the natural frequency of the system without TMD.

$$\mathrm{H}_a(s) = g_a \frac{(s+\propto)^2}{s^2} \tag{8.4}$$

where $\propto$ represents the controller constant and g_a represents the controller gain

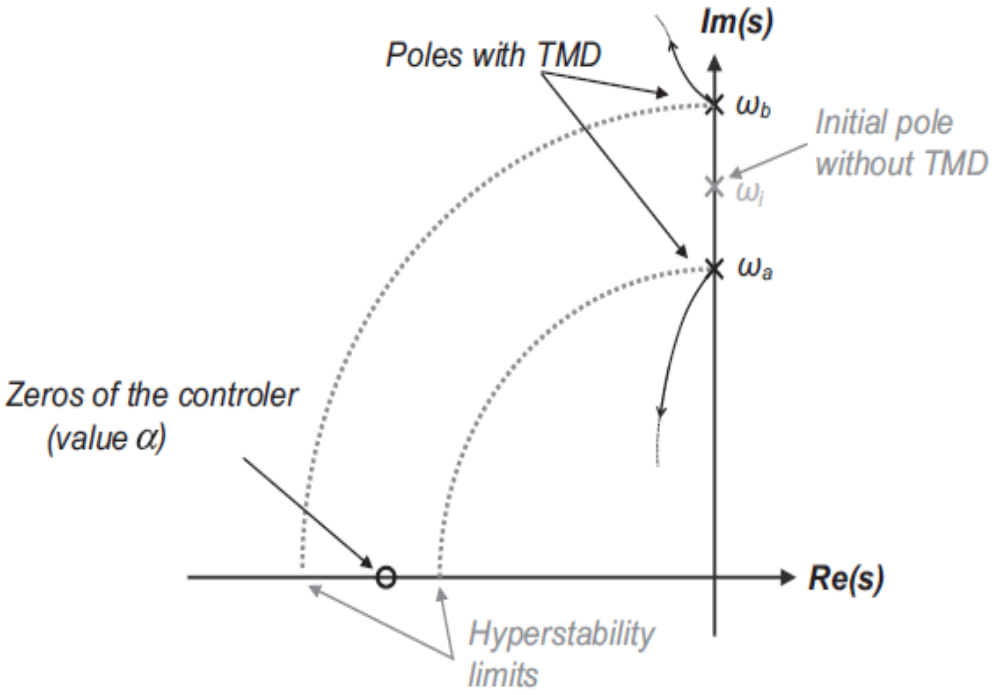

Figure 8.2 Stability limits on the pole map, without structural damping (Collette & Chesné, 2016)

If the α controller, whose operating logic is explained in an undamped system, is used in a damped system, the added damping coefficients will shift the roots on the imaginary axis towards the left half plane and increase the stability of the system. In order to explain how the α value should be selected over the frequency response, the frequency response of the structure, with $\xi = 0.025$, is shown in Figure 8.3. In Figure 8.3, ω_1 and ω_2 represent the natural frequencies of the system using TMD. The $\propto$ value in the control equation Equation (8.4) should be chosen between the first and second natural frequencies of structures (Chesné & Collette, 2018; Paknejad et al., 2022). Provided that the $\propto$ value is selected within the specified range, the control design ensures the stability of the structure for each positive control gain.

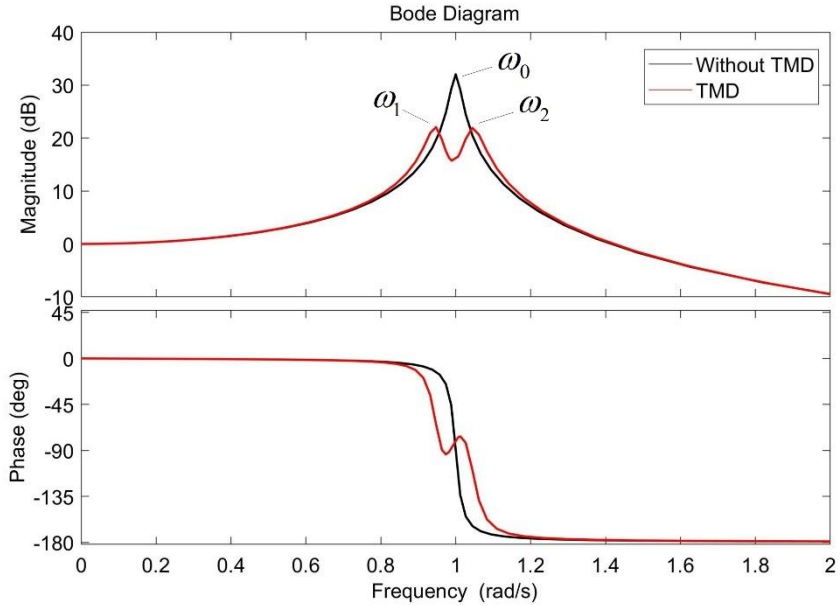

Figure 8.3 Bode plot of the structural system without TMD and TMD

8.2.2 Nonlinear Damping Approach (NLD)

Although the proposed α-controller is quite successful in damping the vibrations occurring in the structure, it cannot prevent high displacements in TMD since it does not contain any control on the displacement of the control mass.

The nonlinear damping approach (NLD) is a control mechanism that prevents ATMD devices from surpassing their stroke limitations. By decreasing the motion of controller mass between the stroke stops, which is determined as κ_0 and κ_1 in Equation (8.6), the NLD method prevents the movable mass from reaching its limitations This is accomplished by including an additional control term in the designed controller equation that becomes active at the physical limit and is zero elsewhere (Venanzi et al., 2015).

The nonlinear damping approach (NLD) in Equation (8.5) and Equation (8.6), originally proposed in (Venanzi & Ubertini, 2014), is a control strategy capable of avoiding stroke limits crossing of ATMD systems.

$$u_f(t) = u_0(t) - g_{NL}\varepsilon_{NL}(x_d(t))\dot{x}_d(t) \tag{8.5}$$

$$\varepsilon_{NL}(x_d(t)) = \begin{cases} 1, & |x_d(t)| \geq \kappa_1 x_{d\_max} \\ 1 - e^{\left(\frac{-1}{1-(|x_d(t)|-\kappa_0 x_{d\_max})^2/(\kappa_1 x_{d\_max}-\kappa_0 x_{d\_max})^2+1}\right)}, & \kappa_0 x_{d\_max} < |x_d(t)| < \kappa_1 x_{d\_max} \\ 0, & |x_d(t)| \leq \kappa_0 x_{d\_max} \end{cases} \tag{8.6}$$

In Equation 8.5 $u_0(t)$ represents the output of the α-controller function and ε_{NL} represents the nonlinear control law in order to apply the limitation to controller mass stroke. $x_d(t)$ and x_{d_max} denote ATMD displacement and maximum stroke limit, respectively. κ_0, κ_1 and g_{NL} denote the control gain constant of the nonlinear control rule. The only rule is the $0 < \kappa_0 < \kappa_1 < 1$ to be followed for the constants κ_0 and κ_1, which are optionally determined according to the desired smoothness level from the ε_{NL} function.

8.3 System Model of SDOF Structure

In this chapter, a controller based on the natural frequency of the structure will be designed for ATMD placed on the top of a skyscraper. The designed controller is first used to reduce the wind-induced vibrations of a skyscraper modeled as SDOF, and then to suppress the earthquake-induced vibrations of a nine-story building.

High-rise structures such as skyscrapers naturally tend to behave in the first mode. For this reason, tall buildings can be modeled as an SDOF system in studies. In this chapter, an SDOF system representing a skyscraper and an ATMD system model placed on it were used.

In Figure 8.1, m_s represents the modal mass of structure $45 \times 10^6\ kg$, k_s represents stiffness coefficient and c_s represents damping coefficient. The mass of ATMD m_d is determined as $1200 \times 10^3\ kg$. By using optimal TMD design calculations in (Krenk, 2005), the necessary damping constant c_d and stiffness constant k_d are calculated for

the TMD system to be used in the building to be optimal. The values of structural parameters are given in Table 8.1.

Table 8.1 Parameters of SDOF structure and TMD system

m_s	45000000 kg
μ	0.02666
k_s	12964746.66 N/m
ω_s	0.5367 rad/s
f_s	0.0854 Hz
c_s	603848.90 N s/m
c_d	71496.07 N s/m

8.4 Numerical Studies for SDOF Structure Against Wind Load

The wind load to which the high-rise building is modeled as SDOF is simulated. The structure and the proposed controller are tested with this realistic wind load. In order to create a virtual wind pattern, the studies in the literature were examined and dominant frequency regions were determined for the winds. The dominant frequency of wind gusts is shown in Figure 8.4. These dominant frequencies are quite low compared to the natural frequencies of building structures. Therefore, these wind gusts activate the first natural frequencies of the structures. (Boggs & Dragovich, 2006)

The fact that the artificial wind breeze desired to be created in this study has a more realistic effect has been taken into account and white noise has not been used. Pink noise is used to simulate the wind and the low-frequency region is also filtered. As a result, the wind force seen in Figure 8.5 was obtained and applied to the structure in the simulation studies.

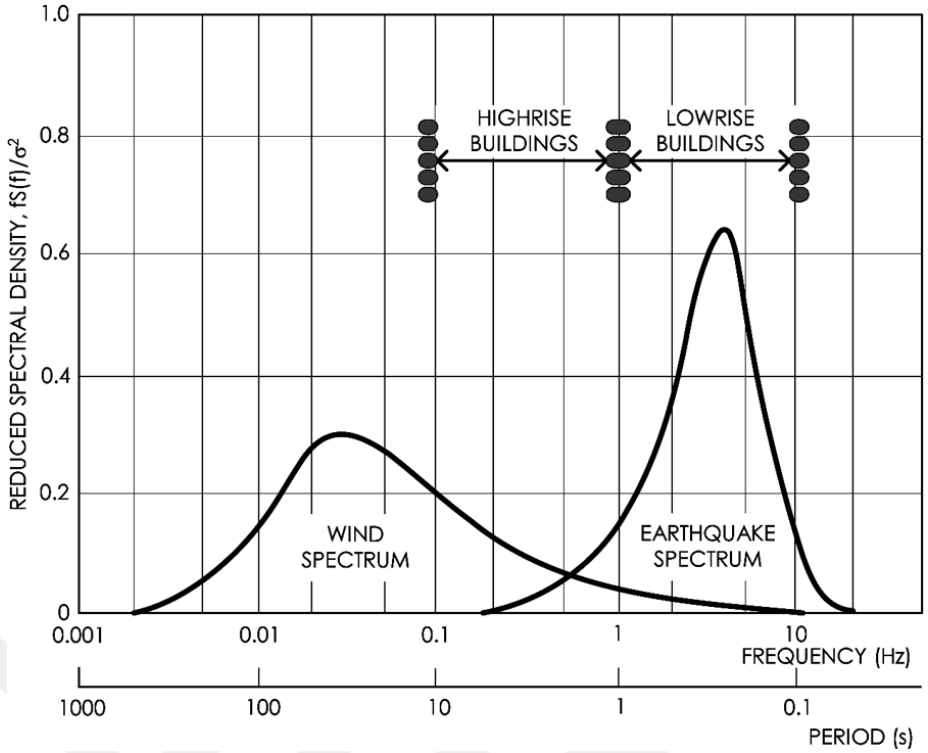

Figure 8.4 Frequency range of structures excited by wind and earthquakes. (Boggs & Dragovich, 2006)

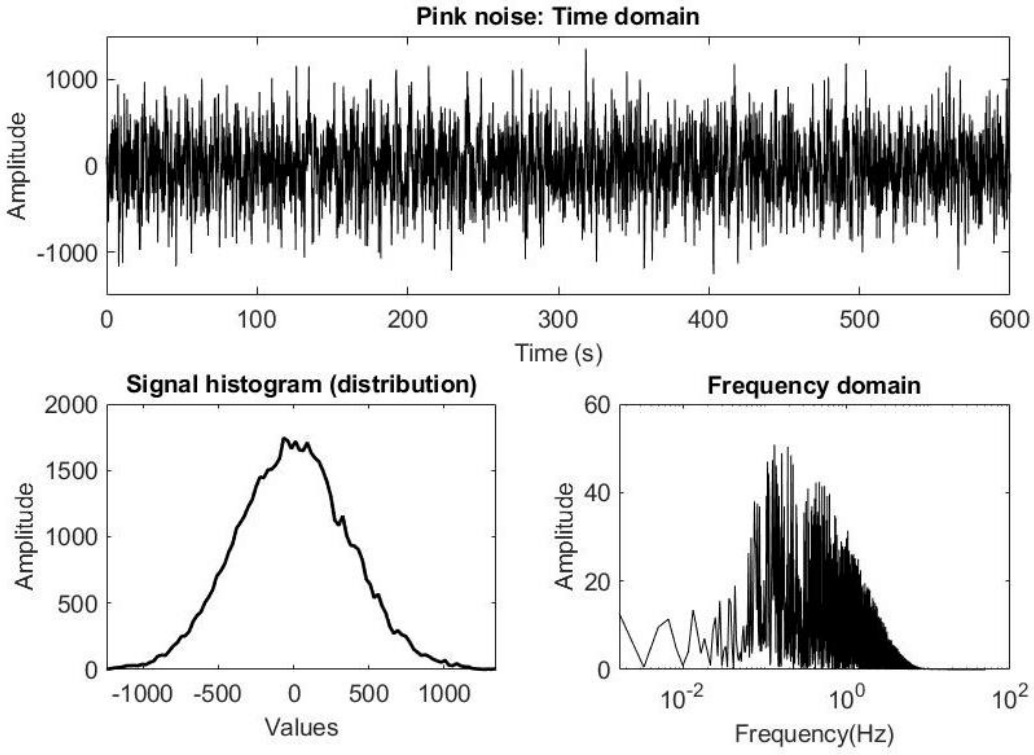

Figure 8.5 Pink noise used for a wind force model

In this chapter, the α-controller gain g_a and NLD controller gain g_{NL} are selected as 2000000 and 500000, respectively. In the α-controller design, the cutoff frequency of H_{HP} and the α values are taken as 0.05367 and 0.5367, respectively, these control parameters are related to the natural frequency of the structure as defined in the controller design section. The constant values of the nonlinear control rule κ_0 and κ_1 are carefully chosen as 0.3 and 0.8, respectively.

Figure 8.6 shows the acceleration response for the modal mass of the wind-loaded structure for four cases: the without TMD system (uncontrolled), the optimally tuned mass damper (TMD) system, the α-controller system, and the α-controller system supported by the NLD. Figure 8.7 shows the displacement results for the same four cases. It is clearly seen in the displacement of structure results that although the TMD system gives better results than the uncontrolled system, the vibration amplitudes are quite high compared to the active systems. Although this success of active control methods in damping the vibrations caused by winds in skyscrapers is an expected result, high amplitudes can be seen as α-controller do not have any control purpose on the controller mass displacement of the system, as seen in Figure 8.8.

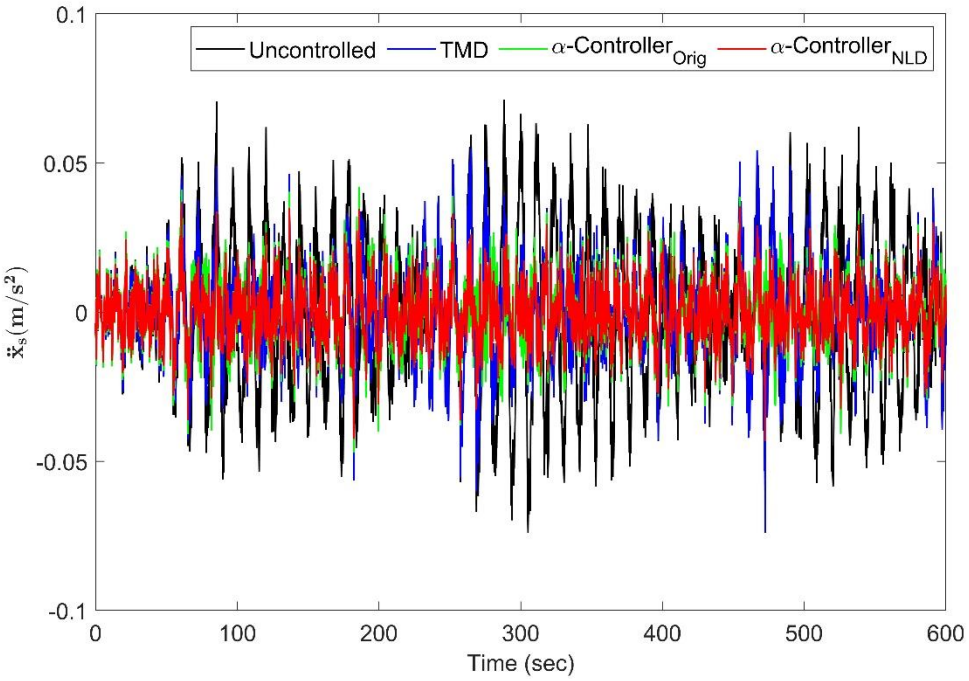

Figure 8.6 Acceleration of structure against a pink noise wind force

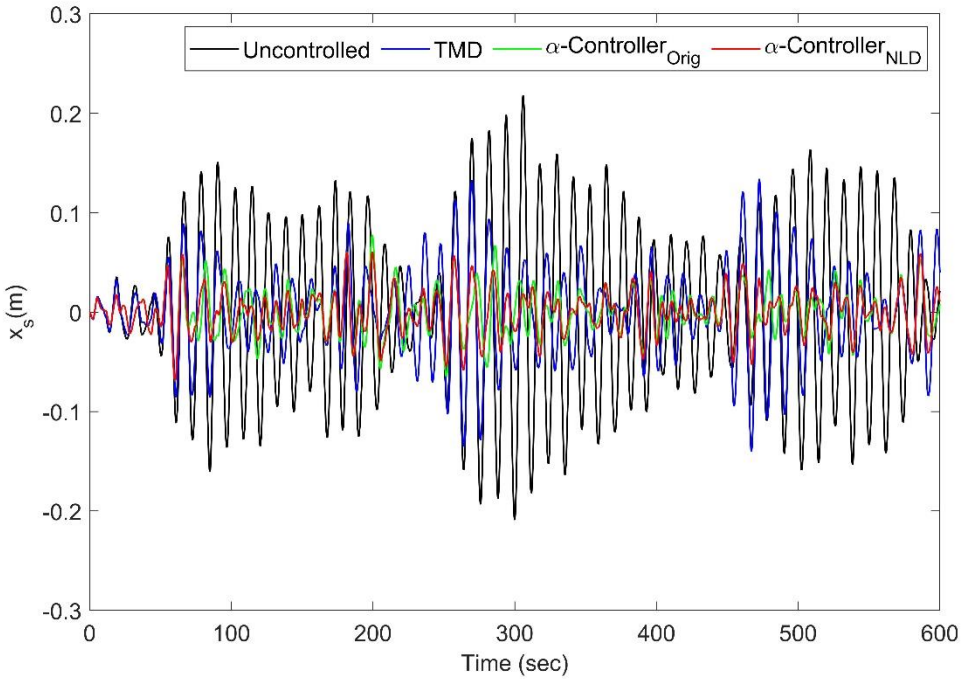

Figure 8.7 Displacement of the structure against a pink noise wind force

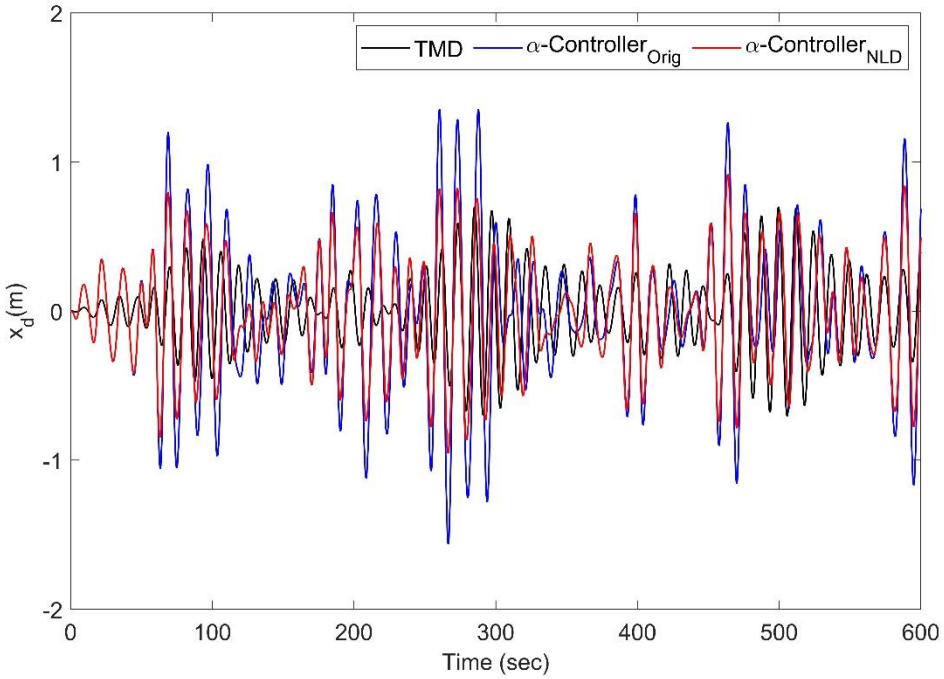

Figure 8.8 Displacement of TMD achieving the control objective

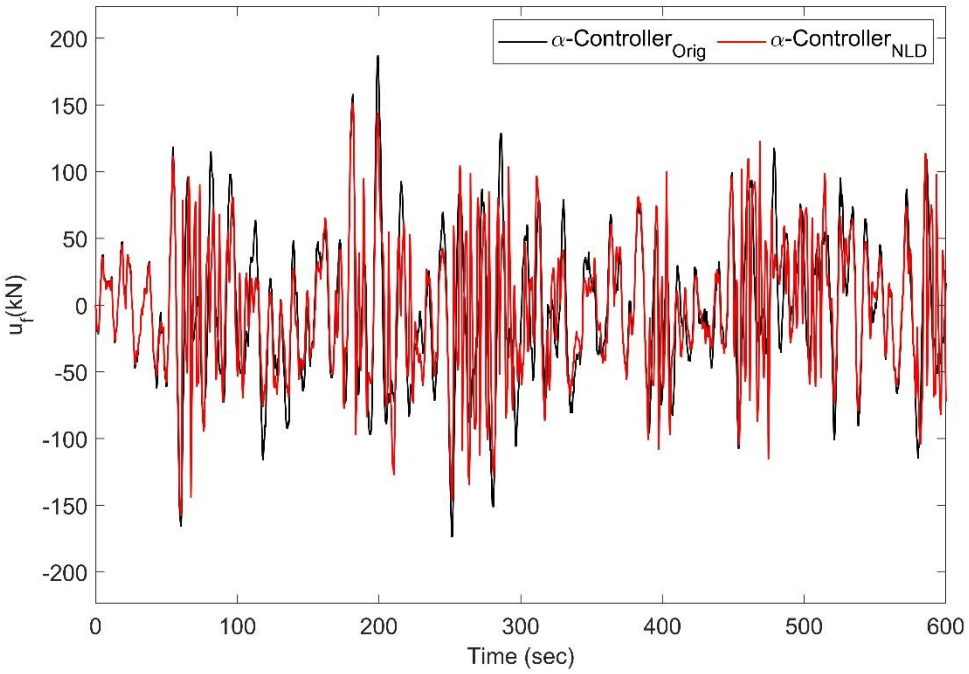

Figure 8.9 Control force for the original ∝-controller and ∝-controller with NLD

Compared to the α controller with the novel α controller, powered by the NLD, has a tremendous effect on the displacement of controller mass, as seen in Figure 8.8. If control effort is compared on two controllers, NLD-supported controls are more successful as seen in Figure 8.9 and Table 8.2. The success of the proposed control design can be seen more strikingly in Table 8.2, which is created with the max and RMS values obtained from the data in Figures 8.6 to Figures 8.9. Controller supported with NLD outperformed the original controls in all Rms and Max values obtained for structure acceleration $\ddot{x}_s$, structure displacement x_s, displacement of controller mass x_d, and control effort u_f parameters.

Tablo 8.2 The statistical results of the uncontrolled structure and the structure using various controllers

	Uncontrolled	TMD	$\propto -\text{Controller}_{Orig}$	$\propto -\text{Controller}_{NLD}$
rms ($\ddot{x}_s$)	$0.02496 m/s^2$	$0.01534 m/s^2$	$0.01126 m/s^2$	$0.01082 m/s^2$
max ($\ddot{x}_s$)	$0.07132 m/s^2$	$0.05475 m/s^2$	$0.04202 m/s^2$	$0.04109 m/s^2$
rms (x_s)	$0.08298 m$	$0.04479 m$	$0.02268 m$	$0.02148 m$
max (x_s)	$0.02181 m$	$0.01341 m$	$0.07779 m$	$0.06091 m$
rms (x_d)		$0.25671 m$	$0.47587 m$	$0.36555 m$

Table 8.2 Continues

max (x_d)		0.70139m	1.3547m	0.9687m
rms (u_f)			52,72 kN	50,76 kN
max (u_f)			187.48 kN	151.66 kN

In order to interpret the acceleration results more meaningfully, the moving RMS technique was used in Figure 8.10. The success of the ATMD system is undoubtedly seen in this figure. It is seen that the α controller supported with NLD gives better results than the original controller, especially at the points where the acceleration value peaks.

An SDOF structure subjected to wind load tends to oscillate at its first natural frequency. The total exposure time of the selected structure to the applied artificial wind breeze is 600 sec. It is known that this structure makes 50 cycles during the simulation run.

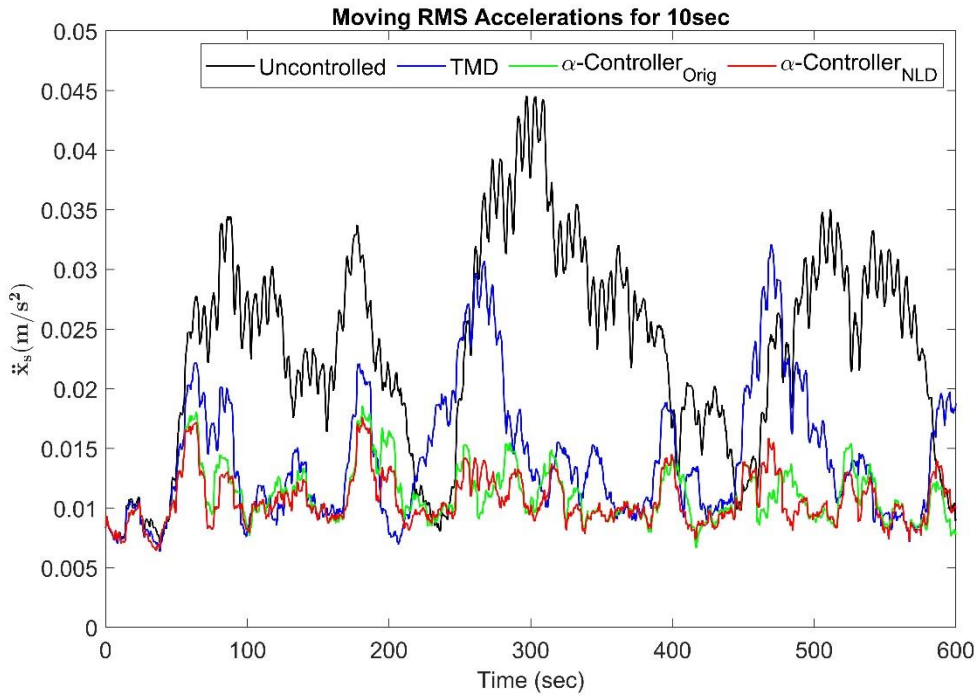

Figure 8.10 Moving RMS of acceleration for 10 seconds

Statistical data of displacement and acceleration values for each cycle were compared in four different situations and the percent success results are given in Table 8.3 and Table 8.4. Table 8.3 gives the percentage results of RMS and Table 8.4 peak value. The results given in the tables are the percentage success of the control methods in the rows compared to the control methods in the columns. For example; When the acceleration data of the structure in Table 8.3 are analyzed in terms of RMS results, it is concluded that TMD results are more successful in 83.67% of 50 cycles than in an uncontrolled situation. The conclusion that can be drawn from both tables is that the α controller supported with NLD produces more successful results than the original controller.

Table 8.3 The success of RMS values of structure accelerations and displacements for each cycle

	Uncontrolled		TMD		$\propto -\text{Controller}_{Orig}$	
	x_s	$\ddot{x}_s$	x_s	$\ddot{x}_s$	x_s	$\ddot{x}_s$
TMD	%89.58	%83.67				
$\propto -\text{Controller}_{Orig}$	%100	%94	%88	%78		
$\propto -\text{Controller}_{NLD}$	%100	%93.88	%90	%84	%64.58	%70.83

Table 8.4 The success of peak values of structure accelerations and displacements for each cycle

	Uncontrolled		TMD		$\propto -\text{Controller}_{Orig}$	
	x_s	$\ddot{x}_s$	x_s	$\ddot{x}_s$	x_s	$\ddot{x}_s$
TMD	%87.83	%84				
$\propto -\text{Controller}_{Orig}$	%100	%90	%84	%72		
$\propto -\text{Controller}_{NLD}$	%97.96	%92	%90	%76	%72	%58

Figure 8.11 shows the displacement responses for the TMD and the α controller,cycle-by-cycle, compared to the uncontrolled condition. Cycles are ordered from largest to smallest according to the uncontrolled (indicated by the black line). Bars give TMD and α controller RMS and peak displacements for the same cycles. Similarly, Figure 8.12 shows acceleration results for each cyclethe for uncontrolled, passive controller (TMD) and proposed controller scenarios. The proposed controls seem to give very satisfactory results, especially in cycles where the optimal TMD fails against the uncontrolled state. On the other hand, in cycles where the α controller with NLD is less successful than TMD, the difference between them is seen to be very small.

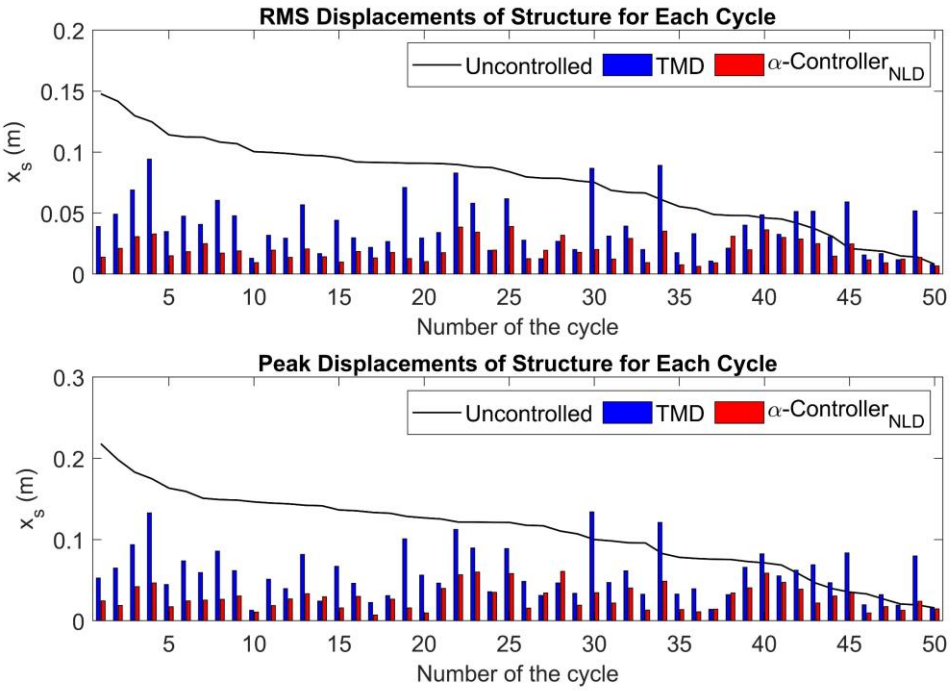

Figure 8.11 RMS and peak displacements of structure for Uncontrolled, TMD, and $\propto -\text{Controller}_{NLD}$ situations cycle by cycle

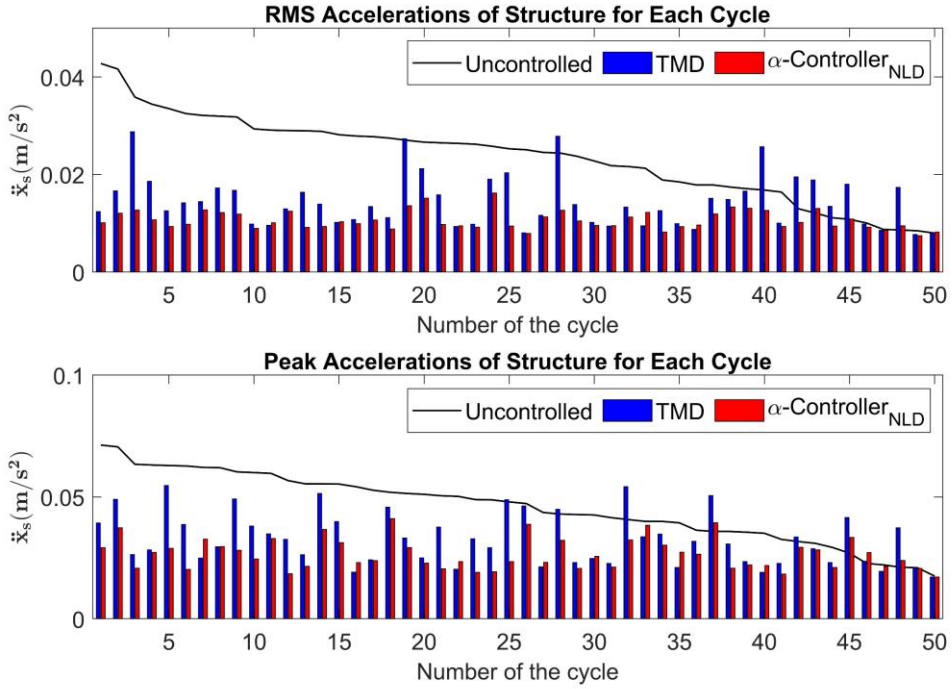

Figure 8.12 RMS and peak accelerations of structure for Uncontrolled, TMD, and $\propto -\text{Controller}_{NLD}$ situations cycle by cycle

8.5 Numerical Studies for Nine-Story Structure Against Earthquake

In this section, it is aimed to test the performance of the new controller, which is modeled as an SDOF system, to reduce the wind response in skyscrapers, with the ATMD system on the nine-story building as shown in Figure 3.1. The specified structure is the structure used in the performance tests of all Lyapunov-based controllers designed throughout the thesis. Within the scope of this test, the new controller is compared with the Linear Regression-based controller selected from among the Lyapunov-based controllers, although it produces results that are close to each other.

The numerical parameters of the nine-story building model used in the simulation studies are given in Table 2.1. These structures were exposed to the East-West direction component of the 1999 Kocaeli earthquake, which was a major earthquake and caused great loss of life and property. The acceleration, velocity, and displacement data of this earthquake are shown in Figure 4.1. The addition of additive white Gaussian noise (AWGN) to all measurement data is represented to simulate external impacts, measurement noise, and possible sensor precision problems. For this control design based on the natural frequency of the structure, 2.20847 rad/s, which is the natural frequency of the structure, is assigned to the α variable. The other control gain parameters, 350000 and 50000, were chosen as g_a and g_{NL}, respectively, by trial and error method.

Figure 8.13 shows the vibration of the ninth floor during the earthquake for two different controller designs: LR model based controller, and $\propto$ - Controller$_{NLD}$. As seen in Figure 8.13, although the results are almost the same, it is seen that the α controller has a slightly better damping success, especially at peak values.

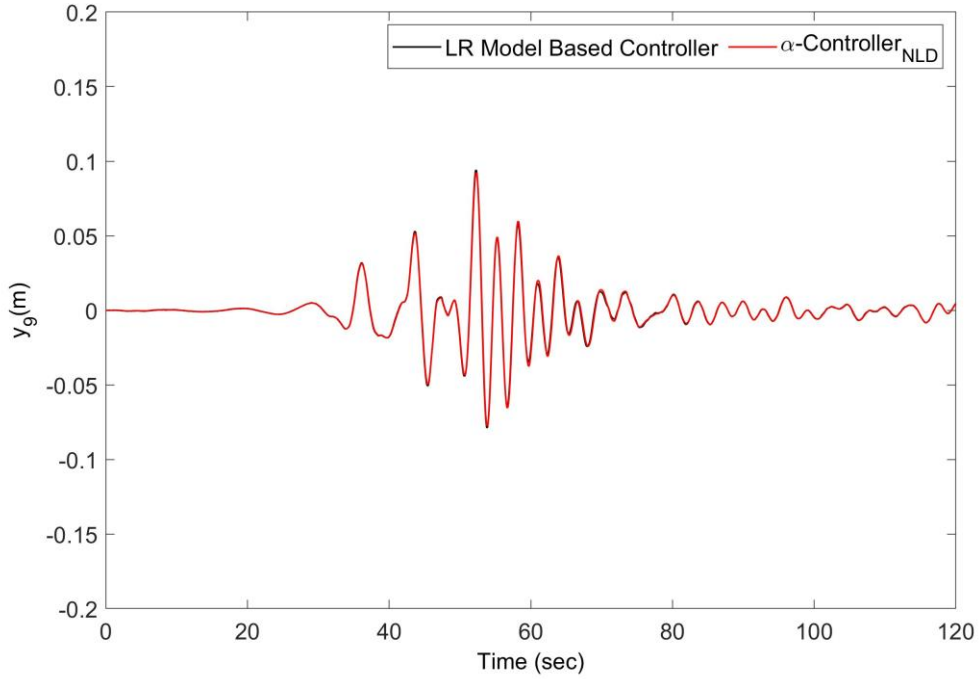

Figure 8.13 Comparison of the displacements of the top floors of the buildings for LR model based controller and ∝ - Controller$_{NLD}$

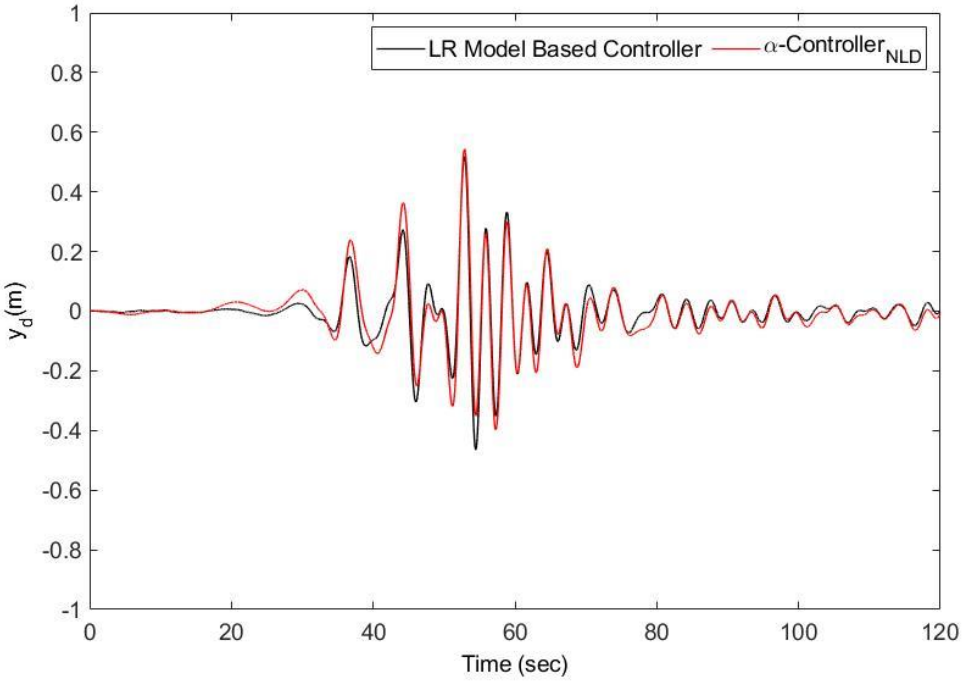

Figure 8.14 Comparison of the displacements of the ATMD systems for LR model based controller and ∝ - Controller$_{NLD}$

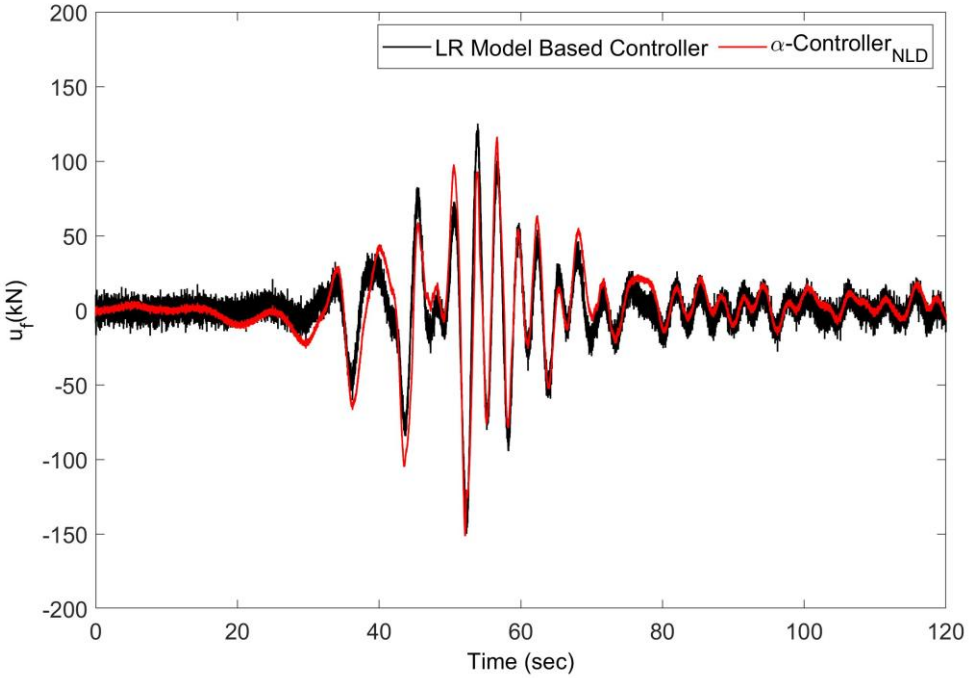

Figure 8.15 Comparison of the control forces for LR model based controller and $\propto$ - Controller$_{NLD}$

In Figure 8.14 it can be seen that the ATMD mass moves within a range considered reasonable by similar studies in the literature. Figure 8.15 shows that the control force required by the $\propto$ controller to achieve the control purpose is quite close to the LR model based controller.

As seen in Figure 8.13, Figure 8.14, and Figure 8.15, the evaluation criteria given in Chapter 5 were applied to compare the performances of these controllers, whose performances are close to each other. Evaluation results are given in Table 8.5.

Table 8.5 Evaluation criteria results for the Kocaeli Earthquake of Linear regression based controller and $\propto -\text{Controller}_{NLD}$ tested in the nine story structure

	$C3$	$\propto -\text{Controller}_{NLD}$		$C3$	$\propto -\text{Controller}_{NLD}$
J_1	0.1946	0.1941	J_7	0.5136	0.5062
J_2	0.1934	0.1931	J_8	0.5098	0.5195
J_3	0.2387	0.2390	J_9	0.6044	0.5934
J_4	0.2417	0.2419	J_{10}	0.6101	0.5969
J_5	1.3647	1.4739	J_{11}	3.3294	3.4860

Table 8.5 Continues

J_6 $(kN\,m/s)$	12.8483	12.9749	J_{12} $(kN\,m/s)$	112.2249	125.7023
σu_f (kN)	24.8585	27.4855	$max\|u_f\|$ (kN)	125.2096	116.3948
σ_{yd} (cm)	9.4951	10.2549	$max\|y_d\|$ (cm)	51.8529	54.2912

In Table 8.5, the results of LR model based controller and $\propto$ - controller tested for the nine-story structure using the original stiffness values are given for the Kocaeli earthquake. When the results are reviewed, it is seen that the $\propto$ - controller gives a little bit better results generally on acceleration based criteria that are J_1, J_2, and J_7 criteria, which are the building acceleration-based criteria. While the LR model based controller is better in the J_3 and J_4 criteria, which are the criteria based on the RMS displacement principle, the $\propto$ - controller seems to be more successful in the J_9 and J_{10} criteria, which are the criteria based on the maximum value of the displacement. J_5 and J_6 are criteria related to controller mass displacement, although the $\propto$ - controller has an NLD limiter, better results are obtained with the LR model based controller. When the two controllers are compared in terms of control effort, LR model based controller has the advantage in RMS, while the $\propto$ - controller has the advantage in peak control effort.

8.6 Conclusions

In this chapter, the $\propto$ - controller designed for the ATMD system to mitigate the wind-induced vibrations on the skyhook structure is modeled as an SDOF structure. This control method is a controller design based on the natural frequency of the structure. The $\propto$ value selected between the first two natural frequencies of an ATMD-containing structure makes the velocity feedback control system hyper-stable. The controller, which gives very successful results against the wind input modeled by pink noise, is enriched with the NLD approach. With this improvement, while the SDOF structure reduces the wind response, the controller mass displacement is considerably limited compared to using the pure α controller. Despite the limited controller stroke, the improved controllers provide greater structural vibration

reduction with less control effort required. Finally, in this chapter, the developed controller has been tested for the purpose of damping earthquake-induced vibrations with a nine-story structure with this structure other Lyapunov-based controllers were also tested throughout this thesis. The results are evaluated with the performance criteria given in Chapter 5 and compared with the novel LR model based controller presented in Chapter 4. The NLD supported αcontroller, which is formed by combining two different control approaches in the literature, can achieve the control purpose only by needing the velocity feedback of the structure and the controller mass. It has the potential to be successfully applied with a simple control structure in vibration damping applications with known natural frequency and ATMD. It should be noted that the αcontroller which gives results close to the Lyapunov-based controller, does not have an adaptive structure and can achieve this success with an α value between the first two natural frequencies of the structure whose vibration amplitude is reduced. Owing to the high gain values used, α values that cannot be selected correctly will cause instability in the system. In addition, since anomalies such as cracks that may occur in the parameters of the structure during an earthquake will also change the natural frequency of the structure, α controllers have the potential to go out of the stable region even if they are stable at the beginning. With its design independent of structural parameters, the LR model based controller can maintain its stable structure against external effects such as earthquakes that may damage the structural integrity. NLD-supported α controller, on the other hand, has a successful performance that can be preferred in the damping of wind-induced vibrations of tall buildings.

CHAPTER NINE
CONCLUSIONS

Vibrations in structures are caused by external factors such as earthquakes, winds, and human-induced forces. This thesis focuses on controller design for active mass systems used to dampen the vibration of structures. Ensuring the stability of the structure while achieving the control purpose is the second main objective of this thesis. One of the most critical parts of controller designs is ensuring system stability. Because the control gains are calculated without knowledge of the system characteristics, especially in robust control schemes, the whole system can be readily destabilized. A controller for the ATMD system that is not ensured the stability of the entire system during the control process may lead to property damage and human casualties. In light of this problem, it is essential to support the developed robust controller with a theoretical stability study that can ensure the stability of the entire system.

In this thesis, all Lyapunov-based controllers are designed and tested to reduce vibrations caused by earthquake-induced vibrations. The α controllers in the eighth chapter have been adapted to minimize the wind-induced vibration amplitudes of skyscraper-like structures. Then, in order to be able to compare it with the other controllers within the scope of the thesis, it is tested with a nine-story linear structure under the earthquake excitation, and its results are compared with the LR model based controller designed in chapter four. All the studies carried out within the scope of this thesis are explained in the previous eight chapters and the conclusions are given at the end of each chapter. To complete this examination in more detail, the results of all chapters are analyzed separately.

- In Chapter 2, a novel robust adaptive controller for ATMD systems that are used to reduce the amplitude of vibration of multi-story buildings is introduced. Theoretically, the designed controller provided the constant control gains are chosen as positive numerical values, the developed controller ensures system stability while attaining the primary control goal owing to the Lyapunov-based stability analysis described. It has been assumed in the literature that the structure

parameters are partially known in the controller design in similar studies designed for ATMD systems in the literature. The most important contribution of this chapter to the literature, unlike its counterparts in the literature, is its design independent of system parameters with adaptive compensation terms. The backstepping control design, which is capable of dealing with parametric uncertainties, offers a generalized control approach for vibration reduction problems in structures using such ATMD systems.

- In Chapter 3, the proposed controller provides a generalized control solution for ATMD systems with a structural parameter-independent control design as in the controller presented in Chapter 2. The designed controller copes with parametric uncertainties by using adaptive compensation terms. The controller proposed in this chapter proposes a solution to a stability problem that is lacking in the literature. While the studies in the literature focused on the stability of the structure, the stability of the controller mass was ignored. In this chapter, besides the stability of the structure, the stability of the control mass is emphasized. In the controller design, the controller mass on which the control force is applied by the actuator and the last floor of a multi-story building are considered together. Owing to this approach, a control scheme that can ensure zero convergence of the ATMD mass and the displacement of the last floor of the structure. It has been demonstrated that a theoretically designed controller that uses Lyapunov-based arguments may accomplish this primary control aim while maintaining the stability of the structure and controller mass.

- In Chapter 4, a novel linear regression model based controller for the ATMD systems is designed. In this control design, as in chapter 2 and chapter 3, the structural parameters are compensated by the designed compensation terms. Similar to the first two control designs, the stability of the structure is mathematically guaranteed by the Lyapunov stability analysis while the earthquake-induced vibrations are reduced. Studies in the literature still assume that at least all states of the top two floors and ATMD system are available to use in the feedback information. The contribution of the controller designed in

this chapter to the literature is a control design that can provide the main control purpose by using only the states of the last floor of the structure as feedback information. In the proposed design, the states of the controller mass and the penultimate floor are obtained by linear regression from the last floor acceleration data. The coefficient vector of the linear regression model is compensated by the compensation terms. Simulation studies performed on nine-story and fifteen-story buildings with the same control gains have shown that the designed controller can be used safely in all buildings with ATMD systems, regardless of the number of floors and system parameters.

- In Chapter 5, the performances of the ATMD system tested controllers designed and placed on a nine-story linear structure in chapters 2, 3, and 4 were compared. In addition to the 12 evaluation criteria based on the control effort as well as the displacement and acceleration values of the structure presented in Yang et al 2001. RMS and peak value of control effort and RMS and peak value of ATMD displacement are added to these evaluation criteria. The three controllers designed were evaluated with a total of 14 criteria for four different earthquakes and three different structures. In order to show that the designed robust controllers can cope with the uncertainty in the structure parameters, the structure stiffness, which is a widely used method in the literature (Nagarajaiah & Varadarajan, 2005; Varadarajan & Nagarajaiah, 2004; J. N. Yang et al., 2001) has been changed to ±15%. In addition, four different major earthquakes are used in the evaluation chapter to test the success of the designed controllers.

  In the displacement based evaluation criteria (J_3, J_4, J_9 and J_{10}), the LR model based controller performs better, but the results are extremely close. In the J_1, J_2, J_7 and J_8 criteria, which are the acceleration-based evaluation criteria, the control design designed in chapter 2, which only guarantees the stability of the structure, is more successful even though it has very close results. In the evaluation criteria related to control effort and control mass displacement, it is clearly seen that the LR model based controller design is more successful. It provides a stronger control performance against disturbance effects such as

measurement error and sensor noise, as it compensates for other states with the help of linear regression using fewer sensor data (only the top floor states are available).

- In Chapter 6, a disturbance function has been added to the mathematical model of the nine-story linear structure used in the control designs in Chapters 2, 3, and 4 in order to obtain a more realistic approach. A band limited white noise is added to the structure model as a nonlinear function to represent unknown external effects like measurement noise, unmodeled dynamics and etc. For the renewed mathematical model, a controller was designed again. In addition to the structural uncertainties, the unknown nonlinearity function is also covered by the designed adaptive compensation terms. The stability of the structure while achieving the control objective is guaranteed by the Lyapunov-based stability analysis. A limited number of studies some of the nonlinear dynamics of multi-story buildings were considered the control designs proposed in these studies were also proposed as linear control inputs by utilizing methods like feedback linearization, linearization around equilibrium points and etc. The main contribution of the controller designed in this section to the literature is the control structure that considers these nonlinear disturbance functions into account in the designed controller. The main purpose of this chapter is to obtain a control design that can partially represent the nonlinear and uncertain effects and to achieve the main control purpose in the presence of these effects.

- In Chapter 7, a robust adaptive controller is designed to mitigate earthquake-induced vibrations of a nonlinear multi-story building using ATMD. By improving the design in Chapter 6, in addition to the nonlinear disturbance function, the structure model used in the controller design is nonlinearized with nonlinear duffing spring elements for a more realistic approach. Robust adaptive backstepping control design has been carried out according to the new nonlinear structure model. Stability of the structure while reaching the control aim is guaranteed by a Lyapunov-based stability criterion that handles all nonlinear and unknown situations. The coefficient vector representing the unknown

parameters of the nonlinear auxiliary function representing the structural parameters and system states is compensated by the adaptive compensation vector. In addition, in this section, ATMD system parameters used in previous studies were recalculated owing to the optimal TMD rules, and an optimal TMD is used as an ATMD in this chapter to reduce the amplitude of vibration of the nine-story building model. The main contribution of the controller designed in this section to the literature is the designed controller that takes these nonlinear disturbance functions and structural nonlinearities into account in the designed controller.

- In Chapter 8, the studies are carried out at Exeter University and the controller structure used is different from the Lyapunov-based robust adaptive controller designs used in other chapters of the thesis. The main aim of the study is to reduce the wind-induced vibrations that occur in a skyscraper modeled as a mass-spring-damper system with a single degree of freedom. The α controller, which is a controller design based on the natural frequency of the structure and developed by Collette & Chesné, (2016), is used as the controller in the ATMD system placed on the structure. This control strategy is focused on the unstable behavior of the system for high gain values, which is the main problem of the velocity feedback control design, which is the most basic control method in ATMD systems. The velocity feedback control approaches used in ATMD systems show stable behavior only for low control gains in relation to the damping constant of the system. The α value to be selected between the first two natural frequencies of the TMD added structure makes the system to be controlled hyperstable. Although the α controller produces very successful results for high control gains, since it does not contain any control over the control mass, the control mass displacement can reach high values. In order to prevent this, the movement stroke of the control mass is limited with the NLD approach, which was first developed by Venanzi & Ubertini, (2014). In the structure simulated with pink noise, the α controller powered by NLD achieved lower control mass displacement compared to the original α controller, as well as lower structural vibration with lower control effort.

In order to preserve the structural integrity of the thesis, the NLD-supported α controller designed in this chapter has been revised to reduce earthquake-induced vibrations on the nine-story linear structure used to simulate the controller performances in other chapters of the thesis. The simulation results were compared with the LR model based controller designed in Chapter 4 with the evaluation criteria recommended in Chapter 5. It gave very close results in terms of structural vibration damping success. When the two controls are compared in terms of control effort, the NLD-supported controls have a lower peak value and a higher RMS value. In terms of control mass displacements, the LR model based controller is more successful. As can be seen, NLD-supported α controllers, which achieved the control purpose by using the natural frequency of the structure, were able to produce performance close to the robust adaptive controllers powered by Lyapunov-based LR. However, it should not be forgotten that the NLD-supported α controller is a control design that is specially designed for the proposed structure and cannot be used without changing the α value in systems with similar models but different structural frequencies. In addition, the natural frequencies of the system need to be determined correctly in the control design. However, the LR model-based control design has a stability analysis independent of system parameters that can be used safely in any similar system. The NLD supported α controller designed in this chapter was obtained by combining the α controller and NLD controller and was used together for the first time in the literature. The controller, which can achieve its control purpose only using the velocity feedback of the structure and the controller mass, is very effective with its simple structure in damping wind-induced vibrations. NLD supported α controller, which also performs well against earthquake-induced vibrations, has disadvantages over LR model based controllers due to its structure depending on the natural frequency of the structure in systems that may cause the parameters of the building to change.

As a result, among the controllers designed within the scope of the thesis, the controller that produces the most successful results for linear structures according to

the performance criteria given in Chapter 5 is the LR model based controller presented in Chapter 4. It can be used successfully in buildings using ATMD systems for the damping of earthquake-induced vibrations with low control effort requirements. With its structure that only needs two sensors, the NLD supported α controller has shown successful performance in damping earthquake-induced vibrations in linear structures. However, due to the design dependent on the natural frequency of the structure, it can be expected to be adversely affected by the changes that may occur in the structural parameters. However, it can be preferred to be used in structures such as steel structures whose structural parameters will not change. The robust adaptive controller designed in Chapter 7 guarantees the stability of the structure while damping earthquake-induced vibrations in nonlinear structures under the effect of unknown nonlinear disturbance. It can be used safely in similar nonlinerar systems. The NLD supported α controller, which needs the natural frequency value of the structure in the control design, has a successful performance that can be preferred in damping the wind-induced vibrations of high-rise buildings with its simple structure.

Future research should be conducted in the following areas:

- The nonlinear structure model should be developed and new controller designs should be made for different nonlinearities.

- Building models should be made more realistic by taking into account torsional vibrations and new controllers should be developed for ATMDs suitable for them.

- Controller designs should be improved by adding a time delay to the system.

- Finally, the proposed controllers should be tested with experimental studies and the successful ones should be used in full scale systems.

REFERENCES

Adhikari, R., Yamaguchi, H., & Yamazaki, T. (1998). Modal space sliding-mode control of structures. *Earthquake Engineering and Structural Dynamics*, *27*(11), 1303–1314. https://doi.org/10.1002/(SICI)1096-9845(1998110)27:11<1303::AID-EQE785>3.0.CO;2-J

Aghabalaei Baghaei, K., Ghaffarzadeh, H., & Younespour, A. (2019). Orthogonal function-based equivalent linearization for sliding mode control of nonlinear systems. *Structural Control and Health Monitoring*, *26*(8), e2372. https://doi.org/10.1002/stc.2372

Akyürek, O., & Suksawang, N. (2021). Vibration control by active integrated control system under bidirectional ground motions. *Advances in Structural Engineering*, *24*(3), 596–610. https://doi.org/10.1177/1369433220963728

Ali, M. M., & Moon, K. S. (2007). Structural developments in tall buildings: current trends and future prospects. *Architectural Science Review*, *50*(3), 205–223. https://doi.org/10.3763/asre.2007.5027

Ali, S. F., & Ramaswamy, A. (2009). Testing and modeling of MR damper and its application to SDOF systems using integral backstepping technique. *Journal of Dynamic Systems, Measurement and Control, Transactions of the ASME*, *131*(2), 1–11. https://doi.org/10.1115/1.3072154

Allan, J. F. (1945). The stabilization of ships by activated fins. *Transactions of The Royal Institution of Naval Architects RINA*, *87*, 123–159.

Alli, H., & Yakut, O. (2005). Fuzzy sliding-mode control of structures. *Engineering Structures*, *27*(2), 277–284.

Aly, A. M. (2014a). Proposed robust tuned mass damper for response mitigation in buildings exposed to multidirectional wind. *Structural Design of Tall and Special*

Buildings, *23*(9), 664–691. https://doi.org/10.1002/tal.1068

Aly, A. M. (2014b). Vibration control of high-rise buildings for wind: A robust passive and active tuned mass damper. *Smart Structures and Systems*, *13*(3), 473–500. https://doi.org/10.12989/sss.2014.13.3.473

Amini, F., & Ghaderi, P. (2013). Seismic motion control of structures: A developed adaptive backstepping approach. *Computers and Structures*, *114–115*, 18–25. https://doi.org/10.1016/j.compstruc.2012.09.011

Andersen, L., Birch, N. W., Hansen, A. H., & Skibelund, J. O. (2001). Response analysis of tuned mass dampers to structures exposed to vortex loading of Simiu-Scanlan type. *Journal of Sound and Vibration*, *239*(2), 217–231. https://doi.org/10.1006/jsvi.2000.3170

Anh, N. D., & Nguyen, N. X. (2012). Extension of equivalent linearization method to design of TMD for linear damped systems. *Structural Control and Health Monitoring*, *19*(6), 565–573.

Bekdaş, G., & Nigdeli, S. M. (2013). Mass ratio factor for optimum tuned mass damper strategies. *International Journal of Mechanical Sciences*, *71*, 68–84. https://doi.org/10.1016/j.ijmecsci.2013.03.014

Boggs, D., & Dragovich, J. (2006). The nature of wind loads and dynamic response. *Special Publication*, *240*, 15–44.

Brock, J. E. (1947). Erratum: a note on the damped vibration absorber *Journal of Applied Mechanics*, 14 (1), A80. https://doi.org/10.1115/1.4009654

Chen, H., Sun, Z., & Sun, L. (2011). Active mass damper control for cable stayed bridge under construction: An experimental study. *Structural Engineering and Mechanics*, *38*(2), 141–156. https://doi.org/10.12989/sem.2011.38.2.141

Chen, X., Li, J., Li, Y., & Gu, X. (2016). Lyapunov-based semi-active control of adaptive base isolation system employing magnetorheological elastomer base isolators. *Earthquake and Structures*, *11*(6), 1077–1099. https://doi.org/10.12989/eas.2016.11.6.1077

Cheng, F. Y., Jiang, H., & Lou, K. (2008). Smart structures: Innovative systems for seismic response control. In *Smart Structures: Innovative Systems for Seismic Response Control*. CRC press.

Chesné, S., & Collette, C. (2018). Experimental validation of fail-safe hybrid mass damper. *JVC/Journal of Vibration and Control*, *24*(19), 4395–4406. https://doi.org/10.1177/1077546317724949

Christenson, R. E. (2001). *Semiactive control of civil structures for natural hazard mitigation: Analytical and experimental studies.* [Ph.D. Thesis]. University of Notre Dame.

Collette, C., & Chesné, S. (2016). Robust hybrid mass damper. *Journal of Sound and Vibration*, *375*, 19–27. https://doi.org/10.1016/j.jsv.2016.04.030

Collins, R., Basu, B., & Broderick, B. (2006). Control strategy using bang-bang and minimax principle for FRF with ATMDs. *Engineering Structures*, *28*(3), 349–356. https://doi.org/10.1016/j.engstruct.2005.08.012

Concha, A., Alvarez-Icaza, L., & Garrido, R. (2016). Simultaneous parameter and state estimation of shear buildings. *Mechanical Systems and Signal Processing*, *70*, 788–810.

Cong, C. (2019). Using active tuned mass dampers with constrained stroke to simultaneously control vibrations in wind turbine blades and tower. *Advances in Structural Engineering*, *22*(7), 1544–1553.

https://doi.org/10.1177/1369433218817892

Constantinou, M., Soong, T., & Dargush, G. (1998). Passive Energy Dissipation Systems for Structural Design and Retrofit. *Multidisciplinary Center for Earthquake Engineering Research*, *1*, 320. http://mceer.buffalo.edu/publications/catalog/reports/Passive-Energy-Dissipation-Systems-for-Structural-Design-and-Retrofit-MCEER-98-MN01.html

Dench, M. R., Brennan, M. J., & Ferguson, N. S. (2013). On the control of vibrations using synchrophasing. *Journal of Sound and Vibration*, *332*(20), 4842–4855. https://doi.org/10.1016/j.jsv.2013.04.044

Dyke, S. J., Spencer, B. F., Quast, P., Kaspari, D. C., & Sain, M. K. (1996). Implementation of an active mass driver using acceleration feedback control. *Computer-Aided Civil and Infrastructure Engineering*, *11*(5), 305–323. https://doi.org/10.1111/j.1467-8667.1996.tb00445.x

Elias, S., & Matsagar, V. (2017). Research developments in vibration control of structures using passive tuned mass dampers. *Annual Reviews in Control*, *44*, 129–156. https://doi.org/10.1016/j.arcontrol.2017.09.015

Etedali, S., Sohrabi, M. R., & Tavakoli, S. (2013). Optimal PD/PID control of smart base isolated buildings equipped with piezoelectric friction dampers. *Earthquake Engineering and Engineering Vibration*, *12*(1), 39–54.

Etedali, S., & Tavakoli, S. (2017). PD/PID Controller Design for Seismic Control of High-Rise Buildings Using Multi-Objective Optimization: A Comparative Study with LQR Controller. *Journal of Earthquake and Tsunami*, *11*(3), 1750009. https://doi.org/10.1142/S1793431117500099

Etedali, S., Zamani, A. A., & Tavakoli, S. (2018). A GBMO-based PIλDμ controller

for vibration mitigation of seismic-excited structures. *Automation in Construction*, *87*, 1–12. https://doi.org/10.1016/j.autcon.2017.12.005

Fang, J. S., Hai, W. H., & Zhang, X. L. (2001). An analytical study for controlling chaos in Duffing oscillator with weak periodic perturbation. *Chinese Physics Letters*, *18*(3), 334–336. https://doi.org/10.1088/0256-307X/18/3/308

Frahm, H. (1911). *Device for damping vibrations of bodies.* US Patent No. US52545509A.

Fuller, C. R., Maillard, J. P., Mercadal, M., & Von Flotow, A. H. (1997). Control of aircraft interior noise using globally detuned vibration absorbers. *Journal of Sound and Vibration*, *203*(5), 745–761. https://doi.org/10.1006/jsvi.1996.0867

Ghaderi, P., & Amini, F. (2017). Adaptive block backstepping control for civil structures with unknown parameters subjected to seismic excitation. *Structural Control and Health Monitoring*, *24*(2), e1875. https://doi.org/10.1002/stc.1875

Ghaderi, P., & Amini, F. (2020). Development of a new method for online parameter identification in seismically excited smart building structures using virtual synchronization and adaptive control design. *Applied Mathematical Modelling*, *87*, 203–221.

Ghaffarzadeh, H., Younespour, A., & Cheng, S. (2020). Design of a tuned mass damper for damped structures using an orthogonal-function-based equivalent linearization method. *Structures*, *28*, 2605–2616.

Ghandchi-Tehrani, M., Wilmshurst, L. I., & Elliott, S. J. (2015). Bifurcation control of a Duffing oscillator using pole placement. *JVC/Journal of Vibration and Control*, *21*(14), 2838–2851. https://doi.org/10.1177/1077546313517586

Ghandchi Tehrani, M., & Elliott, S. J. (2014). Extending the dynamic range of an

energy harvester using nonlinear damping. *Journal of Sound and Vibration*, *333*(3), 623–629. https://doi.org/10.1016/j.jsv.2013.09.035

Ghosh, A., & Basu, B. (2007). A closed-form optimal tuning criterion for TMD in damped structures. *Structural Control and Health Monitoring*, *14*(4), 681–692. https://doi.org/10.1002/stc.176

Guclu, R. (2006). Sliding mode and PID control of a structural system against earthquake. *Mathematical and Computer Modelling*, *44*(1–2), 210–217. https://doi.org/10.1016/j.mcm.2006.01.014

Guclu, R., & Yazici, H. (2008). Vibration control of a structure with ATMD against earthquake using fuzzy logic controllers. *Journal of Sound and Vibration*, *318*(1–2), 36–49. https://doi.org/10.1016/j.jsv.2008.03.058

Gutierrez Soto, M., & Adeli, H. (2013). Tuned Mass Dampers. *Archives of Computational Methods in Engineering*, *20*(4), 419–431. https://doi.org/10.1007/s11831-013-9091-7

Hacioglu, Y., & Yagiz, N. (2012). Adaptive backstepping control with estimation for the vibration isolation of buildings. *JVC/Journal of Vibration and Control*, *18*(13), 1996–2005. https://doi.org/10.1177/1077546311429052

Heidari, A. H., Etedali, S., & Javaheri-Tafti, M. R. (2018). A hybrid LQR-PID control design for seismic control of buildings equipped with ATMD. *Frontiers of Structural and Civil Engineering*, *12*(1), 44–57. https://doi.org/10.1007/s11709-016-0382-6

Hoang, N., Fujino, Y., & Warnitchai, P. (2008). Optimal tuned mass damper for seismic applications and practical design formulas. *Engineering Structures*, *30*(3), 707–715. https://doi.org/10.1016/j.engstruct.2007.05.007

Hort, H. (1934). Beschreibung und Versuchsergebnisse ausgeführter Schiffsstabilisierungsanlagen. *Jahrb. Schiffbautechn. Ges*, *35*, 292–312.

Huo, L., Song, G., Li, H., & Grigoriadis, K. (2008). H∞ robust control design of active structural vibration suppression using an active mass damper. *Smart Materials and Structures*, *17*(1), 15021. https://doi.org/10.1088/0964-1726/17/01/015021

Kamgar, R., Samea, P., & Khatibinia, M. (2018). Optimizing parameters of tuned mass damper subjected to critical earthquake. *Structural Design of Tall and Special Buildings*, *27*(7), e1460. https://doi.org/10.1002/tal.1460

Karami, K., Manie, S., Ghafouri, K., & Nagarajaiah, S. (2019). Nonlinear structural control using integrated DDA/ISMP and semi-active tuned mass damper. *Engineering Structures*, *181*, 589–604. https://doi.org/10.1016/j.engstruct.2018.12.059

Kardoutsou, V., Taflampas, I., & Psycharis, I. N. (2017). A new pulse indicator for the classification of ground motions. *Bulletin of the Seismological Society of America*, *107*(3), 1356–1364. https://doi.org/10.1785/0120160301

Kareem, A., Kijewski, T., & Tamura, Y. (1999). Mitigation of motions of tall buildings with specific examples of recent applications. *Wind and Structures, An International Journal*, *2*(3), 201–251. https://doi.org/10.12989/was.1999.2.3.201

Kayabekir, A. E., Bekdaş, G., Nigdeli, S. M., & Geem, Z. W. (2020). Optimum design of PID controlled active tuned mass damper via modified harmony search. *Applied Sciences (Switzerland)*, *10*(8), 2976. https://doi.org/10.3390/APP10082976

Kaynia, A. M., Veneziano, D., & Biggs, J. M. (1981). Seismic Effectiveness of Tuned Mass Dampers. *ASCE J Struct Div*, *107*(8), 1465–1484.

Khalil, H. K. (2010). Lyapunov stability. *The Control Systems Handbook: Control System Advanced Methods, Second Edition*, 1005–1014. https://doi.org/10.1201/b10384

Khatibinia, M., Mahmoudi, M., & Eliasi, H. (2020). Optimal Sliding Mode Control for Seismic Control of Buildings Equipped With Atmd. *Iran University of Science & Technology*, *10*(1), 1–15.

Kobori, T., & Minai, R. (1960). Analytical study on active seismic response control. *Journal of Structural Control Engineering (Transactions of the Architectural Institute of Japan)*, *66*(2), 257–260.

Krenk, S. (2005). Frequency analysis of the tuned mass damper. *Journal of Applied Mechanics, Transactions ASME*, *72*(6), 936–942. https://doi.org/10.1115/1.2062867

Krstic, M., Kokotovic, P. V, & Kanellakopoulos, I. (1995). *Nonlinear and adaptive control design*. John Wiley & Sons, Inc.

Krstic, M., & Smyshlyaev, A. (2007). Backstepping boundary control for first order hyperbolic PDEs and application to systems with actuator and sensor delays. *Proceedings of the IEEE Conference on Decision and Control*, *57*(9), 225–230. https://doi.org/10.1109/CDC.2007.4434474

Lavasani, S. H. H., Alizadeh, H., Doroudi, R., & Homami, P. (2020). Vibration control of suspension bridge due to vertical ground motions. *Advances in Structural Engineering*, *23*(12), 2626–2641. https://doi.org/10.1177/1369433220919079

Li, C., & Cao, L. (2019a). Active tuned tandem mass dampers for seismic structures. *Earthquake and Structures*, *17*(2), 143–162. https://doi.org/10.12989/eas.2019.17.2.143

Li, C., & Cao, L. (2019b). High performance active tuned mass damper inerter for structures under the ground acceleration. *Earthquake and Structures*, *16*(2), 149–163. https://doi.org/10.12989/eas.2019.16.2.149

Li, Z., & Adeli, H. (2016). New discrete-time robust H2/H∞ algorithm for vibration control of smart structures using linear matrix inequalities. *Engineering Applications of Artificial Intelligence*, *55*, 47–57. https://doi.org/10.1016/j.engappai.2016.05.008

Luft, R. W. (1979). Optimal tuned mass dampers for buildings. *Journal of the Structural Division*, *105*(12), 2766–2772. https://doi.org/10.1061/jsdeag.0005323

Mallock, A. (1905). A method of preventing vibration in certain classes of steamships. *Transactions of the Royal Institution of Naval Architects*, *47*, 227–230.

Mamat, N., Yakub, F., Shaikh Salim, S. A. Z., & Mat Ali, M. S. (2020). Seismic vibration suppression of a building with an adaptive nonsingular terminal sliding mode control. *JVC/Journal of Vibration and Control*, *26*(23–24), 2136–2147. https://doi.org/10.1177/1077546320915324

Mañosa, V., Ikhouane, F., & Rodellar, J. (2005). Control of uncertain non-linear systems via adaptive backstepping. *Journal of Sound and Vibration*, *280*(3–5), 657–680. https://doi.org/10.1016/j.jsv.2003.12.033

Marian, L., & Giaralis, A. (2014). Optimal design of a novel tuned mass-damper-inerter (TMDI) passive vibration control configuration for stochastically support-excited structural systems. *Probabilistic Engineering Mechanics*, *38*, 156–164. https://doi.org/10.1016/j.probengmech.2014.03.007

Nagarajaiah, S., & Varadarajan, N. (2005). Short time Fourier transform algorithm for wind response control of buildings with variable stiffness TMD. *Engineering*

Structures, *27*(3), 431–441. https://doi.org/10.1016/j.engstruct.2004.10.015

Novak, S., & Frehlich, R. G. (1982). Transition to chaos in the Duffing oscillator. *Physical Review A*, *26*(6), 3660–3663. https://doi.org/10.1103/PhysRevA.26.3660

Ormondroyd, J., & Den, H. J. P. (1928). Theory of the dynamic vibration absorber. *Transactions of the American Society of Mechanical Engineers*, *50*, 9–22.

Ouyang, Y., Shan, J., Shi, W., & Spencer, B. F. (2019). Adaptive control for smart-actuated base isolation structures regarding various reference-tracking strategies. *Engineering Structures*, *198*, 109574. https://doi.org/10.1016/j.engstruct.2019.109574

Ouyang, Y., Shi, W., Shan, J., & Spencer, B. F. (2019). Backstepping adaptive control for real-time hybrid simulation including servo-hydraulic dynamics. *Mechanical Systems and Signal Processing*, *130*, 732–754. https://doi.org/10.1016/j.ymssp.2019.05.042

Paknejad, A., Zhao, G., Chesné, S., Deraemaeker, A., & Collette, C. (2022). Design and optimization of a novel resonant control law using force feedback for vibration mitigation. *Structural Control and Health Monitoring*, *29*(6), e2939. https://doi.org/10.1002/stc.2939

Palazzo, B., & Petti, L. (1999). Optimal structural control in the frequency domain: Control in norm H2 and H∞. *Journal of Structural Control*, *6*(2), 205–221. https://doi.org/10.1002/stc.4300060202

Petrini, F., Giaralis, A., & Wang, Z. (2020). Optimal tuned mass-damper-inerter (TMDI) design in wind-excited tall buildings for occupants' comfort serviceability performance and energy harvesting. *Engineering Structures*, *204*, 109904. https://doi.org/10.1016/j.engstruct.2019.109904

Pourzeynali, S., Lavasani, H. H., & Modarayi, A. H. (2007). Active control of high rise building structures using fuzzy logic and genetic algorithms. *Engineering Structures*, *29*(3), 346–357.

Pozo, F., Ikhouane, F., Pujol, G., & Rodellar, J. (2006). Adaptive backstepping control of hysteretic base-isolated structures. *JVC/Journal of Vibration and Control*, *12*(4), 373–394. https://doi.org/10.1177/1077546306063254

Preumont, A., Alaluf, D., & Bastaits, R. (2014). Hybrid mass damper: A tutorial example. *CISM International Centre for Mechanical Sciences, Courses and Lectures*, *558*, 179–211. https://doi.org/10.1007/978-3-7091-1821-4_3

Rana, R., & Soong, T. T. (1998). Parametric study and simplified design of tuned mass dampers. *Engineering Structures*, *20*(3), 193–204.

Randall, S. E., Halsted, D. M., & Taylor, D. L. (1981). Optimum vibration absorbers for linear damped systems. *Journal of Mechanical Design, Transactions of the ASME*, *103*(4), 908–913. https://doi.org/10.1115/1.3255005

Rasouli, S. K., & Yahyai, M. (2002). Control of response of structures with passive and active tuned mass dampers. *Structural Design of Tall Buildings*, *11*(1), 1–14. https://doi.org/10.1002/tal.181

Ricciardelli, F., & Vickery, B. J. (1999). Tuned vibration absorbers with dry friction damping. *Earthquake Engineering and Structural Dynamics*, *28*(7), 707–723. https://doi.org/10.1002/(SICI)1096-9845(199907)28:7<707::AID-EQE836>3.0.CO;2-C

Shan, J., Ouyang, Y., & Shi, W. (2018). Adaptive control of earthquake-excited nonlinear structures with real-time tracking on prescribed performance criteria. *Structural Control and Health Monitoring*, *25*(10), e2247.

https://doi.org/10.1002/stc.2247

Shariatmadar, H., & Razavi, H. M. (2014). Seismic control response of structures using an ATMD with fuzzy logic controller and PSO method. *Structural Engineering and Mechanics*, *51*(4), 547–564.

Shing, P. B., Dixon, M. E., Kermiche, N., Su, R., & Frangopol, D. M. (1996). Control of building vibrations with active/passive devices. *Earthquake Engineering and Structural Dynamics*, *25*(10), 1019–1039. https://doi.org/10.1002/(SICI)1096-9845(199610)25:10<1019::AID-EQE584>3.0.CO;2-Y

Sladek, J. R., & Klingner, R. E. (1983). Effect of tuned-mass dampers on seismic response. *Journal of Structural Engineering*, *109*(8), 2004–2009. https://doi.org/10.1061/(asce)0733-9445(1983)109:8(2004)

Snowdon, J. C. (1959). Transient behavior of the dynamic absorber. *Journal of the Acoustical Society of America*, *31*(12), 1668–1675. https://doi.org/10.1121/1.1907676

Socha, L., & Blachuta, M. (2000). Application of linearization methods with probability density criteria in control problems. *Proceedings of the 2000 American Control Conference. ACC (IEEE Cat. No. 00CH36334)*, *4*, 2775–2779.

Soleymani, M., Abolmasoumi, A. H., Bahrami, H., Khalatbari, A., Khoshbin, E., & Sayahi, S. (2018). Modified sliding mode control of a seismic active mass damper system considering model uncertainties and input time delay. *JVC/Journal of Vibration and Control*, *24*(6), 1051–1064. https://doi.org/10.1177/1077546316657477

Soong, T. T., & Spencer, B. F. (1992). Active structural control: theory and practice. *Journal of Engineering Mechanics*, *118*(6), 1282–1285. https://doi.org/10.1061/(asce)0733-9399(1992)118:6(1282)

Soong, T. T., & Spencer, B. F. (2002). Supplemental energy dissipation: State-of-the-art and state-of-the-practice. *Engineering Structures*, *24*(3), 243–259. https://doi.org/10.1016/S0141-0296(01)00092-X

Spence, R., & So, E. (2021). Why do buildings collapse in earthquakes? John Wiley \& Sons. https://doi.org/10.1002/9781119619475

Talib, E., Shin, J. H., & Kwak, M. K. (2019). Designing multi-input multi-output modal-space negative acceleration feedback control for vibration suppression of structures using active mass dampers. *Journal of Sound and Vibration*, *439*, 77–98. https://doi.org/10.1016/j.jsv.2018.09.052

Thenozhi, S., & Yu, W. (2013). Advances in modeling and vibration control of building structures. *Annual Reviews in Control*, *37*(2), 346–364. https://doi.org/10.1016/j.arcontrol.2013.09.012

Thenozhi, S., & Yu, W. (2014). Stability analysis of active vibration control of building structures using PD/PID control. *Engineering Structures*, *81*, 208–218. https://doi.org/10.1016/j.engstruct.2014.09.042

Tokhi, M. O., Veres, S., & Veres, S. M. (2002). *Active sound and vibration control: theory and applications* (Vol. 62). Iet.

Ümütlü, R. C., Bidikli, B., & Ozturk, H. (2022). A backstepping control design for ATMD systems of building structure against earthquake excitations in the presence of parametric uncertainty. *Structural Control and Health Monitoring*, *29*(3), e2893. https://doi.org/10.1002/stc.2893

Ümütlü, R. C., Ozturk, H., & Bidikli, B. (2021). A robust adaptive control design for active tuned mass damper systems of multistory buildings. *JVC/Journal of Vibration and Control*, *27*(23–24), 2765–2777.

https://doi.org/10.1177/1077546320966236

Varadarajan, N., & Nagarajaiah, S. (2004). Wind response control of building with variable stiffness tuned mass damper using empirical mode decomposition/hilbert transform. *Journal of Engineering Mechanics*, *130*(4), 451–458. https://doi.org/10.1061/(asce)0733-9399(2004)130:4(451)

Venanzi, I., Ierimonti, L., & Ubertini, F. (2015). An enhanced nonlinear damping approach accounting for system constraints in active mass dampers. *Journal of Sound and Vibration*, *357*, 2–15.

Venanzi, I., & Ubertini, F. (2014). Free vibration response of a frame structural model controlled by a nonlinear active mass driver system. *Advances in Civil Engineering*, *2014*.

Vickery, B. J., & Davenport, A. G. (1970). An investigation of the behaviour in wind of the proposed Centrepoint Tower. *Sydney, Australia; Engineering Science Report No. BLWT-1-70; University of Western Ontario: London, ON, Canada*.

Warburton, G. B., & Ayorinde, E. O. (1980). Optimum absorber parameters for simple systems. *Earthquake Engineering \& Structural Dynamics*, *8*(3), 197–217.

Weisner, K. (1979). Tuned mass dampers to reduce building wind motion. *ASCE Convention and Exposition*, *3510*.

Wirsching, P. H., & Campbell, G. W. (1973). Minimal structural response under random excitation using the vibration absorber. *Earthquake Engineering & Structural Dynamics*, *2*(4), 303–312. https://doi.org/10.1002/eqe.4290020402

Xu, L., Cui, Y., & Wang, Z. (2020). Active tuned mass damper based vibration control for seismic excited adjacent buildings under actuator saturation. *Soil Dynamics and Earthquake Engineering*, *135*, 106181.

Yakut, O., & Alli, H. (2011). Neural based sliding-mode control with moving sliding surface for the seismic isolation of structures. *Journal of Vibration and Control*, *17*(14), 2103–2116.

Yang, D.-H., Shin, J.-H., Lee, H., Kim, S.-K., & Kwak, M. K. (2017). Active vibration control of structure by active mass damper and multi-modal negative acceleration feedback control algorithm. *Journal of Sound and Vibration*, *392*, 18–30.

Yang, J. N., Agrawal, A. K., Samali, B., & Wu, J. C. (2001). A benchmark problem for response control of wind-excited tall buildings. *Proceedings of the International Modal Analysis Conference - IMAC*, *1*(4), 151–157. https://doi.org/10.1061/(asce)0733-9399(2004)130:4(437)

Yao, J. T. P. (1972). Concept of Structural Control. *ASCE J Struct Div*, *98*(ST7), 1567–1574. https://doi.org/10.1061/jsdeag.0003280

Yazici, H., Guclu, R., Kucukdemiral, I. B., & Alpaslan Parlakci, M. N. (2012). Robust delay-dependent H ∞ control for uncertain structural systems with actuator delay. *Journal of Dynamic Systems, Measurement and Control, Transactions of the ASME*, *134*(3). https://doi.org/10.1115/1.4005500

Younespour, A., & Ghaffarzadeh, H. (2015). Structural active vibration control using active mass damper by block pulse functions. *JVC/Journal of Vibration and Control*, *21*(14), 2787–2795. https://doi.org/10.1177/1077546313519285

Yu, W., & Thenozhi, S. (2016). *Active Structural Control with Stable Fuzzy PID Techniques*. Springer. https://doi.org/10.1007/978-3-319-28025-7

Zapateiro, M., Karimi, H. R., Luo, N., Phillips, B. M., & Spencer, B. F. (2009). Semiactive backstepping control for vibration reduction in a structure with magnetorheological damper subject to seismic motions. *Journal of Intelligent*

Material Systems and Structures, *20*(17), 2037–2053. https://doi.org/10.1177/1045389X09343024

Živanović, S., Pavic, A., & Reynolds, P. (2005). Vibration serviceability of footbridges under human-induced excitation: A literature review. *Journal of Sound and Vibration*, *279*(1–2), 1–74. https://doi.org/10.1016/j.jsv.2004.01.019

APPENDICES

- **List of Publications**

  - Article:

Ümütlü, R. C., Öztürk, H., & Bidikli, B., (2021). A robust adaptive control design for ATMD systems of multi-story buildings. *Journal of Vibration and Control*, 27(23-24), 2765-2777. DOI: 10.1177/1077546320966236

Ümütlü, R. C., Bidikli, B., & Öztürk, H., (2022) A backstepping control design for ATMD systems of building structure against earthquake excitations in the presence of parametric uncertainty. *Structural Control and Health Monitoring*, e2893. DOI: 10.1002/stc.2893

Ümütlü, R. C., Öztürk, H., & Bidikli, B., (2022) an adaptive controller design for ATMD system used in structures under the effect of unknown nonlinear effects. *Dokuz Eylül Üniversitesi Mühendislik Fakültesi Fen ve Mühendislik Dergisi*. DOI: 10.21205/deufmd.2022247121

- Bulletin:

Ümütlü, R. C., Öztürk, H., & Bidikli, B., (2021). Design of a Lyapunov based controller for vibration control of multi-story buildings with nonlinear approach. Presented at ISSC 2021, Izmir/Turkey